Aus der Medizinischen Universitätsklinik und Poliklinik
Tübingen

Abteilung Innere Medizin II
(Schwerpunkt: Onkologie, Hämatologie, Klinische
Immunologie, Rheumatologie und Pulmologie)

Oscillating mRNA expression of neutrophil granule proteins and preleukemic *CSF3R/RUNX1* mutations in cyclic neutropenia patients

Inaugural-Dissertation
zur Erlangung des Doktorgrades
der Medizin

der Medizinischen Fakultät
der Eberhard Karls Universität
zu Tübingen

vorgelegt von

Reinel, Elisa-Kathrin

2019

Dekan:	Professor Dr. I. B. Autenrieth
1. Berichterstatter:	Professor Dr. J. Skokowa
2. Berichterstatter:	Professor Dr. R. Handgretinger
Tag der Disputation:	28.03.2019

Meiner Familie

Table of contents

Abbreviations VII

List of figures XI

List of tables XIII

1 Introduction 1

1.1 Pathophysiology of neutropenia 1

1.1.1 Basic classification of the human immune system 1

1.1.2 Neutrophil function 1

1.1.3 Physiology of neutrophil maturation 3

1.1.4 Pathophysiology of genetic chronic neutropenia 7

1.2 Clinical information about CyN 10

1.2.1 Definition 10

1.2.2 Epidemiology and etiology 11

1.2.3 Clinical symptoms 11

1.2.4 Diagnosis 12

1.2.5 Therapy 12

1.2.6 Prognosis and risks associated with CyN 13

2 Aim 14

3 Probands, materials and methods 16

3.1 Proband samples 16

3.1.1 Selection of CyN patients 16

3.2 Materials 19

3.2.1 Chemicals 19

3.2.1.1 Standard chemicals 19

3.2.1.2 Media 21

3.2.1.3 Primers 21

3.2.1.4 Antibodies and isotypes 23

3.2.1.5 Enzymes 23

3.2.1.6 Molecular weight standards 24

Table of contents

3.2.2 Buffers and standard compositions 24
3.2.3 Consumables 24
3.2.4 Equipment 25
3.2.5 Software 26
3.3 Methods 27
3.3.1 Preparation and quantification of RNA samples 27
3.3.1.1 Isolation of MNCs from bone marrow samples 27
3.3.1.2 Magnetic separation of $CD33^+$ and $CD34^+$ cells 27
3.3.1.3 Detection of isolated cell fractions by FACS 28
3.3.1.4 Total RNA purification protocol 28
3.3.1.5 Quantification of RNA products by NanoDrop 28
3.3.2 Preparation and quantification of cDNA samples 29
3.3.2.1 Reverse transcription 29
3.3.2.2 WTA Ovation protocol 30
3.3.2.3 Quantification of cDNA products by Qubit 31
3.3.3 Real-time quantitative PCR 31
3.3.4 PCR 32
3.3.5 Restriction digestion of wild type allele sequences 33
3.3.6 Molecular cloning 35
3.3.7 Sanger sequencing 36
3.3.8 Gel electrophoresis 36

4 Results 37
4.1 Explanatory approach for neutrophil oscillation in CyN 37
4.1.1 Neutrophil protein gene expression of a CyN patient in the microarray 37
4.1.2 Validation of microarray data by qPCR 38
4.1.2.1 Cycling gene expression pattern in CyN patient 1 39
4.1.2.2 Expression of granule protein genes in CyN patient 1 vs. HDs 44
4.1.2.3 Expression of granule protein genes in four other CyN patients 48
4.1.2.4 Expression of granule protein genes in four CyN patients vs. HDs 51
4.1.3 *C/EBPe* and *TNFRSF1A* mutations of CyN patient 1 53
4.1.3.1 Expression of *C/EBPe* in CyN patients vs. HDs 56
4.2 *CSF3R* and *RUNX1* mutations in CyN patients 63

4.2.1 *CSF3R* and *RUNX1* mutation in CyN patient 6 64
4.2.2 *CSF3R* mutation in CyN patient 4 65

5 Discussion 68
5.1 Oscillating granule protein gene expression in CyN patient 1 68
5.1.1 Discussion of data collection and experimental setup 68
5.1.2 Basic findings about cycling genes in CyN patient 1 69
5.1.3 *C/EBPe* mutation correlated with cycling genes in CyN patient 1 70
5.2 Discussion of pathomechanism in general CyN 73
5.2.1 Role of ELANE as a cycling gene in CyN patients 73
5.2.2 Regeneration of neutrophil production at the ANC nadir 74
5.2.3 Biological difference of SCN and CyN in neutrophil production 75
5.3. Cooperativity of CSF3R and RUNX1 mutations in CyN 75
5.3.1 *CSF3R* and *RUNX1* mutations in SCN 75
5.3.2 *CSF3R* and *RUNX1* mutations in CyN 75
5.3.3 G-CSF dose dependence of *CSF3R* mutation 76
5.4 Perspectives in CyN treatment 76

6 Summary 78
6.1 Summary (English version) 78
6.2 Summary (German version) 79

7 References 81

8 Declaration of Authorship 90

9 Publication 92

Acknowledgement 93

Abbreviations

AML	acute myeloid leukemia
ANC	absolute neutrophil count
AP	ammonium persulfate
b-actin	beta-actin
BC	band cell
BFU-E	burst-forming unit-erythrocyte
BFU-Eo	burst-forming unit-eosinophil
BFU-G	burst-forming unit-granulocyte
BFU-M	burst-forming unit-monocyte/macrophage
BFU-MK	burst-forming unit-megakaryocyte
BM	bone marrow
bp	base pairs
BSA	bovine serum albumin
C/EBP	CCAAT/enhancer binding protein
CD33/CD34/CD38	cluster of differentiation 33/34/38
cDNA	complementary deoxyribonucleic acid
CFU-E	colony-forming unit-erythrocyte
CFU-Eo	colony-forming unit-eosinophil
CFU-G	colony-forming unit-granulocyte
CFU-M	colony-forming unit-monocyte/macrophage
CFU-MK	colony-forming unit-megakaryocytes
CLP	common lymphoid progenitors
CMP	common myeloid progenitors
Cp	crossing point
CRISP3	cysteine-rich secretory protein 3
CSF3R	colony stimulating factor 3 receptor gene
CyN	cyclic neutropenia

ddH2O	double distilled water
Deep seq	deep sequencing
DEFA4	defensin alpha 4
Diff	differentiation
DMSO	dimethyl sulfoxide
DNA	deoxyribonucleic acid
dNTP	deoxynucleoside triphosphate
dsDNA	double strand deoxyribonucleic acid
dT	deoxythymidine
EDTA	ethylenediaminetetraacetic acid
ELANE	elastase - neutrophil expressed gene
EPO	erythropoietin
FACS	fluorescence activated cell sorting
FcR	fragment crystallizable region
FCS	fetal calf serum
G6PC3	glucose 6 phosphatase catalytic 3
G-CSF	granulocyte colony stimulating factor
GM-CSF	granulocyte/monocyte colony stimulating factor
GMP	granulocyte/macrophage progenitors
HAX1	HCLS1-associated protein X-1
HD	healthy donor
HSC	hematopoietic stem cells
Ig	immunoglobulin
IL	interleukin
LCN2	lipocalin 2
M-CSF	monocyte/macrophage colony stimulating factor
MAF	mutant allele frequency

MAX	maximum
MB	myeloblast
MC	myelocyte
MDS	myelodysplastic syndrome
MEP	megakaryocyte/erythroid progenitors
MIN	minimum
MMC	metamyelocyte
MMP8	matrix metallopeptidase 8
MNC	mononuclear cell
MPO	myeloperoxidase
MPP	multipotent progenitors
mRNA	messenger ribonucleic acid
NAMPT	nicotinamide phosphoribosyltransferase
NE	neutrophil elastase protein
NTC	negative template control
OLFM4	olfactomedin 4
PB	peripheral blood
PBS	phosphate-buffered saline
PCR	polymerase chain reaction
PFA	paraformaldehyde
PM	polymorphonuclear
PMN	polymorphonuclear leukocytes
PolyPhen-2	Polymorphism Phenotyping v2 online tool
qPCR	quantitative polymerase chain reaction
RNA	ribonucleic acid
rpm	rounds per minute
RT	reverse transcriptase
RUNX1	runt related transcription factor 1

Abbreviations

SCN	severe chronic neutropenia
SCNIR	Severe Chronic Neutropenia International Registry
SDS	sodium dodecyl sulfate
Seg	segmented cell
SIFT	Sorting intolerant from tolerant online tool
SLPI	secretory leukocyte protease inhibitor
SNP	single nucleotide polymorphism
TFRC	transferrin receptor
TNC1	transcobalamin 1
TNFRSF1A	TNF receptor superfamily member 1A
TPO	thrombopoietin
vs	versus
wt	wild type
WTA	whole transcriptome amplification

List of figures

Figure 1: The dependence of neutrophil granules on granulopoiesis stages. 3

Figure 2: Classical view of the differentiation of hematopoietic cells. 6

Figure 3: *ELANE* mutations in SCN and CyN patients. 9

Figure 4: Maturation arrest of the myeloid cells in CyN and SCN. 10

Figure 5: Family trees of examined CyN patients. 17

Figure 6: ANC courses of CyN patients 1, 3 and 4. 18

Figure 7: Restriction digestion of *RUNX1* allele by BtSCI enzyme. 34

Figure 8: Sample selection for microarray setup. 38

Figure 9: Graphic representation of group of patients and experimental setup. 39

Figure 10: Gene expression in $CD33^+$ cells of CyN patient 1. 40

Figure 11: Five oscillating genes of interest in $CD33^+$ cells of CyN patient 1. 42

Figure 12: Gene expression in $CD34^+38^+$ cells of CyN patient 1. 43

Figure 13: Relative gene expression of CyN patient 1 vs. HDs. 47

Figure 14: Relative *TFRC* expression of CyN patient 1 vs. HDs. 48

Figure 15: Relative gene expression of CyN patients 2, 3, 4 and 5 vs. b-actin. 49

Figure 16: Relative gene expression of four further CyN patients vs. CyN patient 1. .. 50

Figure 17: Relative gene expression of four CyN patients vs. HDs. 52

Figure 18: Overview of different *C/EBPe* isoforms. 55

Figure 19: Overview of *C/EBPe* mRNA sequence with primer binding sites. 56

Figure 20: Relative *C/EBPe* expression of CyN patient 1 vs. HDs. 57

Figure 21: Relative *C/EBPe* expression of four CyN patients vs. HDs. 57

Figure 22: Relative *C/EBPe* expression of four CyN patients vs. HDs. 58

Figure 23: Relative *C/EBPe* C-terminal expression of CyN patient 1 vs. HDs. 59

Figure 24: Relative *C/EBPe* C-terminal expression of four CyN patients vs. HDs. 59

Figure 25: Relative *C/EBPe* N-terminal expression of CyN patient 1 vs. HDs. 61

List of figures

Figure 26: Relative *C/EBPe* N-terminal expression of four CyN patients vs. HDs. 61

Figure 27: Acquired mutations in cytoplasmic domain of *G-CSFR*. 63

Figure 28: Time line of *CSF3R* and *RUNX1* mutation acquisition in CyN patient 6. .. 64

Figure 29: Sanger sequencing results of *RUNX1* mutation in CyN patient 6. 65

Figure 30: Time line of *CSF3R* mutation acquisition in CyN patient 4. 66

Figure 31: Sanger sequencing results of *CSF3R* mutation in CyN patient 4. 67

Figure 32: Influence of ANC on G-CSF level and *C/EBPe* expression. 73

List of tables

Table 1: Patient data with appropriate *ELANE* mutation. 17

Table 2: Standard chemicals. 19

Table 3: Media. 21

Table 4: Primers for qPCR. 22

Table 5: Primers for PCR. 23

Table 6: Primers for reverse transcription. 23

Table 7: Antibodies and isotypes for FACS. 23

Table 8: Enzymes. 23

Table 9: Molecular weight standards. 24

Table 10: Consumables. 24

Table 11: Equipment. 25

Table 12: Softwares. 26

Table 13: Master mixes for reverse transcription. 29

Table 14: Thermocycler setup for reverse transcription. 29

Table 15: Master mixes for WTA Ovation protocol. 30

Table 16: Thermocycler setup for WTA Ovation protocol. 31

Table 17: Master mix 1 for qPCR. 32

Table 18: Thermocycler setup for qPCR. 32

Table 19: Master mix for standard PCR 33

Table 20: Thermocycler setup for PCR (CSF3R_NGS5F/R). 33

Table 21: Thermocycler setup for PCR (RUNX1ex3D17N_F/RUNX1D171N309.R).. 33

Table 22: Master mix for restriction digestion with BtsCI enzyme. 35

Table 23: Master mix for ligation. 35

Table 24: Overview of *C/EBPe* expression in CyN patients. 62

Table 25: Simplified WTA qPCR and gel electrophoresis results of Figure 13. 71

1 Introduction

1.1 Pathophysiology of neutropenia

1.1.1 Basic classification of the human immune system

In general, the main function of the human immune system is to discriminate between own and foreign cells. This is performed by the innate, inborn immune system and the adaptive or acquired immune system. Adaptive immunity reacts specifically and with a time delay to foreign tissue with the production of B and T lymphocytes. In contrast, the innate immune system nonspecifically protects the body from exogenous threat, immediately after penetration. It consists of mechanical barriers (e.g., the skin), the humoral defense (e.g., the complement system) and finally the cellular components (e.g., phagocyting cells) (Beutler, 2004; Orkin et al., 2014).

1.1.2 Neutrophil function

The phagocyte system, as a substantial part of the innate immune system, consists of granulocytes (neutrophils, eosinophils and basophils) and mononuclear phagocytes (tissue macrophages and monocytes). It has the principal function to defend the host against microorganisms. When these permeate into tissue usually protected by the skin, or mucous membranes, the microbes themselves or macrophages activate endothelial cells that attract neutrophils through chemotactic signals. In the presence of the focus of infection, the neutrophils are able to detect the particulate matter with the aid of surface markers and thus ingest and phagocyte it (Iwasaki & Medzhitov, 2010; Borregaard, 2010).

For this phagocytic process, neutrophils make use of different kinds of antimicrobial toxic substances that are transported in granules. These organelles, which originate from the Golgi, were historically separated in four distinct groups according to their constituents. The first group is the azurophilic granules or primary granules, which are formed in the early stages of granulopoiesis and contain not only antimicrobial enzymes such as myeloperoxidase (MPO) but also defensins and the neutrophil elastase (NE). The second group is the specific granules, also called secondary granules, which are present in further

matured myelocytes and metamyelocytes. Proteins such as cysteine-rich secretory protein 3 (CRISP3), lipocalin 2 (LCN2), secretory leukocyte peptidase inhibitor (SLPI), and lactoferrin are part of these structures. The third group is the gelatinase or tertiary granules, which still carry some antimicrobial toxics but rather serve as a storage for various metalloproteases, such as gelatinase. As a final group to mention are the secretory vesicles, which are not produced by the Golgi. These are built in the latest stages of neutrophil differentiation and no longer serve as antimicrobial containers but encase proteins such as the plasma protein albumin (Figure 1).

Migrated by chemotaxis to the epicenter of inflammation, the activated neutrophils release their granule components through fusion with the plasma membrane or phagocyting organelles (Borregaard, 2010; Borregaard & Cowland, 1997; Borregaard et al., 2007; Nüsse & Lindau, 1988; Amulic et al., 2012; Borregaard et al., 1995).

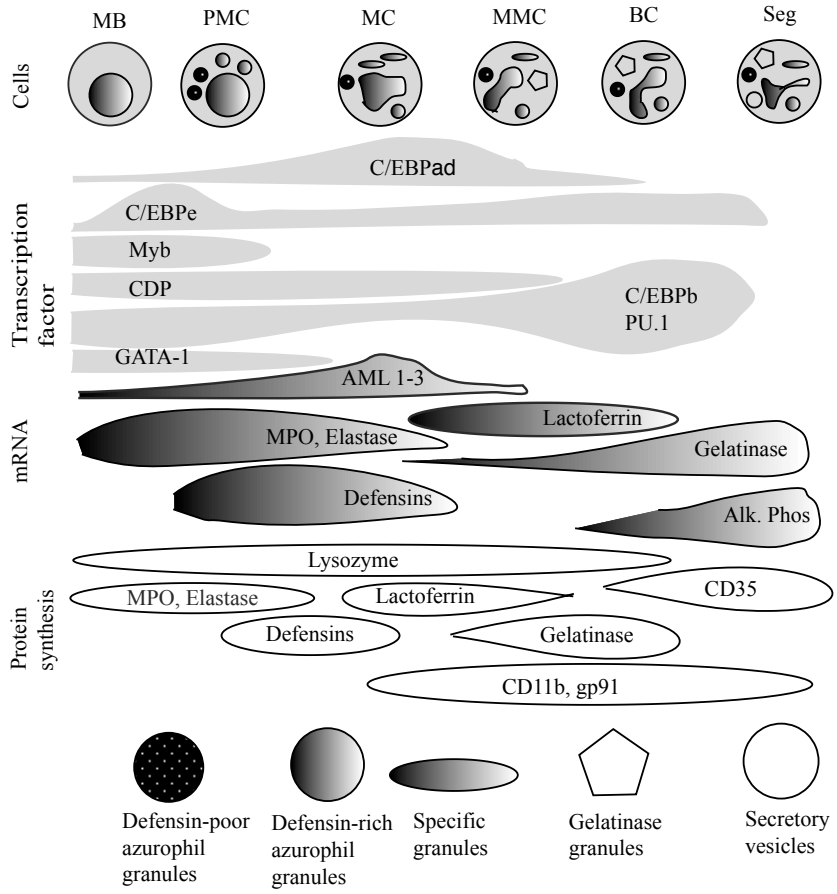

Figure 1: The dependence of neutrophil granules on granulopoiesis stages. According to the respective stage of differentiation, neutrophils are influenced by diverse transcription factors. Correspondingly, stage-dependent expression of genes at the mRNA level control the synthesis of proteins. These proteins compose the characteristic formation of granules. The neutrophil granules can thus be separated according to their presence during neutrophil maturation. Also, the respective term reflects their characteristic compound. MB, myeloblast; PMC, promyelocyte; MC, myelocyte; MMC, metamyelocyte; BC, band cell; Seg, segmented cell (Modified from Borregaard & Cowland, 1997; Koschmieder et al., 2005).

1.1.3 Physiology of neutrophil maturation

The formation of granulocytes and monocytes as part of hematopoiesis takes place in the bone marrow, where on average 1 to 2 x 10^{11} neutrophils are produced per day. The origin of various types of blood cells are the hematopoietic stem cells (Maximow, 1909). Human hematopoietic stem cells that settle in niches built by osteoblasts are multipotent and self-renewing (Borregaard, 2010; Winkler et al., 2010). Traditionally, according to the classical model of hematopoiesis, the hematopoietic differentiation is structured as a pyramidal hierarchy. From their apex, stem cells undergo restriction into oligopotent progenitors, which further develop into unipotent cells. Thus, hematopoietic cells

undergo a specification with a continuing loss of their differentiation potential. Previously, a multipotent progenitor cell was considered to follow two different paths – the myeloid or the lymphoid lineage (Figure 2). However, recent developments in this field have led to a new concept, which organizes the classical model of hematopoiesis in a new order. First, according to Notta et al., development of the fetal blood has to be delimited from that of the adult. While the fetal model still contains oligopotent progenitor cells, these should now no longer exist in the adult blood hierarchy. In contrast, a two-tier structure is defined in theory with multipotent stem cells and multipotent progenitors (MPPs) on the one plane and committed unipotent progenitors on the other plane. Second, concerns have arisen about the heterogeneity of classically defined oligopotent common myeloid progenitors (CMPs). Originally, they are expected to differentiate into the erythroid, megakaryocytic and myeloid lineage, while common lymphoid progenitors (CLPs) take the lymphoid direction. However, in the light of the recent findings, the first bifurcation in hematopoiesis is much more compound than the previous separation into the myeloid and lymphoid way. As an example, the megakaryocytic development is now expected to originate directly from multipotent cells (Notta et al., 2016). Although this approach is very fascinating, and might even be groundbreaking and challenging the classical view on hematopoiesis, it has not been dealt with in-depth sufficiently. Therefore, the following issues will be linked to the current scheme.

Turning now to myeloid differentiation, neutrophil progenitors have a high requirement for different transcription factors and growth factors to eventually reach their fully endowed quality (Doulatov et al., 2012). The most important representatives are the transcription factors PU.1 and the CCAAT/enhancer-binding protein (C/EBP) family (Figures 1 and 2) (Koschmieder et al., 2005). PU.1 plays an essential role in the maturation control of early myeloid precursors (Iwasaki et al., 2005), whereas the C/EBP family has a number of representatives that are important at different times of granulopoiesis. Moreover, members of the C/EBP factors are required needs-based (Bedi et al., 2009). C/EBPa plays an active role in the progression of common myeloid progenitors (CMPs) to granulocyte/macrophage progenitors (GMPs) (Zhang et al., 2004). Additionally, it is said to be required for steady-state neutrophil production. In contrast, C/EBPb is highly expressed in situations with increased neutrophil demand such as stress

and infections (Hirai et al., 2006). C/EBPe, on the other hand, leads to the final differentiation steps of eosinophils and neutrophils, regulating the maturation from promyelocyte to myelocyte stage (Antonson et al., 1996; Friedman, 2007; Hirai et al., 2006; Bedi et al., 2009).

Besides, a number of cytokines serve as proliferation and differentiation factors of neutrophil and monocyte production and, moreover, cover the requirements for increased cell demand. These glycoprotein growth factors are referred to as colony-stimulating factors (CSF), among them interleukin 3 (IL-3, also called multi-CSF), IL-6, granulocyte-macrophage CSF (GM-CSF), granulocyte CSF (G-CSF) and macrophage CSF (M-CSF) (Welte et al., 1985; Wong et al., 1985). While multi-CSF and GM-CSF stimulate immature cells of both cell lines, namely granulocytes and monocytes, G-CSF and M-CSF influence more mature progenitor cells only on the corresponding cell lineage and thus occur later during maturation (Metcalf, 1989; Sieff, 1987). Thus, G-CSF plays an important role in the steady-state neutrophil production. It is also known to be responsible for the mobilization of neutrophils from the bone marrow into peripheral blood. Another function attributed to G-CSF is to inhibit neutrophil apoptosis and accelerate the neutrophil production (Basu et al., 2002; Haurie et al., 1998; Williams et al., 1990). While the G-CSF levels in healthy donors are usually below the detection limit of < 30 pg/ml, it increases strongly in the case of infections and consequently also induces proliferation under stress conditions (K. Watari et al., 1989).

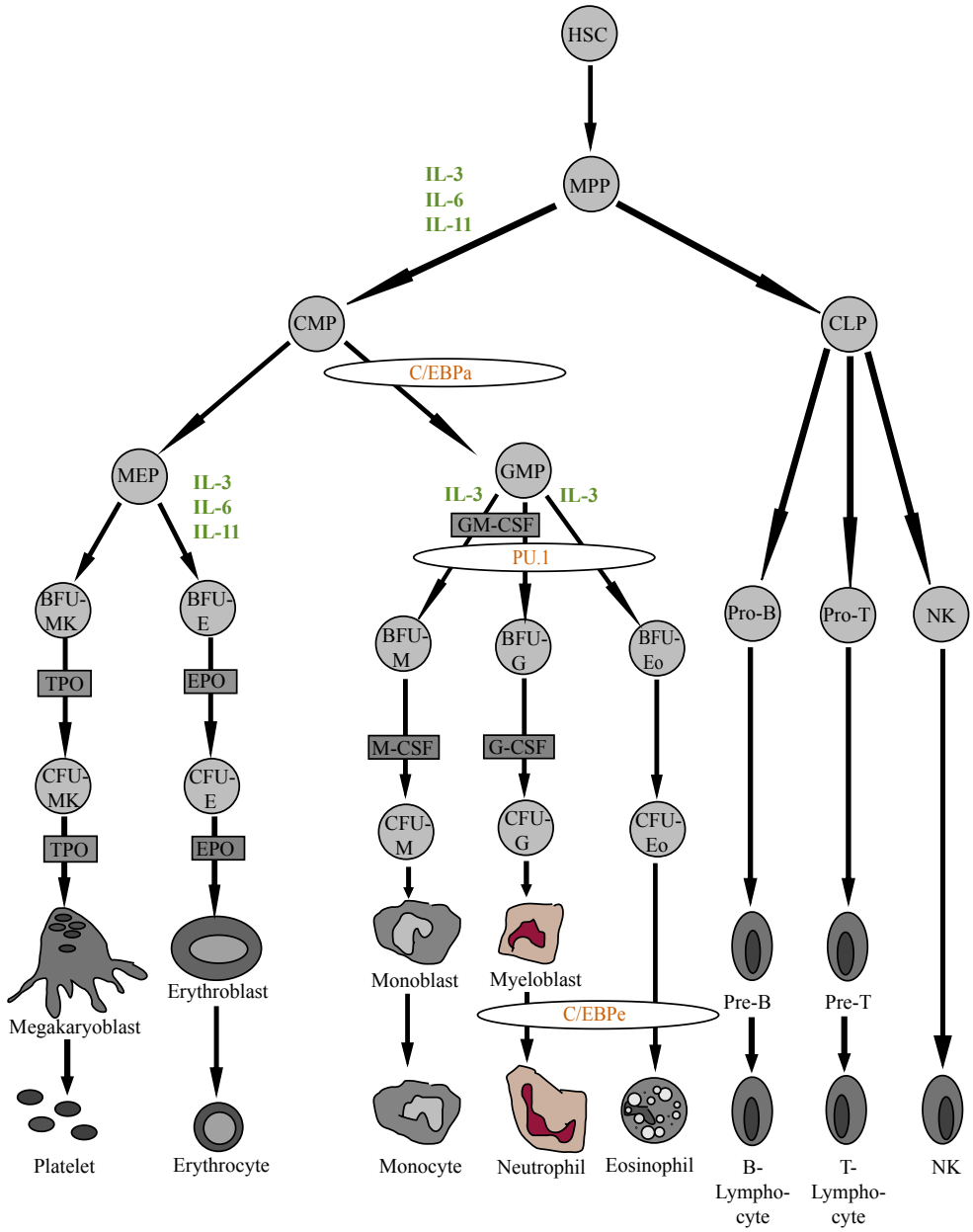

Figure 2: Classical view of the differentiation of hematopoietic cells.
The origin of hematopoiesis is the hematopoietic stem cell, which can differentiate into two different lineages, the myeloid and the lymphoid path. Neutrophils develop out of the granulocyte/macrophage progenitors. The various growth and transcription factors that are necessary for this are represented in this graph. Early-represented hematopoietic growth factors are written in green. Transcription factors are in white round boxes. Growth factors, represented in later steps of hematopoiesis, are shown in little gray boxes: HSC, hematopoietic stem cells; MPP, multipotent progenitors; CMP, common myeloid progenitors; CLP, common lymphoid progenitors; MEP, megakaryocyte/erythroid progenitors; GMP, granulocyte/macrophage progenitors; BFU-MK, burst-forming unit-megakaryocyte; BFU-E, burst-forming unit-erythrocyte; BFU-M, burst-forming unit-monocyte/macrophage; BFU-G, burst-forming unit-granulocyte; BFU-Eo, burst-forming unit-eosinophil; CFU-MK, colony-forming unit-megakaryocytes; CFU-E, colony-forming unit-erythrocyte; CFU-M, colony-forming unit-monocyte/macrophage; CFU-G, colony-forming unit-granulocyte; CFU-Eo, colony-forming unit-eosinophil; TPO, thrombopoietin; EPO, erythropoietin; M-CSF, monocyte/macrophage colony-stimulating factor; G-CSF, granulocyte colony stimulating factor; GM-CSF, granulocyte/(monocyte/macrophage) colony stimulating factor (Modified from Fernández & de Alarcón, 2013; Koschmieder et al., 2005).

1.1.4 Pathophysiology of genetic chronic neutropenia

While the described maturation process leads to a neutrophil count of 1500 to 7500 cells/µl in peripheral blood of healthy adults, gene defects are known to cause different forms of chronic neutropenia (Osgood et al., 1939).

Congenital neutropenia, first mentioned by Kostmann in 1956, describes a group of hematopoietic disorders that are all characterized by diminished absolute neutrophil counts (ANC) (Kostmann, 1956; Welte & Boxer, 1997). On the one hand, non-cycling continuous absolute neutrophil counts (ANC) below 500 cells/µl, which produce the phenotype of severe neutropenia, are summarized as severe congenital neutropenia (SCN). On the other hand, a characteristic pattern of oscillating neutrophil counts, which was already observed in 1910, was delimited from SCN and defined as cyclic neutropenia (CyN) (Donadieu et al., 2011; Skokowa et al., 2017). This historical separation of SCN and CyN was questioned when causative mutations were found in the same gene, elastase - neutrophil expressed gene *(ELANE)*. Since then, a continuum between SCN and CyN has been considered, with CyN being a type of SCN (Dale et al., 2000; Horwitz et al., 1999). The list of genes associated with SCN is growing every year. In 2017, according to Skokowa et al., 29 neutropenia-related genes were counted. These can be sorted according to their type of inheritance. Mutations in five of 29 genes are known to show an autosomal dominant inheritance pattern. The most common gene of this group is *ELANE*, which causes 45% of all SCN cases (Dale et al., 2000; Horwitz et al., 1999). Among the 19 mutated, autosomal-recessive inherited genes are the HCLS1-associated protein X-1 gene (*HAX1*), causing 7% of the SCN cases, and the glucose 6 phosphatase catalytic 3 gene (*G6PC3*), associated with 2% of all SCN patients (Klein et al., 2007; Boztug et al., 2009). Besides, mixed autosomal inheritance, X-linked and mitochondrial DNA inheritance are published. This thesis focuses on CyN cases with mutations in *ELANE* (Donadieu et al., 2011; Skokowa et al., 2017).

Due to the permanently low ANC, SCN shows clinical signs of persistent severe bacterial and fungal infections. The symptoms already appear in early infancy, making therapy with filgrastim (recombinant human granulocyte colony-stimulating factor [r-metHuG-CSF]; Neupogen, Amgen, Thousand Oaks, CA) essential (Bonilla et al., 1989).

CyN, as a subtype of SCN, was first described in 1910 with recurrent furunculosis, fever, and an atypical blood picture (Leale, 1910). It is an autosomal dominant inherited disorder that commonly also appears sporadically from new germline mutations (Horwitz et al., 1999; Morley et al., 1967). Similarly to SCN, most cases of CyN are the consequence of heterozygous mutations in *ELANE*. SCN is actually associated with *ELANE* mutations in 35-63% and CyN in 80-100% of cases. (Boxer & Newburger, 2007; Dale et al., 2000; Newburger et al., 2010). In contrast to typical SCN, CyN shows a cycling periodical pattern of ANC ranging between less than 200 cells/µl and near-physiological values. As a consequence of the recurring recovery of ANC, CyN appears in a milder clinical severity, and thus, lower doses of G-CSF treatment are required than in typical SCN (further information in Chapter 1.2) (Hammond et al., 1989; Leale, 1910; Skokowa et al., 2017; Welte et al., 2006).

The *ELANE* gene is located on chromosome 19p.13.3. Mutations occur especially on intron 4 and exon 5 of the *ELANE* gene, while exons 2, 3 and 4, as well as intron 3, may also be affected. At this point, more than 200 mutations in the *ELANE* gene have been reported (Horwitz et al., 1999; Makaryan et al., 2015). Interestingly, there is an overlap of *ELANE* mutations that can be detected in SCN as well as in CyN patients (Figure 3).

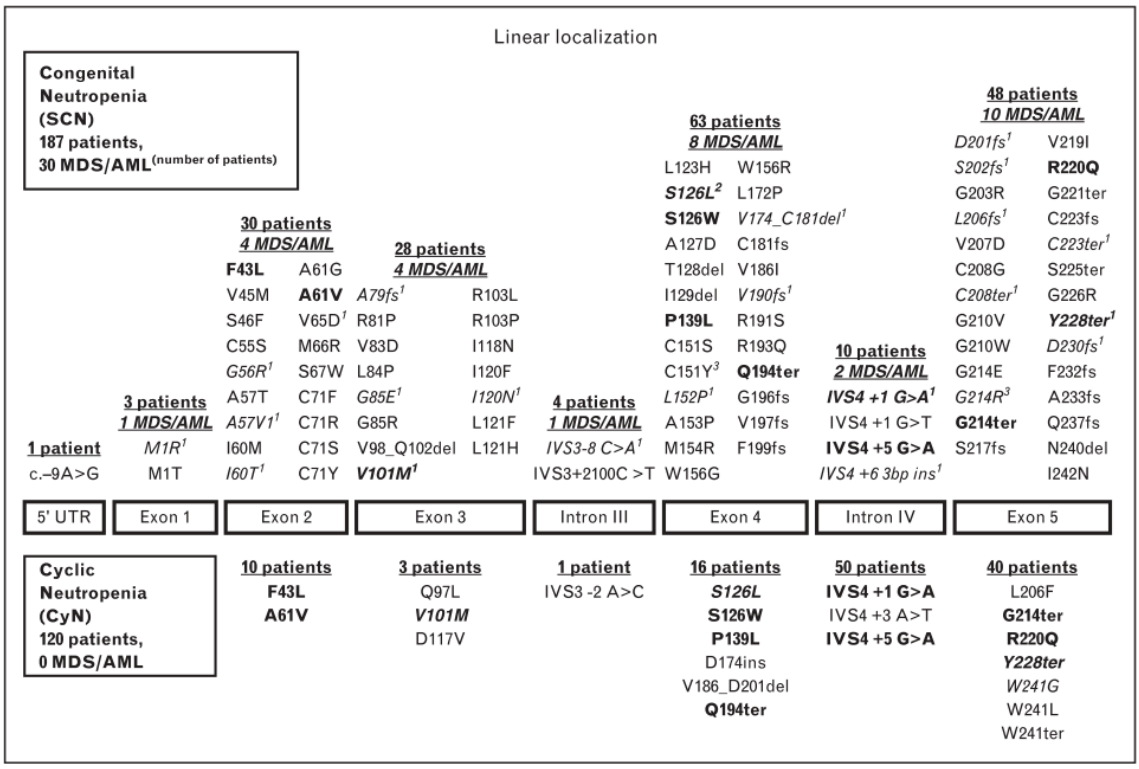

Figure 3: *ELANE* mutations in SCN and CyN patients.
The various *ELANE* mutations with their respective gene locations of in a total 307 patients are indicated in a linear representation, showing 120 CyN cases in the lower part and 187 SCN cases above. Mutations that could be detected in both neutropenia forms are indicated in bold. Reported cases of neutropenic patients who developed myelodysplasia or acute myeloid leukemia are presented: AML, acute myeloid leukemia; CyN, cyclic neutropenia; MDS, myelodysplasia; SCN, severe congenital neutropenia (Makaryan et al., 2015).

The cytotoxic serine protease ELANE is expressed in the promyelocyte and myelocyte stages. Being stored as a part of the innate immune system in the azurophil granules of the neutrophils, it is, among others, involved in the identification and degradation of microorganisms (Borregaard & Cowland, 1997; Dale et al., 2000; Germeshausen et al., 2013; Ohlsson & Odsson, 1974; Spicer & Hardin, 1969). The precise pathomechanism how *ELANE* mutations induce neutropenia is not yet understood. However, several explanations have been made, one of which describes the cause of the elastase misfolding. Misfolded elastase induces stress in the endoplasmic reticulum and activates an unfolded protein response, which in turn leads to cell apoptosis and cell arrest of granulopoiesis (Grenda et al., 2007; Köllner et al., 2006).

Moreover, the effects of the *ELANE* mutations are visible on the bone marrow level. There, SCN is associated with a maturation arrest of granulocyte differentiation at the promyelocyte stage, continuously in case of SCN, whereas a fluctuating cell production

can be examined in CyN (Figure 4). In turn, an increased amount of promyelocytes is observed in the bone marrow. However, the number of matured neutrophils in peripheral blood appear to be reduced, which causes an elevated risk of bacterial and fungal infections in SCN and CyN. (Klein, 2011; Dale & Hammond, 1988; Welte et al., 2006; Wriedt et al., 1970).

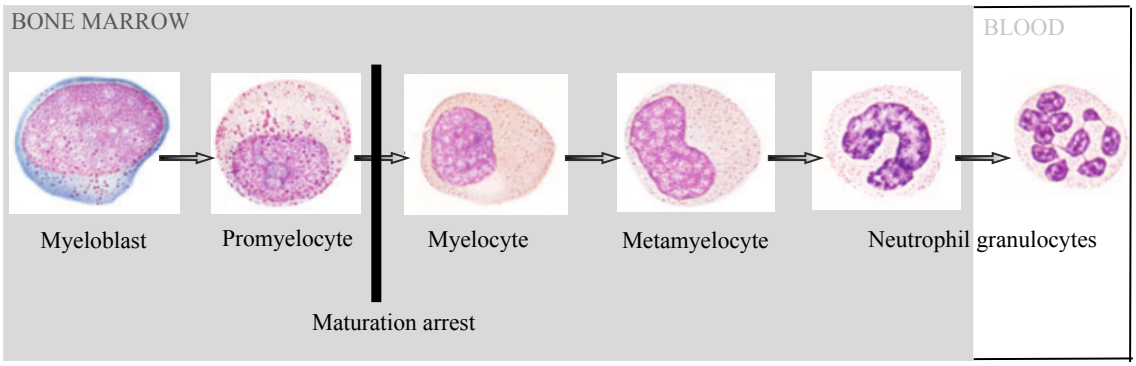

Figure 4: Maturation arrest of the myeloid cells in CyN and SCN.
(Modified from Klein, 2011; Dale & Hammond, 1988).

While the neutrophils periodically cyclize in CyN as a result of the maturation arrest at the cycle nadir, other blood cells are known to show oscillating counts with the same cycle duration as neutrophils. First, monocyte counts may fluctuate in the opposite direction compared to neutrophils. Nevertheless, monocytosis can often be diagnosed by the time cycle. Next, platelet counts peak at the end of neutrophil recovery. Finally, reticulocyte counts reach their highest levels at the neutrophil nadir, and oscillating lymphocytes can also be registered (Guerry et al., 1973; Hammond et al., 1989; Wright et al., 1981).

1.2 Clinical information about CyN

1.2.1 Definition

CyN is characterized by a regular periodic oscillation of peripheral blood neutrophils in an average 21-day rhythm. Characteristically, the ANC drops to a nadir of fewer than 200 neutrophils per µl and does not increase much higher than 2000 neutrophils per µl at the cycle peak (Dale et al., 2000; Dale & Hammond, 1988).

1.2.2 Epidemiology and etiology

The incidence of CyN ranges between 0.5 and 1 patient per million population (Orkin et al., 2014). As described in Chapter 1.1.4, CyN is an autosomal dominant inherited or sporadically appearing disorder that is generally due to a gene mutation in *ELANE*. The reason how this mutation leads to the typical cycling ANC remains unclear (Horwitz et al., 1999; Morley et al., 1967).

1.2.3 Clinical symptoms

At the cycle nadir, which usually lasts three to six days, the untreated patients usually present with a typical symptom complex, which varies, however, from patient to patient and from cycle to cycle. Characteristically, CyN patients have fungal and bacterial infections triggered by the diminished neutropenic host defense. In contrast, viral or parasitic infections are not part of the typical appearance, as they are not affected by the neutrophil count. The cardinal symptoms during the neutropenic stage are various types of purulent inflammations, caused especially by Staphylococcus aureus and gram-negative bacteria. Among them, furunculosis and cellulitis, abscesses, pneumonia, otitis media, stomatitis, gingivitis and periodontitis. In the first period of dropping neutrophil counts, the patients develop anorexia and malaise. Myalgia, headache, mouth ulcers and pharyngitis appear at the time the ANC reaches its nadir. Fever and cervical lymphadenopathy occur next. Once the ANC exceeds 500/µl, the patients are in general clinically silent except for chronic persistent gingivitis and periodontitis (Dale & Hammond, 1988; Leale, 1910). The symptoms generally appear in the first year after birth and occasionally show an improvement in early adulthood based on an increase of neutrophils at the cycle nadir. While the clinical appearances listed above are all cardinal symptoms of CyN, there are sporadically more serious, life-threatening complications. These range from intestinal perforation with peritonitis, necrotizing enterocolitis, mastoiditis, pneumonia, and Clostridium or Escherichia coli sepsis (Wright et al., 1981; Dale, 2002).

1.2.4 Diagnosis

A reliable diagnosis of CyN, besides the clinical appearance, requires an ANC measurement at least three times a week for a total of six to eight weeks. In this way, ANC nadirs should be detected at levels lower than 200 neutrophils per µl. It should be noted, however, that less than 5% of the patients are known to show variable patterns, depending on the cycle duration or the amplitude of oscillations. Additionally, oscillations of other cells such as lymphocytes, eosinophils and platelets may increase suspicion. The examination of bone marrow aspirate is often helpful in proving the diagnosis. Thus, the neutrophil maturation arrest at the promyelocyte or myelocyte stage could be detectable during the cycle nadir as compared to the normal neutrophil formation at the remainder of the cycle. Finally, the clinically-based diagnosis can be confirmed by sequencing the *ELANE* gene (Dale et al., 2003; Dale, 2002).

1.2.5 Therapy

Prior to the introduction of treatment with G-CSF, there was no known long-term management that would improve the prognosis of CyN effectively. The conventional approaches have been to diminish acute clinical symptoms by antibiotic treatment, glucocorticosteroids, gamma globulin infusions or other methods. The only successful therapy to cure CyN was bone marrow transplantation. Finally, in 1987, clinical trials were initiated that confirmed that G-CSF led to a selective increase of neutrophil production. Since then, it is known as the gold standard for CyN and SCN treatment with the best benefits for patient health (Cottle et al., 2002; Hammond et al., 1989; Rappeport et al., 1980). As a stimulator of myeloid proliferation and maturation, G-CSF induces an approximately 16-fold increase in ANCs in CyN patients (Dale et al., 1993). At the bone marrow level, an increased percentage of polymorphonuclear leukocytes (PMNs), as well as an increased count of postmitotic neutrophils, demonstrated increased neutrophil production. Thus, G-CSF treatment decreases the risk and frequency of oropharyngeal inflammation, fever and bacterial infections. As the cycle amplitude increases, the cycle length decreases from about 21 to 14 days (Hammond et al., 1989; Dale et al., 1993). Applied subcutaneously once a day, the dose ranges from 0.0 - 11.2 µg/kg/day with a median dose of 2.1 µg/kg/day for CyN patients. G-CSF is generally well tolerated for

long-term treatment, showing a relatively low number of side effects. Among them, bone pain and splenomegaly appear predominantly at the beginning of therapy and usually resolve spontaneously. In very few cases, osteoporosis, thrombocytopenia, vasculitis and proteinuria were observed (Cottle et al., 2002; Makaryan et al., 2015).

1.2.6 Prognosis and risks associated with CyN

While SCN is known to be a preleukemic bone marrow failure syndrome, CyN has long been known as a benign disease (Gilman et al., 1970; Skokowa et al., 2014). Approximately 20% of SCN patients develop myelodysplastic syndrome (MDS) or acute myeloid leukemia (AML) after 20 years. Eighty percent of those who develop AML are heterozygous for the acquired mutation of the colony stimulating factor 3 receptor gene *(CSF3R)*. Thus, an association of *CSF3R* mutation with leukemogenesis can be expected. However, recent investigations have shown that *CSF3R* mutation itself is not entirely sufficient for leukemic transformation. Rather, it is considered an initial driver of AML development and only induces leukemogenesis in cooperation with mutations in the Runt-related transcription factor 1 gene (*RUNX1)* (Cho & Jeon, 2014; Rosenberg et al., 2006; Rosenberg et al., 2010; Touw, 2015). The combination of *RUNX1* mutations and *CSF3R* mutations could be found in > 65% of SCN patients suffering from MDS/AML. *CSF3R* and *RUNX1* are consequently considered as combined drivers of leukemogenesis. In contrast, until 2016 CyN was predicted to be a disease with no risk of leukemic transformation (Klimiankou et al., 2016; Skokowa et al., 2014).

2 Aim

SCN and CyN are considered as two related immunodeficiency diseases with similar clinical symptoms and overlapping heterozygous mutations in *ELANE*. However, they can be distinguished from each other by examining the severity and length of infectious diseases as well as the ANC counts. While SCN patients show a constant low level of neutrophils below 500 cells/µl, CyN patients are known to have a cycling count of neutrophils (Donadieu et al., 2011; Horwitz et al., 1999; Kostmann, 1956; Leale, 1910).

It is still completely unclear which factors are responsible for the different ANC intervals and the cycling ANC in CyN patients. Within the framework of this poorly understood phenomenon, this work examines the gene expression of a CyN index patient using qPCR. The genes of interest included neutrophil granule proteins, the nicotinamide phosphoribosyltransferase gene (*NAMPT*) and the transferrin receptor gene (*TFRC*). Thereby, the gene expressions at the ANC cycle nadir and peak were compared to each other. This experiment aims to prove the hypothesis of a feedback regulation of neutrophil counts. Accordingly, the fluctuating ANC might be induced by a negative feedback loop and thus is reflected in an opposite oscillation of neutrophil proteins. With minimal ANC, neutrophil production and protein gene expression might be boosted. In contrast, granulopoiesis seems to be downregulated in CyN at the ANC peak. The elucidation of this principle could contribute to the fundamental understanding of CyN and, in the long term, lead to the development of new therapeutic approaches.

Furthermore, the two forms of neutropenia could be distinguished by their propensity to develop leukemia (Chapter 1.2.6). SCN is known to be associated with MDS and AML. Especially, acquired mutations in *CSF3R* and *RUNX1* contribute to leukemic progression. On the other hand, CyN was known as a benign disease (Skokowa et al., 2014). In 2016, however, Klimiankou et al. screened CyN patients for acquired *CSF3R* mutations using deep sequencing and identified one patient with the *CSF3R* mutation. Three years after the CSF3R acquisition, the *RUNX1* mutation could be found in this patient and AML was diagnosed. With this in mind, a group of CyN patients was examined to detect the preleukemic *CSF3R* mutation prematurely (Klimiankou et al., 2016). This screening

aimed to identify those patients at risk of developing MDS, and if necessary, to provide them with regular follow-up monitoring.

3 Probands, materials and methods

3.1 Proband samples

In total, six patients suffering from CyN were examined. All of them are registered in the *Severe Chronic Neutropenia International Registry* (SCNIR) and diagnosed with CyN showing an approximately 21-day oscillating pattern and having a mutation at different positions of the gene *ELANE* (Table 1). As a comparison to CyN subjects, six healthy donor controls were used. Bone marrow samples were isolated by sterile puncture through the pelvis bone at the *Universitätsklinikum Tübingen*. All patients signed informed consent forms to take part in this study.

3.1.1 Selection of CyN patients

The first aim of this research was to broaden current knowledge of trigger mechanisms leading to neutrophil oscillations in CyN patients (Chapter 4.1). To shed light on this question, samples of five CyN patients were examined, namely CyN patients 1-5 (Table 1). The patient cohort was selected according to the criteria of a diagnosed CyN, the existence of the cell fraction of interest and the sampling date. Only those samples were integrated that were taken at the time of the neutrophil peak corresponding to the cycle maximum or those at the neutrophil nadir. In this way, a direct comparison of gene expressions between the two cycle time points could be drawn. The investigated cell fractions were $CD33^+$ and $CD34^+38^+$.

For the second research aspect, *CSF3R* mutations in CyN patients (Chapter 4.2), CyN patients 4 and 6 were included (Table 1).

Table 1: Patient data with appropriate *ELANE* mutation.

CyN patient	Year of birth	*ELANE* mutation	Sample material	
			Cell lineage	ANC/µl
CyN patient 1	1978	NP_001963.1:p.Trp241Cys	$CD34^+38^+$	3.200 (MIN↓)
			$CD33^+$	3.200 (MIN↓)
			$CD34^+38^+$	9.100 (MAX)
			$CD33^+$	9.100 (MAX)
CyN patient 2	1963	NP_001963.1:p.Val190_Phe199del	$CD34^+38^+$	1.200 (MIN↑)
CyN patient 3	1989	NP_001963.1:p.Val190_Phe199del	$CD34^+38^+$	2.000 (MIN↑)
CyN patient 4	2000	NP_001963.1:p.Val190_Phe199del	$CD34^+38^+$	23.400 (MAX)
			$CD33^+$	17.700 (MAX)
CyN patient 5	1992	NP_001963.1:p.Arg220Gln	$CD34^+38^+$	6.900 (MAX)
			$CD33^+$	6.900 (MAX)
CyN patient 6	1997	NP_001963.1:p.Ala233Pro NP_001963.1:p.Val235TrpfsX5 Two mutations were found on the same allele.		

Table 1 shows the data of the CyN patients included in this research work. Besides, their *ELANE* mutation, the isolated cell lineage, and the ANC/µl measured at the sample collection day are described. Whether the ANC is equivalent to the maximum or minimum of the neutrophil cycle is written in brackets. ANC, absolute neutrophil count; CyN, cyclic neutropenia; MAX, maximum; MIN, minimum; (MIN↓), shortly before cycle minimum, ANC still decreasing; (MIN↑), shortly after the cycle minimum, ANC increasing again.

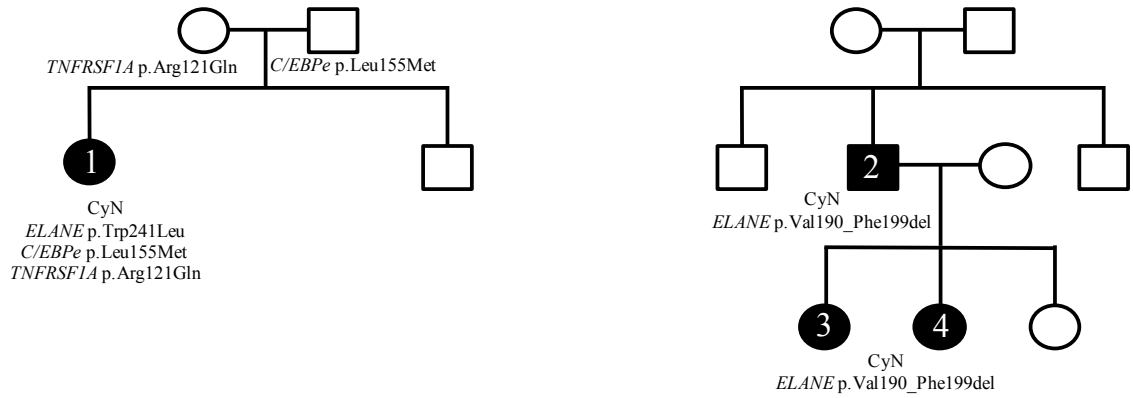

Figure 5: Family trees of examined CyN patients.
The family tree of CyN patient 1 is indicated on the left and of CyN patients 2, 3 and 4 on the right side. Affected CyN patients are symbolized in black and numbered in the form of a white cipher according to Table 1. The corresponding mutations are indicated below each patient. CyN; cyclic neutropenia.

Two family cases of CyN were included in this study (Figure 5). First, CyN patient 1 is presented with the sporadically appearing *ELANE* mutation and the TNF receptor superfamily member 1A gene (*TNFRSF1A*) mutation inherited from the mother, while the *C/EBPe* mutation is inherited from the father. In addition, the second family case of CyN includes CyN patients 2, 3 and 4, concerning a parent with his two female offspring, all bearing the same *ELANE* mutation, which was autosomal dominantly inherited (Table 1). Figure 6 presents ANC courses collected by the SCNIR. For CyN patient 1, the ANC at the two time points of sample collection is depicted. The courses of CyN patients 3 and 4 represent exemplary neutrophil oscillations.

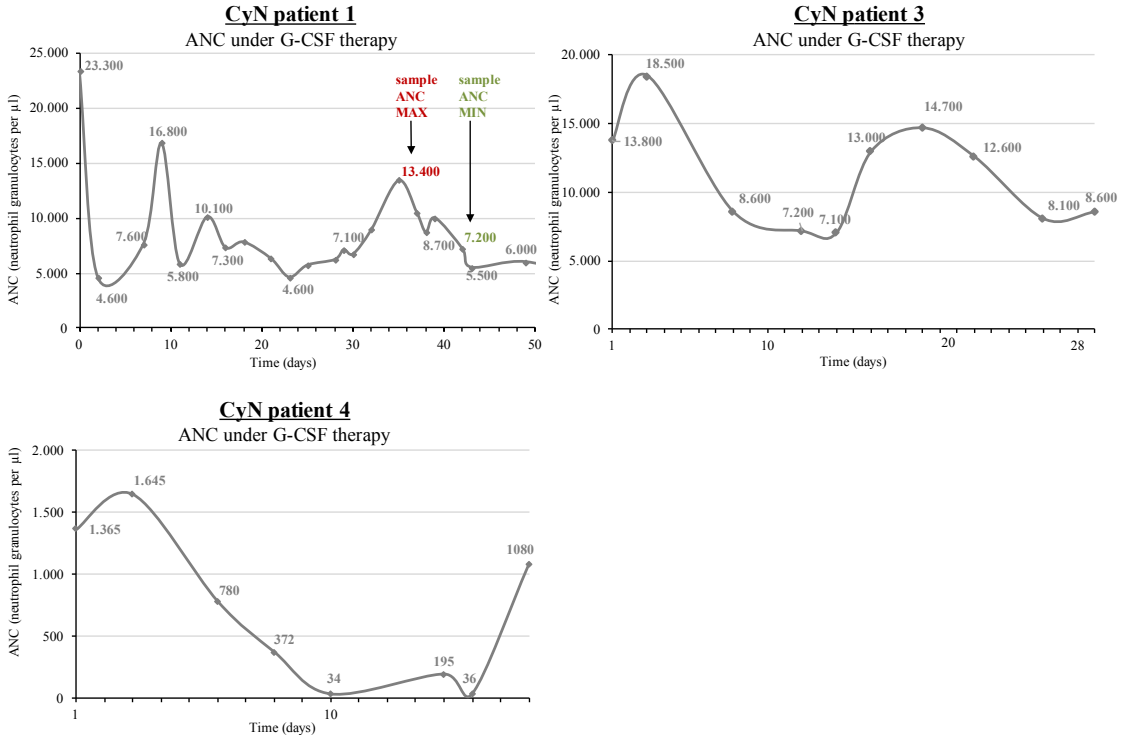

Figure 6: ANC courses of CyN patients 1, 3 and 4.
In the case of CyN patients 3 and 4, a representative ANC is illustrated. The graph, picturing the ANC course of CyN patient 1 shows the two points colored in red and green indicating the time and the corresponding ANC when the samples used for this research were obtained. ANC, absolute neutrophil count; CyN, cyclic neutropenia; G-CSF, granulocyte colony-stimulating factor; MAX, maximum; MIN, minimum (data have been kindly made available by Dr. C. Zeidler, Medizinische Hochschule Hannover).

3.2 Materials

3.2.1 Chemicals

3.2.1.1 Standard chemicals

Table 2: Standard chemicals.

Chemical	Company, headquarter, country
0.5% PFA FACS fixation	Sigma Aldrich, St. Louis, USA
1% BSA	Sigma Aldrich, St. Louis, USA
2-Mercaptoethanol 98%	Sigma Aldrich, St. Louis, USA
3% Acetic Acid with Methylene Blue	Stem cell Technologies, Vancouver, Canada
5x Colorless GoTaq Flexi Buffer	Promega, Fitchburg, USA
5x Green GoTaq Flexi Buffer	Promega, Fitchburg, USA
6x DNA Loading Dye	Thermo Fisher Scientific, Waltham, USA
AccuGene 10x TBE Buffer	Lonza, Basel, Switzerland
Agencourt RNAClean XP Beads	Roche, Basel, Switzerland
Ampicillin sodium salt	Roth, Karlsruhe, Germany
Ampuwa ddH2O	Fresenius, Homburg, Germany
Anti-Biotin MicroBeads, isotype: mouse IgG1	Miltenyi Biotec, Auburn, USA
Bromophenol blue	Sigma Aldrich, St. Louis, USA
CD33 MicroBeads, human, isotype: mouse IgG1	
CD34 MicroBeads, human, isotype: mouse IgG1	Miltenyi Biotec, Auburn, USA
CD38-Biotin MicroBeads, human, isotype: mouse IgG2a	Miltenyi Biotec, Auburn, USA
CutSmart Buffer	New England Biolabs, Hitchin, UK
DMSO	Sigma Aldrich, St. Louis, USA
Ethanol absolute 100%, AnalaR NORMAPUR	VWR Prolabo Chemicals, Radnor, USA
FcR Blocking Reagent	Miltenyi Biotec, Auburn, USA
FCS, inactivated	Sigma Aldrich, St. Louis, USA
Ficoll-Paque-Plus	GE Healthcare Life Sciences, Chalfont St. Giles, UK
GelRed Nucleic Acid Gel Stain	Biotium, Hayward, USA
Glycerol	Fluka, St. Gallen, Switzerland
GoTaq Hot Start Polymerase	Promega, Fitchburg, USA
HCL 2N	Roth, Karlsruhe, Germany

HCL 32%	Roth, Karlsruhe, Germany
Human CD33 MicroBead Kit	Miltenyi Biotec, Auburn, USA
KCl 0.6 M	Carl Roth, Karlsruhe, Germany
LightCycler 480 SYBR Green I Master	Roche, Basel, Switzerland
MACS buffer	Miltenyi Biotec, Auburn, USA
Methanol	Roth, Karlsruhe, Germany
MgCl2 25mM	Promega, Fitchburg, USA
MultiSort Release Reagent	Miltenyi Biotec, Auburn, USA
MultiSort Stop Reagent	Miltenyi Biotec, Auburn, USA
NaCl	Roth, Karlsruhe, Germany
NaOH	Merck Millipore, Billerica, USA
NEB PCR Cloning Kit	New England Biolabs, Hitchin, UK
Omniscript RT Kit (200)	Qiagen, Hilden, Germany
Ovation Pico WTA System 2 (Kit)	NuGEN, San Carlos, USA
PBS buffer	Lonza, Basel, Switzerland
PCR Nucleotide Mix	Roche, Basel, Switzerland
QIAquick PCR Purification Kit (250)	Qiagen, Hilden, Germany
Qubit dsDNA HS Assay Kit	Thermo Scientific, Waltham, USA
RLT buffer	Qiagen, Hilden, Germany
RNase-Free DNase Set	Qiagen, Hilden, Germany
RNase-Free Water	Qiagen, Hilden, Germany
RNeasy Micro Kit	Qiagen, Hilden, Germany
RNeasy Mini Kit	Qiagen, Hilden, Germany
SDS	Roth, Karlsruhe, Germany
SeaKem LE Agarose	Lonza, Basel, Switzerland
Tris Base 0.5M, pH 6.8	Roth, Karlsruhe, Germany

3.2.1.2 Media

Table 3: Media.

Media	Company, headquarter, country
Agar Agar Kobe I	Roth
LB-Medium (Luria/Miller)	New England Biolabs, Hitchin, UK
SOC Outgrowth Medium	New England Biolabs, Hitchin, UK

LB-Agar-Ampicillin Medium

200 ml LB-Medium

3 g Agar

200 µl Ampicillin (final concentration: 100 µg/ml)

3.2.1.3 Primers

The primers for qPCR were selected from Harvard Medical School's PrimerBank database (Wang et al., 2012) and rechecked by NCBI Primer-Blast (Ye et al., 2012) for their specificity. They were synthesized by Eurofins Genomics (Ebersberg, Germany) and aliquoted in concentrations of 100 µg/ml before being stored at -20 °C.

Table 4: Primers for qPCR.

Gene of interest	Primer sequence (5' → 3')	Product length	Melting temperature
cebpε_qF1	TCCATTGACCTCTCCGCCTA	72	60.03
cebpε_qR1	TGGCTTCACGGCAAAGAGAT		59.96
DEFA4_qF1	TCTTCAGGTTTCAGGCTCAACA	93	59.83
DEFA4_qR1	ATGAGGCAGTTCCCAACACG		60.61
ELA2_qF	GGCTCTACCCCGATGCCT	69	60.84
ELA2_qR	AGCGTTGGATGATAGAGTCGATC		60.06
h beta-actin_qF	TTCCTGGGCATGGAGTC	84	55.57
h beta-actin_qR	CAGGTCTTTGCGGATGTC		55.79
hCEBPE C-term F	CCCTTACACAAGGGCAAGAA	153	57.71
hCEBPE C-term R	CTCTGCCATGTACTCCAGCA		59.46
hCEBPE N-term F	TCTCCGCCTACATCGAGTCT	163	59.82
hCEBPE N-term R	CCGAAGGTATGTGGAGGGTA		58.22
HSLPI_qF	TCTCAGCCATCCACCCAGAC	142	61.27
HSLPI_qR	TCACCTTGCCTTTGGCCTC		60.23
LCN2_qF1	ACCCTCTACGGGAGAACCAA	82	59.88
LCN2_qR1	CAGGGAGGCCCAGAGATTTG		60.11
MMP8_qF1	AGCCAGGAGGGGTAGAGTTT	145	59.88
MMP8_qR1	TCCAGGTAGTCCTGAACAGTTT		58.69
NAMPT_310_qF	AGGGCTTTGTCATTCCCAGA	254	58.92
NAMPT_563_qR	GCCAGCAGTCTCTTGGGAAG		60.68
OLFM4-634_qF	ATTCGCCGAGAAATCGTGG	201	58.32
OLFM4-834_qF	GTAATCCCTACCCCAAGCACC		60.13
qCRISP3_F	TACAGACACAGTAACCCAAAGGA	98	59.03
qCRISP3_R	TGGATTGCTTGTGACCATGAG		58.56
TCN1_qF	CATCCGCCTAAAACCTCTGTT	179	57.9
TCN1_qR	CCGAGCTTACATCTGACAATCTG		60.6
TFRC_qF	GGCTACTTGGGCTATTGTAAAGG	156	60.6
TFRC_qR	CAGTTTCTCCGACAACTTTCTCT		58.9

Table 5: Primers for PCR.

Gene of interest	Primer sequence (5' → 3')	Product length	Melting temperature
CSF3R_RNA4_837-F	GCCCGCCAGTCTGTATCAC	823	60.52
CSF3R_RNA4_837-R	GTCATGGGCTTATGGACCCT		59.15
RUNX1ex3D171N_qF	CCTCAGGTTTGTCGGTCGAA	705	59.97
RUNX1ex3D171N_qR	CAGATCCAACCATCCCCACC		60.11
RUNX1ex3D171N_qF	CCTCAGGTTTGTCGGTCGAA	309	59.97
RUNX1D171N309.R	GGCTGAGGGTTAAAGGCAGT		59.4

Table 6: Primers for reverse transcription.

Primer	Company, headquarters, country
Oligo(dT)18 Primer 100 µM	Thermo Scientific, Waltham, USA
Random Primer Hexamer 100 µM	Thermo Scientific, Waltham, USA

3.2.1.4 Antibodies and isotypes

Table 7: Antibodies and isotypes for FACS.

Antibody and isotype	Company, headquarters, country
APC CD34 (8G12), order number: 345804	BD, Franklin Lakes, USA
APC-Mouse IgG1 k Isotype Control, order number: 555751	BD, Franklin Lakes, USA
PE Mouse Anti-Human CD38, order number: 555460	BD, Franklin Lakes, USA
PE Mouse IgG1, k Isotype Control, order number: 556650	BD, Franklin Lakes, USA

3.2.1.5 Enzymes

Table 8: Enzymes.

Enzymes	Company, headquarters, country
Restriction enzyme BtsCI	New England Biolabs, Hitchin, UK

3.2.1.6 Molecular weight standards

Table 9: Molecular weight standards.

Molecular weight standard	Company, headquarters, country
Gene Ruler 100 bp DNA Ladder	Thermo Scientific, Waltham, USA
Quick-Loading 1 kb DNA Ladder	New England Biolabs, Hitchin, UK

3.2.2 Buffers and standard compositions

AccuGene 10x TBE Buffer

Tris-borate 0.89 M

EDTA (disodium salt) 0.02 M

pH 8.3

FACS Buffer

PBS buffer

1% BSA

MACS Buffer

PBS buffer, pH 7.2

0.5% bovine serum albumin

EDTA 2 mM

3.2.3 Consumables

Table 10: Consumables.

Consumable	Company, headquarters, country
Bacterial cell spreader	Roth, Karlsruhe, Germany
Hemocytometer (C-Chip disposable)	NanoEnTek, Seoul, Korea
LightCycler plate with adhesive seal (96 wells)	Sarstedt, Nümbrecht, Germany
MS- and LS-column	Miltenyi Biotec, Bergisch Gladbach, Germany
Petri Dish 94x16	Greiner Bio-One, Kremsmuenster, Austria
Pipette filter tips:	
- Biosphere plus Filter Tips	Sarstedt, Nümbrecht, Germany

- Filter Tips Safeguard	Peqlab, Erlangen, Germany
- Filter Tip Ultrapoint TipOne	Starlab, Hamburg, Germany
Pre-separation filters 30 µm	Miltenyi Biotec, Bergisch Gladbach, Germany
Reaction tubes:	
- DNA LoBind Tube 0.5, 1.5 ml	Eppendorf, Hamburg, Germany
- PCR tubes 0.2 ml	Starlab, Hamburg, Germany
- Qubit assay tubes	Life technologies, Carlsbad, USA
- Falcon tube 15, 50 ml	Sarstedt, Nümbrecht, Germany
- Polystyrene Round-Bottom Tube	Thermo Fisher Scientific, Waltham, USA

3.2.4 Equipment

Table 11: Equipment.

Equipment	**Company, headquarters, country**
Automatic Ice Flaker Machine (AF 100 AS)	Scotsman, Vernon Hills, USA
Centrifuges:	
- Centrifuge 5424	Eppendorf, Hamburg, Germany
- Crystal 8 Micro Centrifuge	LMS, Brigachtal, Germany
- Megafuge 1.0 R	Heraeus, Hanau, Germany
Erlenmeyer flasks	Th. Geyer, Erlangen, Germany
FACSCanto II Flow Cytometer	BD, Franklin Lakes, USA
Fluorometer (Qubit 2.0)	Life technologies, Carlsbad, USA
Gel electrophoresis equipment	Bio-Rad, Hercules, USA
(Wide Mini-Sub Cell GT Complete Systems)	
Hoods:	
- Safety Workbench LaminAir HB 2448	Heraeus, Hanau, Germany
- Hood Biowizard Golden Line	Kojair, Vilppula, Finland
- Air Clean 600 PCR Workstation	Starlab, Hamburg, Germany
- DNA/RNA UV-Cleaner UVC/T-AR	Biosan, Riga, Lativa
Ice Pan (9l “Magic Touch 2”)	Bel-Art SP Scienceware, Wayne, USA
Incubator (Kelvitron T)	Heraeus, Hanau, Germany
LightCycler 480 (96-well version)	Roche, Basel, Switzerland
Magnet (DynaMag-2)	Thermo Fisher Scientific, Waltham, USA

Microscope (Laborlux S)	Leitz, Wetzlar, Germany
Microwave (Micromat 15-w)	AEG, Nuremberg, Germany
NanoDrop 2000/2000c Spectrophotometer	Thermo Fisher Scientific, Waltham, USA
Pipettes:	
- Pipetus 100-240 V	Hirschmann, Eberstadt, Germany
- Reference variable	Eppendorf, Hamburg, Germany
- Research plus variable	Eppendorf, Hamburg, Germany
- Serological pipette 5, 10, 25 ml	Sarstedt, Nümbrecht, Germany
- Transfer pipette	Sarstedt, Nümbrecht, Germany
Precision balance (EMB)	Kern, Balingen, Germany
Refrigerators	Liebherr, Bulle, Switzerland
Separator	Miltenyi Biotec, Bergisch Gladbach, Germany
(MACS Multi Stand, QuadroMACS Separator)	
Thermocycler (Mastercycler nexus GX2)	Eppendorf, Hamburg, Germany
Thermomixer compact	Eppendorf, Hamburg, Germany
UV transilluminator (Gel iX Imager)	Intas Science Imaging, Göttingen, Germany
Vortex mixer (Genius 3)	IKA, Staufen, Germany

3.2.5 Software

Table 12: Software.

Software	**Company, headquarters, country**
Chromas Pro 1.7.7	Technelysium, South Brisbane, Australia
EazyDraw	EazyDraw, Poynette, USA
FACSCanto II Software	BD Biosciences, Franklin Lakes, USA
FACSDiva	BD Biosciences, Franklin Lakes, USA
FlowJo	Tree Star, Ashland, USA
LightCycler 480 Software release 1.5.0	Roche, Basel, Switzerland
Microsoft Office	Microsoft, Redmond, USA
- Microsoft Word for Mac version 15.19.1	
- Microsoft Excel for Mac version 15.19.1	
- Microsoft PowerPoint for Mac version 15.19.1	
NanoDrop 2000 Software	Thermo Fisher Scientific, Waltham, USA

3.3 Methods

3.3.1 Preparation and quantification of RNA samples

The following two steps, which resulted in separate cell fractions, were performed in cooperation with medical technical assistants.

3.3.1.1 Isolation of MNCs from bone marrow samples

The bone marrow samples were diluted in a ratio of 1:2 with PBS buffer, overlaid on Ficoll-Plaque Plus and centrifuged (25 min, 1600 rpm). Thus, a gradient of the different blood components was obtained, from which the interphase containing mononuclear cells was isolated. Then, the mononuclear cells (MNCs) were washed in two steps with 30 ml 4 °C cold PBS buffer and centrifuged (8 min, 1300 rpm). For the cell counting, the remaining pellet was resuspended in 1-5 ml PBS buffer, mixed with methylene blue in a 1:10 ratio and then pipetted onto a Neubauer chamber. Depending on the cell material of interest (RNA, DNA or proteins), different lysis solutions were added before freezing. To freeze MNCs, a mixture of 900 µl FCS and 100 µl DMSO was added. AllPrep and RNA samples were mixed with 350 µl RLT buffer for up to 5x10^6 cells. To obtain proteins, 20 µl Lämmli buffer was used for approximately 1x10^5 cells. When a special cell fraction, such as $CD33^+$ for example, should be obtained, the magnetic separation protocol was started immediately.

3.3.1.2 Magnetic separation of $CD33^+$ and $CD34^+$ cells

To separate the different cell fractions, the freshly isolated cells were resuspended with MACS buffer and then mixed with the appropriate magnetic beads. For this, the $CD33^+$/$CD34^+$/$CD38^+$ MultiSort Kit protocols of Miltenyi Biotec were used. In the case of the $CD34^+38^+$ fraction, the $CD34^+$ cells were first separated before adding the second $CD38^+$ marker. Corresponding to the MNC isolation protocol, the cell number was counted under the microscope.

3.3.1.3 Detection of isolated cell fractions by FACS

After having isolated a cell lineage of interest by magnetic separation, its percentage was determined by FACS, a method that makes it possible to verify the success of the magnetic bead protocol. The separated cells were evenly distributed to the FACS tubes, which were then filled up to 2 ml with FACS buffer and centrifuged (5 min, 300 g, 4 °C). The corresponding antibodies or isotypes were then added to the cells before being incubated (20 min, 4 °C in the dark). After a washing and centrifugation step, the supernatant was aspirated. Next, 200 µl of 0.5% PFA were added as a cell fixative before the cells were stored at 4 °C. The measurement was performed under standard conditions using the Canto II flow cytometer and analyzed with the software FACSDiva and Flowjo. Unstained cells were used as negative control. The isotypes were then measured to set a gate for the following measurements between negative and positive cells. Both monochrome and multicolored samples were prepared to detect double positive cells. To prevent false positive results due to cell duplicates, these were excluded by gating. Furthermore, a gating step helped to prevent neutrophils from being measured by FACS.

3.3.1.4 Total RNA purification protocol

The total RNA purification protocol was used to isolate RNA from cells lysed in RLT buffer. Depending on the number of cells, two different protocols were used: ≤ 5x10^5 cells - Micro kit and ≤ 5x10^6 cells - Mini kit.

3.3.1.5 Quantification of RNA products by NanoDrop

The NanoDrop spectrophotometer was used to measure RNA concentration. Therefore, 1 µl of RNase-free water served as blank. The samples were also measured in an amount of 1 µl.

3.3.2 Preparation and quantification of cDNA samples

3.3.2.1 Reverse transcription

RNA samples in the range of 500 to 1000 ng were transcribed into cDNA with a low expenditure of time according to the Omniscript Reverse Transcription Kit protocol. First, the master mix 1 was prepared and incubated with program 1 (Table 13 and 14). Next, the master mix 2 was pipetted. After the first incubation step was completed, 9 µl of the master mix 2 was added to the first sample solution and then again incubated with program 2. The completed cDNA was finally stored at -20 °C.

Table 13: Master mixes for reverse transcription.

Master mix	Master mix components	Amount
Master mix 1	Oligo(dT) 18 primer (10 µM)	2 µl
	Random Hexamer Primer (10 µM)	2 µl
	ddH2O-RNA mixture	27 µl
	Total volume	**31 µl**
Master mix 2	10x RT buffer	4 µl
	dNTPs	4 µl
	RT enzyme	1 µl
	Total volume	**9 µl**

Table 14: Thermocycler setup for reverse transcription.

	Temperature	Time
Program 1	70 °C	5 min
Program 2	RT 42 °C 72 °C 4 °C	2 min 60 min 10 min hold

3.3.2.2 WTA Ovation protocol

The Ovation Pico WTA system amplifies cDNA out of a small quantity of RNA. The procedure includes the synthesis of a DNA/RNA heteroduplex double-stranded cDNA, followed by the SPIA amplification (Kurn et al., 2005). The Ovation Pico WTA System V2 protocol starts with the synthesis of first strand cDNA from total RNA. For this purpose, master mix 1 was prepared and incubated with program 1 (Table 15 and 16). Then master mix 2 was mixed, added to mix 1 and incubated with program 2. The result of this step was single cDNA strands with a unique RNA portion at the 5' end. Next, the generation of the second strand of cDNA was started. Master mix 3 was prepared, pipetted into the reaction tube of the first strand cDNA synthesis and then incubated with program 3. Then, the cDNA was purified using magnetic separation. The last step consisted in the SPIA amplification, which relied on the application of chimeric primer, DNA polymerase, and RNase H to finally obtain a strong accumulation of cDNA (Kurn et al., 2005). Master mix 4 was prepared and added to the reaction tube that was incubated with program 4. The tube was then again transferred to the magnet. The cleared supernatant containing SPIA cDNA could finally be collected and purified using the QIAquick PCR Purification Kit.

Table 15: Master mixes for WTA Ovation protocol.

Master mix	Master mix components	Amount
Master mix 1	First Strand Primer Mix	2 µl
	Total RNA sample (500 pg to 50 ng)	5 µl
	Total volume	**7 µl**
Master mix 2	First Strand Buffer Mix	2.5 µl
	First Strand Enzyme (RT)	0.5 µl
	Total volume	**2.5 µl**
Master mix 3	Second Strand Buffer Mix	9.7 µl
	Second Strand Enzyme Mix (DNA polymerase)	0.3 µl
	Total volume	**10 µl**
Master mix 4	SPIA Buffer Mix	50 µl
	SPIA Primer Mix	25 µl
	SPIA Enzyme Mix	25 µl
	Total volume	**100 µl**

Table 16: Thermocycler setup for WTA Ovation protocol.

	Temperature	Time
Program 1	65 °C 4 °C	2 min hold
Program 2	4 °C 25 °C 42 °C 70 °C 4 °C	2 min 30 min 15 min 15 min hold
Program 3	4 °C 25 °C 50 °C 80 °C 4 °C	1 min 10 min 30 min 20 min hold
Program 4	4 °C 47 °C 95 °C 4 °C	1 min 75 min 4 min hold

3.3.2.3 Quantification of cDNA products by Qubit

The cDNA samples were measured by Qubit by mixing 1 µl sample with 1 µl fluorescent dye and 199 µl buffer. After an incubation of 2 min at RT, the tube was transferred to the fluorometer.

3.3.3 Real-time quantitative PCR

Real-time quantitative PCR (qPCR) enables the quantification of amplified PCR products in real time, according to the log phase of accumulation. It shows highly reproducible results, allows a high throughput of samples and provides a broad dynamic range (Heid et al., 1996). This method is intended to measure the expression of different granule protein genes in patient samples. The qPCR uses fluorescent technologies; in this setup, the dye SYBR Green I was used (Fraga et al., 2008). All cDNA dilutions were adjusted to a b-actin average Cp value of 21.5, with b-actin being selected as the reference housekeeping gene. First, master mix 1 was prepared and pipetted into a 96-well plate, followed by centrifugation (Table 17). According to the LightCycler 480 protocol of Roche, the reaction setup of program 1 was used (Table 18). Beside non-template controls used as contamination control, each gene was tested in triplicate (Bustin et al., 2009). The data were finally interpreted and checked for specificity using the LightCycler Software.

The checked data were then transferred to an Excel table to calculate the triplicate's Cp average and the Δ-Cp value (deviation of the target's Cp average to the housekeeping gene's Cp average) (Bustin et al., 2009). Based on this Δ-Cp value, further calculations as ratios could be performed.

Table 17: Master mix 1 for qPCR.

Master mix	**Master mix components**	**Amount**
Master mix 1	SYBR Green 10 mmol	5 µl
	Primer mix (F and R primer)	0.8 µl
	cDNA	4.2 µl
	Total volume	**10 µl**

Table 18: Thermocycler setup for qPCR.

	Temperature	**Time**	**Cycles**
Program 1: (1) Pre-incubation	95 °C	10 min	1x
(2) Amplification - Denaturation - Annealing - Amplification	 95 °C 60 °C 72 °C	 10 sec 10 sec 30 sec	45x
(3) Melting program	95 °C 65 °C	4 sec 1 min	1x
(4) Cooling Program	40 °C	10 sec	1x

3.3.4 PCR

PCR was used to detect the *CSF3R* and *RUNX1* mutations. The PCR products were purified with the QIAquick PCR Purification Kit (250) and further used for restriction digestion or directly sent for Sanger sequencing. The standard master mix used for each PCR reaction and the primer-specific thermocycler installations are shown in Table 19, 20 and 21.

Table 19: Master mix for standard PCR .

Master mix	Master mix components	Amount
PCR master mix (1x)	Green Flexi buffer	4 µl
	25 mM MgCl2	1 µl
	10 mM dNTPs	0.5 µl
	GoTaq polymerase	0.2 µl
	Forward Primer 10 pmol/µl	1 µl
	Reverse Primer 10 pmol/µl	1 µl
	ddH2O	10.3 µl
	Template	2 µl
	Total volume	**20 µl**

Table 20: Thermocycler setup for PCR (CSF3R_NGS5F/R).

CSF3R setup	**Temperature**	**Time**	**Cycles**
	98 °C	30 sec	1x
Denaturation	98 °C	40 sec	30x
Annealing	58 °C	7 sec	30x
Amplification	72 °C	7 sec	30x
	72 °C	5 min	1x
	8 °C	hold	hold

Table 21: Thermocycler setup for PCR (RUNX1ex3D17N_F/RUNX1D171N309.R).

RUNX1 setup	**Temperature**	**Time**	**Cycles**
	95 °C	10 min	1x
Denaturation	95 °C	40 sec	35x
Annealing	63 °C	20 sec	35x
Amplification	72 °C	30 sec	35x
	72 °C	2 min	1x
	8 °C	hold	hold

3.3.5 Restriction digestion of wild type allele sequences

This method served to increase the ratio of acquired, mutated alleles that would otherwise be below the detection limit of Sanger sequencing. The principle is based on a restriction enzyme that binds to a specific nucleotide of a PCR product and cuts the strand into two parts at this position. If the enzyme binds precisely to the nucleotide that is partially mutated, only the wild-type alleles will be cut. The enzyme will not work with the mutated

alleles because there is no binding site for the enzyme due to the change of nucleotide. Next, PCR followed, and only the resistant complete mutated strands were amplified.

In this case, the restriction enzyme BtSCI was used, which binds and cuts the wild type of the *RUNX1* gene (Figure 7). The master mix (Table 22) was prepared and then incubated in the thermocycler (15 min, 300 rpm, 50 °C). To see whether the digestion had worked, a 15 µl sample was pipetted into a 2% agarose gel, where, in the case of a healthy donor sample, two bands were expected. For further examinations, the enzyme in the remaining sample was inactivated at 80 °C for 20 minutes in the thermocycler. After the inactivation, the probes were again amplified by PCR using the same protocol as usual, purified, and then sent for Sanger sequencing.

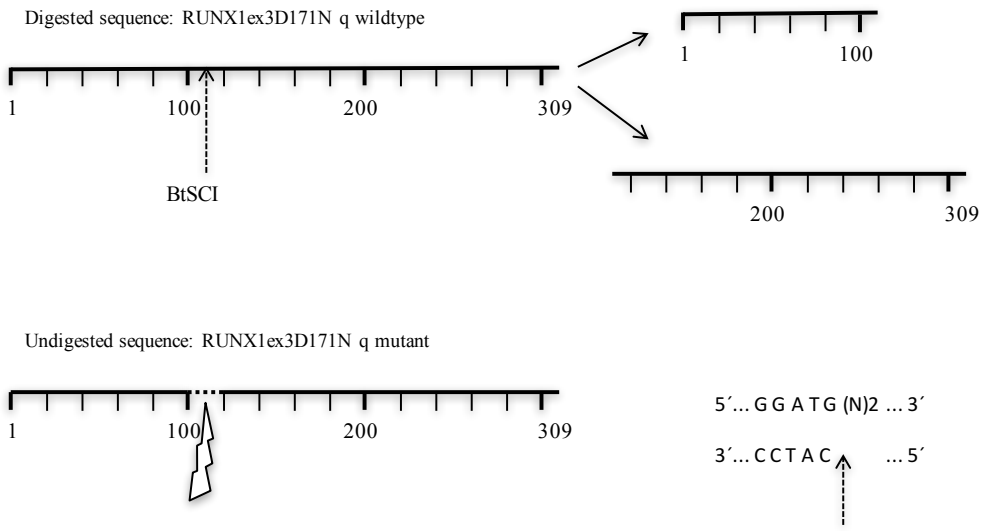

Figure 7: Restriction digestion of *RUNX1* allele by BtSCI enzyme.
While the wild type allele is cut into two pieces, the mutant allele has its mutation exactly at the position where the enzyme would cut and is thereby protected.

Table 22: Master mix for restriction digestion with BtsCI enzyme.

Master mix	Master mix components	Amount
Master mix 1	Restriction enzyme BtsCI	10 units = 1 µl
	DNA (PCR product)	1 µg
	10X CutSmart Buffer	5 µl
	ddH2O	Filled up to total volume of 50 µl
	Total Volume	**50 µl**

3.3.6 Molecular cloning

With the molecular cloning method, patient DNA was ligated in a vector, which was then introduced into the host organisms, which were E. coli bacteria. For this, the gene segment of interest, the *CSF3R* gene, was first worked out by PCR using the CSF3R_RNA4_837 F and CSF3R_RNA4_837 R primers. The PCR product was tested for its specificity by gel electrophoresis, purified with the QIAquick PCR Purification Kit (250) and measured with Qubit. According to the sample concentration, the product was diluted to a final concentration of 6.5 ng/µl. Then the ligation process began, starting with the preparation of the following master mix (Table 23) containing the chemicals of the NEB-PCR Cloning Kit.

Table 23: Master mix for ligation.

Master mix	Master mix components	Amount
Ligation master mix	DNA (PCR product)	4 µl
	Linearized pMiniT Vector	1 µl
	Cloning master mix	2 µl
	Total volume	**7 µl**

This ligation master mix was incubated (15 min at 25 °C and then 2 min on ice). In the meanwhile, the NEB 10-beta Competent E. coli cells stored at -80 °C were thawed on ice. After the incubation time, 2 µl of the completed ligation reaction was added to the competent cells, mixed together and again incubated (25 min on ice). In the following transformation step, the bacteria-ligation mix was heat shocked (30 sec, 42 °C) and then incubated (5 min on ice). Next, 950 µl of SOC medium was added for the outgrowth

process, and the mixture could then be incubated (1 h, 250 rpm, 37 °C) in the thermoblock. In the end, 50 µl of the suspension was spread on an ampicillin LB medium petri dish, which was then incubated (18 h, 37 °C). Afterward, the clones could be picked, and every single one was mixed with 20 µl of ddH2O. Of these, another PCR was performed with the same primers as before under the standard conditions. The PCR product could then be purified with the QIAquick PCR Purification Kit (250) and sent for Sanger sequencing.

3.3.7 Sanger sequencing

With Sanger sequencing, the patient DNA could be examined at the nucleotide level, whereby single nucleotide mutations could be detected with very high specificity. The method was performed by the GATC Sequencing Service offered by GATC Biotech in Konstanz. Two 1.5 µl tubes were prepared, each containing 10 µl of purified PCR product and 0.25 µl of either the forward or the reverse primer. The results were finally analyzed with Chromas Pro 1.7.7.

3.3.8 Gel electrophoresis

Agarose gel electrophoresis was done to check the specificity of qPCR and to confirm the quantitative amount of cDNA amplified by qPCR. This procedure was performed by default with an agarose concentration of 2% in a 1x TBE buffer system. As nucleic acid gel stain, 10 µl of GelRed was used. The samples were stained with 6x DNA loading dye and thickened. As a molecular-weight size marker, 3 µl of a 100 bp ladder was utilized. Subsequently, the samples were separated in their fragments by a constant voltage of 80 V for 50 min. When the run was complete, the bands were visualized by UV transillumination at a wavelength of 312 nm and recorded by a documentation system.

4 Results

4.1 Explanatory approach for neutrophil oscillation in CyN

This chapter is dedicated to the project on the cycling ANC phenomenon in CyN, which constitutes the main difference to SCN.

4.1.1 Neutrophil protein gene expression of a CyN patient in the microarray

A microarray run had been performed by the research group of Prof. Dr. J. Skokowa/Prof. Dr. K. Welte with the samples of a CyN patient, CyN patient 1 (Table 1). In this context, it was found that several granule protein genes, as well as *NAMPT* and *TFRC*, showed an oscillating expression between the cycle peak and nadir of ANC. The hypothesis here is that the ANC course has an inhibitory or excitatory influence on granulopoiesis. To validate the microarray data received from the bone marrow samples of CyN patient 1, alternative methods had to be performed and additional CyN patients examined.

The samples used for this microarray originated from a CyN patient (CyN patient 1) and a healthy donor treated with G-CSF as a control. In both cases, $CD34^{+}38^{-}$ (hematopoietic stem cells, HSC) and $CD33^{+}$ (myeloid progenitor) cells were collected. CD33, CD34 and CD38 are detectable at different points of hematopoietic differentiation and are therefore used to select cells and examine their gene expressions at specific maturity levels (Nielsen & McNagny, 2008). Additionally, in the case of the CyN patient, two samples of each cell line, $CD33^{+}$ and $CD34^{+}38^{-}$, were chosen. Samples were obtained at different times of the ANC cycle. One was obtained at the ANC peak of the patient, and the other was obtained at the ANC nadir (Figures 6 and 8). In this way, gene expressions could be compared over the time of hematopoietic maturation and also over the time of neutrophil oscillation. As those RNA expression oscillations reproduced the patient's ANC oscillations, an induction and cycling of granulopoiesis in stem cells ($CD34^{+}$ $CD38^{-}$) and myeloid progenitors ($CD33^{+}$) was deduced. Finally, candidates were selected from the top list of upregulated/downregulated genes in microarray assays that showed a very low expression at the cycle peak compared to the cycle nadir of the CyN patient 1. These genes of interest were the granule protein genes called cysteine-rich secretory protein 3

(*CRISP3*), defensin alpha 4 (*DEFA4*), elastase - neutrophil expressed (*ELANE*), lipocalin 2 (*LCN2*), matrix metallopeptidase 8 (*MMP8*), olfactomedin 4 (*OLFM4*), secretory leukocyte protease inhibitor (*SLPI*) and transcobalamin 1 (*TCN1*). Additionally, nicotinamide phosphoribosyltransferase gene (*NAMPT*) was analyzed, which induces neutrophil activation, myeloid differentiation and also prevents neutrophil apoptosis (Skokowa et al., 2009). The transferrin receptor gene (*TFRC*) served as a reference gene and is expressed in various cell types (Vorachek et al., 2013).

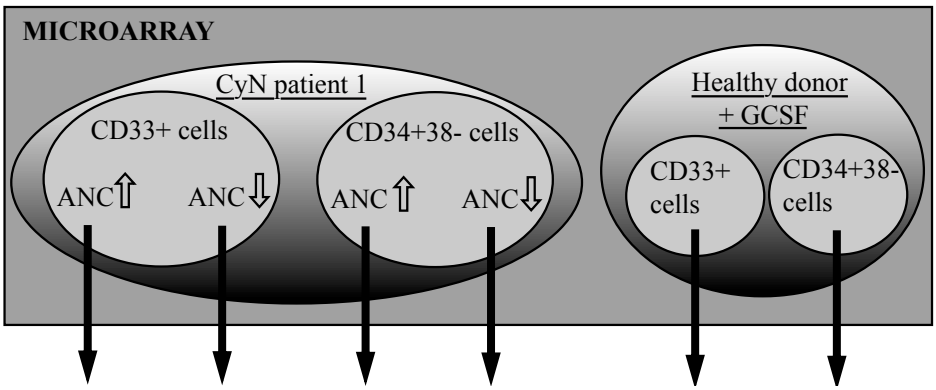

Figure 8: Sample selection for microarray setup.
In total, four samples of CyN patient 1 were chosen. The $CD33^{+}$ and $CD34^{+}38^{-}$ cell populations were processed, from which in both cases two samples were taken (ANC peak and nadir respectively). A healthy donor treated with G-CSF served as a control. From these data, ten genes were selected that all showed a different expression at the ANC peak and nadir of the CyN patient. ANC, absolute neutrophil count; CyN, cyclic neutropenia; G-CSF, Granulocyte colony-stimulating factor.

4.1.2 Validation of microarray data by qPCR

To confirm microarray data, qPCR is usually performed. The validity of microarray data was proven by using the same samples of CyN patient 1 for qPCR. First, the gene expression at the cycle peak was compared to the expression at the cycle nadir in CyN patient 1. Next, CyN patient 1 was compared to healthy donors. The following step was to analyze CyN patient 1 against four other CyN patients. To fulfill the criteria for being included in this study, the additional CyN patient samples had to be obtained at either the ANC peak or the nadir (Table 1). The final step was to compare the four CyN patients to healthy donors (Figure 9).

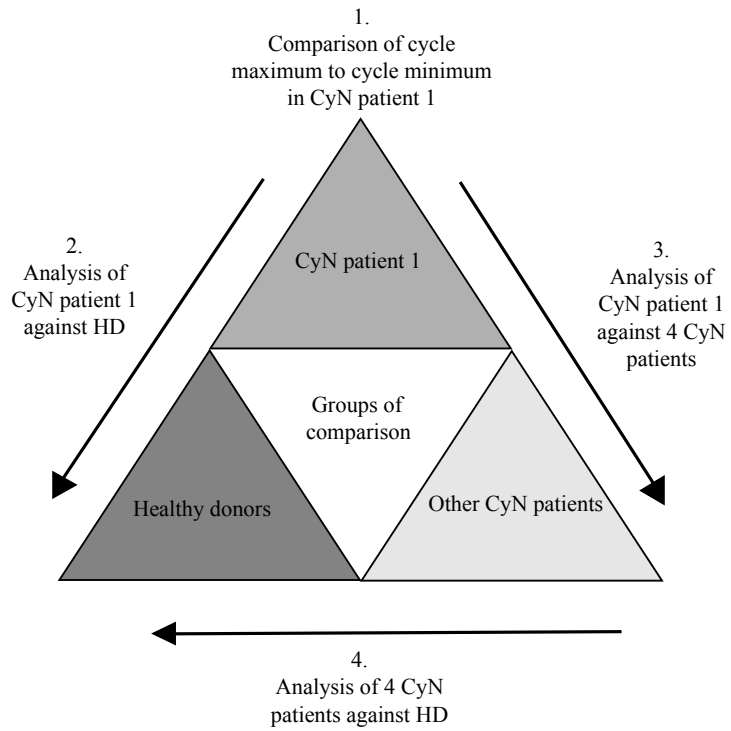

Figure 9: Graphic representation of group of patients and experimental setup.
The scheme represents the order of steps performed by qPCR with the aim to confirm the approach based on the microarray data. The first experiments were performed on the samples of CyN patient 1, which were then correlated with healthy donor samples. Afterward, the results were to be verified by analyzing four additional CyN patients. CyN, cyclic neutropenia; HD, healthy donors.

4.1.2.1 Cycling gene expression pattern in CyN patient 1

First, the cycling gene expression of granule proteins, *NAMPT* and *TFRC* in CyN patient 1, previously detected in the microarray, was verified (Figure 9). Due to the small amount of RNA from the patient's samples, the RNA was amplified using the WTA Ovation protocol (Chapter 3.3.2.2). Consequently, as an intermediate target, the reproducibility of data should be evaluated by using either the WTA Ovation protocol or the usual reverse transcription protocol (Chapter 3.3.2.1). In the case of the $CD33^+$ cells, the same cell populations could be utilized for qPCR. However, the $CD34^+38^-$ cell fraction examined in microarray could not be reevaluated, so $CD34^+38^+$ cells were used instead for qPCR.

The gene expression of eight granule protein genes of interest as well as of *NAMPT* and *TFRC* in $CD33^+$ cells of CyN patient 1 was measured. To correlate the expression of granule protein genes with the ANC in CyN patients, the ratio of the gene expression at

the ANC peak and the expression at the ANC nadir was calculated in each case. This ratio is illustrated as the fold change in the form of a bar graph (Figure 10).

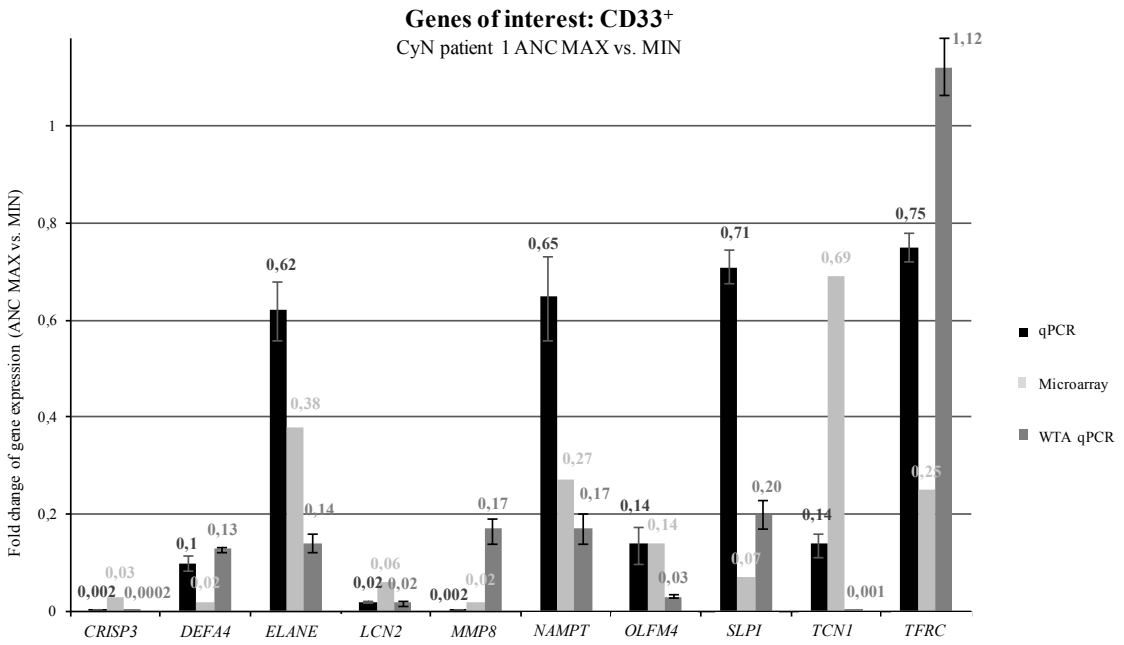

Figure 10: Gene expression in CD33$^+$ cells of CyN patient 1.
The bar graph illustrates the fold changes in gene expression at the ANC maximum compared to the ANC minimum of CyN patient 1 measured by microarray, qPCR and WTA qPCR. MAX, maximum; MIN, minimum; qPCR, real-time quantitative polymerase chain reaction; vs., versus; WTA, whole transcriptome amplification.

First, the RNA expression fold changes from microarray data were confirmed by using qPCR of normal cDNA or qPCR of WTA cDNA for *CRISP3, DEFA4, LCN2, MMP8* and *OLFM4*. The same trend in RNA expression fold changes was observed for *ELANE, NAMPT, SLPI* and *TCN1*. Only the microarray data of *TFRC* could not be reproduced. As a result, WTA samples were used instead of conventional reverse transcription samples for further investigation.

Next, for both methods, WTA qPCR and microarray, a trend could be analyzed for five out of ten genes of interest (Figure 10). Here, the gene expression at the ANC nadir is strikingly higher compared to the ANC maximum. This was detectable in *CRISP3, DEFA4*, *LCN2, MMP8* and *OLFM4*. Whereas, *ELANE, NAMPT, SLPI* and *TCN1* showed the same trend with a higher expression at the cycle nadir compared to the peak in a less remarkable way. The WTA qPCR results showed an increased fold change in gene expression between the ANC minimum and maximum in every tested gene, despite

TFRC. The fold change ranged between 5,000 for *CRISP3* expression and 5.9 for *NAMPT* expression, comparing the cycle nadir to the peak. Only *TFRC* gene expression behaved differently according to the WTA qPCR results. Here, the expression at the ANC maximum had a 1.1-fold increase compared to the minimum (Figure 10).

The five mentioned genes (*CRISP3, DEFA4, LCN2, MMP8* and *OLFM4*), which showed a high reproducibility and a pronounced expression oscillation, are presented in detail (Figure 11). Thereby, the qPCR results of *CRISP3, LCN2* and *OLFM4* were confirmed by gel electrophoresis. In the case of those samples that were obtained at the minimum of ANC, the bright PCR product bands appeared. In contrast, there was no, or rather a weaker, band in the CyN samples at the ANC maximum. A possible method limitation is that the qPCR difference between the ANC maximum and minimum of *DEFA4* and *MMP8* is not large enough to be visualized in gel electrophoresis.

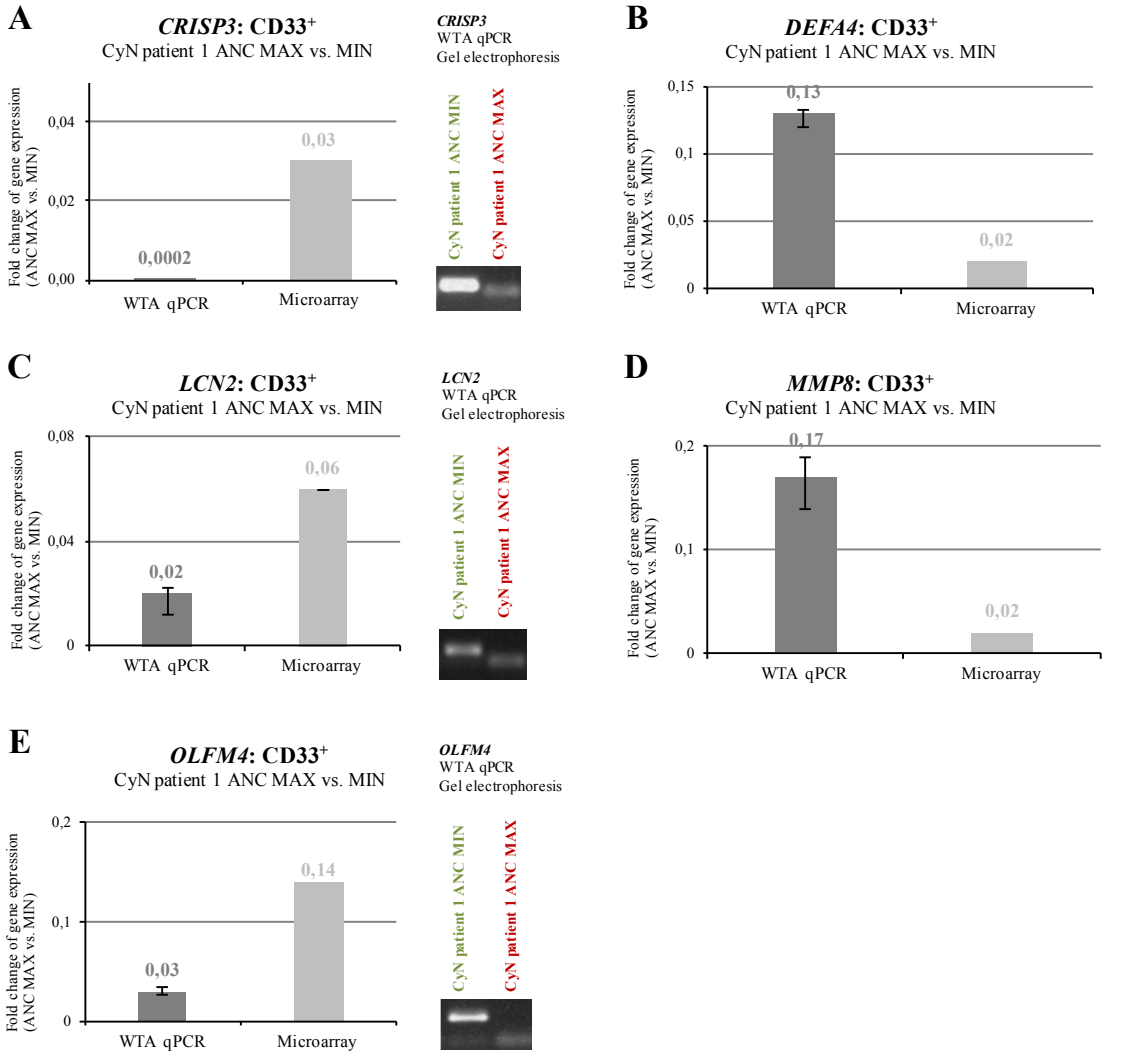

Figure 11: Five oscillating genes of interest in CD33$^+$ cells of CyN patient 1.
This detailed illustration shows the fold change difference in the expression of five granule protein genes with a high expression oscillation in CD33$^+$ cells of CyN patient 1. The bars in dark gray represent the fold change in the expression at the ANC maximum compared to the ANC minimum in qPCR data, while the bars in light gray represent the fold change in microarray data. At the right of three bar graphs, gel electrophoresis data underline the results of the corresponding gene. ANC, absolute neutrophil count; MAX, maximum; MIN, minimum; qPCR, real-time quantitative polymerase chain reaction; vs., versus; WTA, whole transcriptome amplification.

Then, a similar experimental setup was performed for $CD34^+38^+$ cells (Figure 12). It was not possible to work with the same samples as utilized for microarray ($CD34^+38^-$ cells) because the samples of the two specific dates were inaccessible. Again, the bars represent the fold change in gene expression at the ANC peak compared to the nadir.

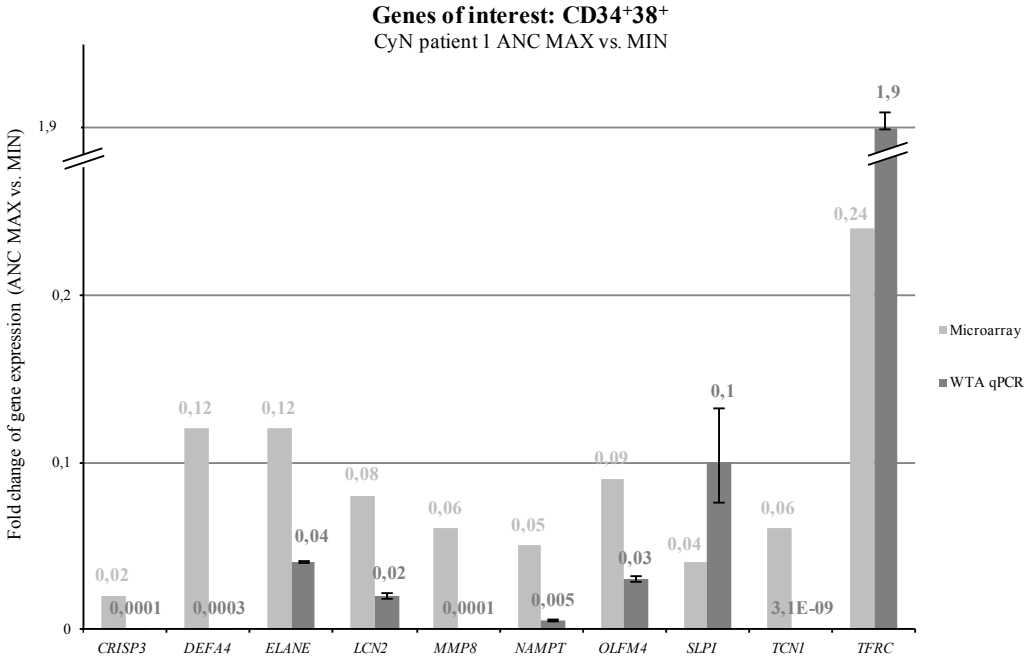

Figure 12: Gene expression in $CD34^+38^+$ cells of CyN patient 1.
The bar graph illustrates the fold changes in gene expression at the ANC maximum compared to the ANC minimum of CyN patient 1 measured by microarray and WTA qPCR. MAX, maximum; MIN, minimum; qPCR, real-time quantitative polymerase chain reaction; vs., versus; WTA, whole transcriptome amplification.

Compared to the microarray results, the WTA qPCR data showed the same trend of gene expression for nine out of ten genes, so the results were considered confirmed. Again, only the microarray data for *TFRC* could not be confirmed. In conclusion, the trend of increased gene expression at the ANC minimum appeared noticeable compared to the ANC maximum. The fold change in gene expression between the ANC minimum and maximum ranged between 1 million for *TCN1* and 1.9 for *TFRC*.

As a first result, oscillating granule proteins and *NAMPT* gene expression in CyN patient 1 could be confirmed for nine out of ten genes. A strong upregulation of the gene expression at the ANC nadir compared to the ANC maximum was detectable. Furthermore, the gene expression of both subpopulations of $CD34^+$ cells, $CD34^+38^-$ and $CD34^+38^+$, showed the same trend. Further gene expression measurements were

continued by using the $CD34^{+}38^{+}$ fraction. Finally, these experiments revealed that the expression of the annotated protein genes displays the same behavior by taking into consideration that nine out of ten genes tested showed the same pattern.

4.1.2.2 Expression of granule protein genes in CyN patient 1 vs. HDs

Having confirmed the oscillating granule protein and *NAMPT* gene expression in the first patient, CyN patient 1, the next aim was to examine this phenomenon in comparison to healthy donors.

For this, $CD33^{+}$ and $CD34^{+}38^{+}$ cells from three healthy donors per cell fraction were measured. The WTA qPCR data from CyN patient 1 (Chapter 4.1.2.1) were then set in relation to the average gene expression of the three healthy donors (Figure 13). In addition, the gel electrophoresis data according to each gene were examined.

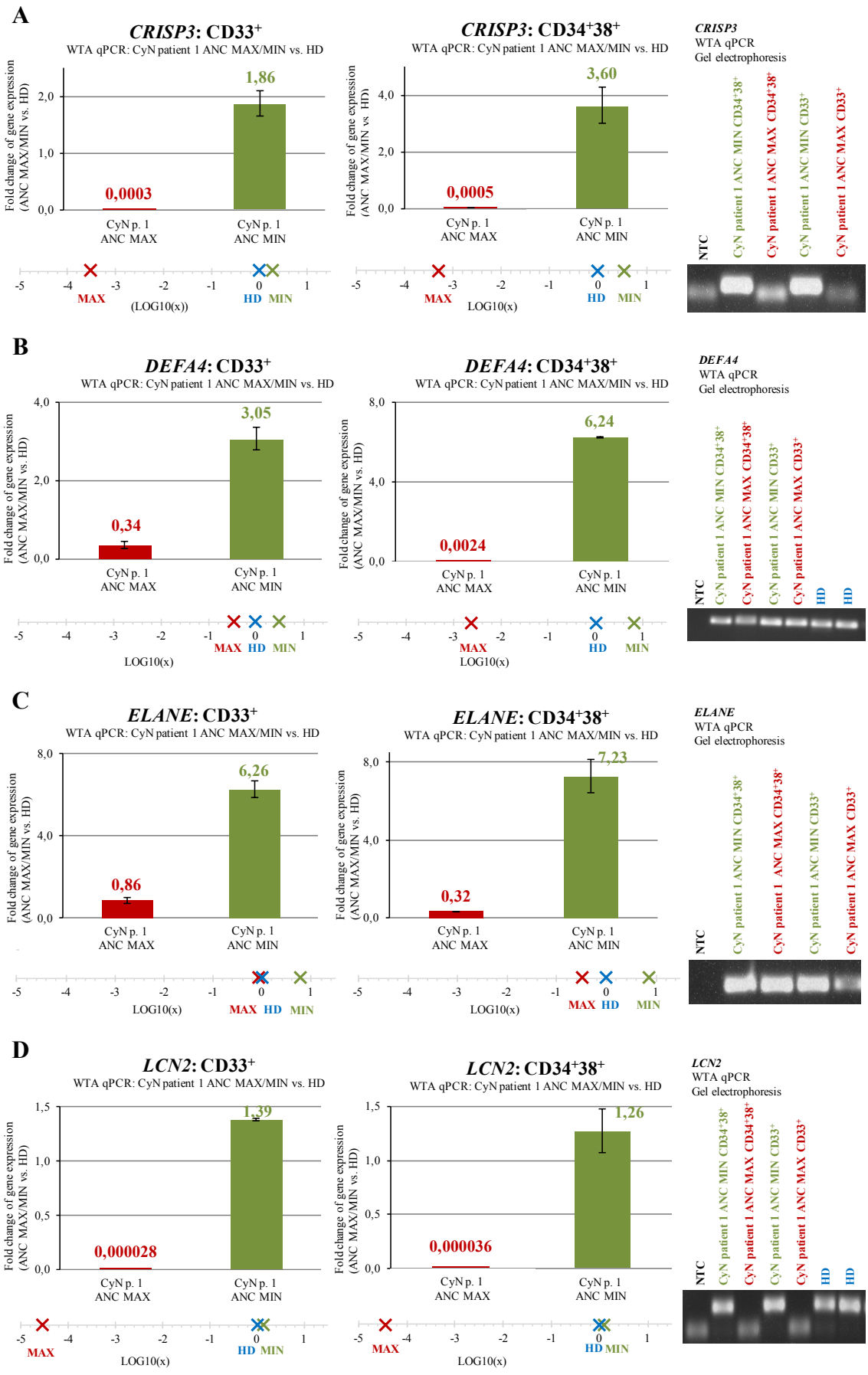
A
CRISP3: CD33+
WTA qPCR: CyN patient 1 ANC MAX/MIN vs. HD
Fold change of gene expression (ANC MAX/MIN vs. HD)
1,86
0,0003
CyN p. 1 ANC MAX
CyN p. 1 ANC MIN
MAX
HD MIN
(LOG10(x))
CRISP3: CD34+38+
WTA qPCR: CyN patient 1 ANC MAX/MIN vs. HD
3,60
0,0005
LOG10(x)
CRISP3
WTA qPCR
Gel electrophoresis
NTC
CyN patient 1 ANC MIN CD34+38+
CyN patient 1 ANC MAX CD34+38+
CyN patient 1 ANC MIN CD33+
CyN patient 1 ANC MAX CD33+
B
DEFA4: CD33+
WTA qPCR: CyN patient 1 ANC MAX/MIN vs. HD
3,05
0,34
DEFA4: CD34+38+
6,24
0,0024
DEFA4
HD
C
ELANE: CD33+
6,26
0,86
ELANE: CD34+38+
7,23
0,32
ELANE
D
LCN2: CD33+
1,39
0,000028
LCN2: CD34+38+
1,26
0,000036
LCN2

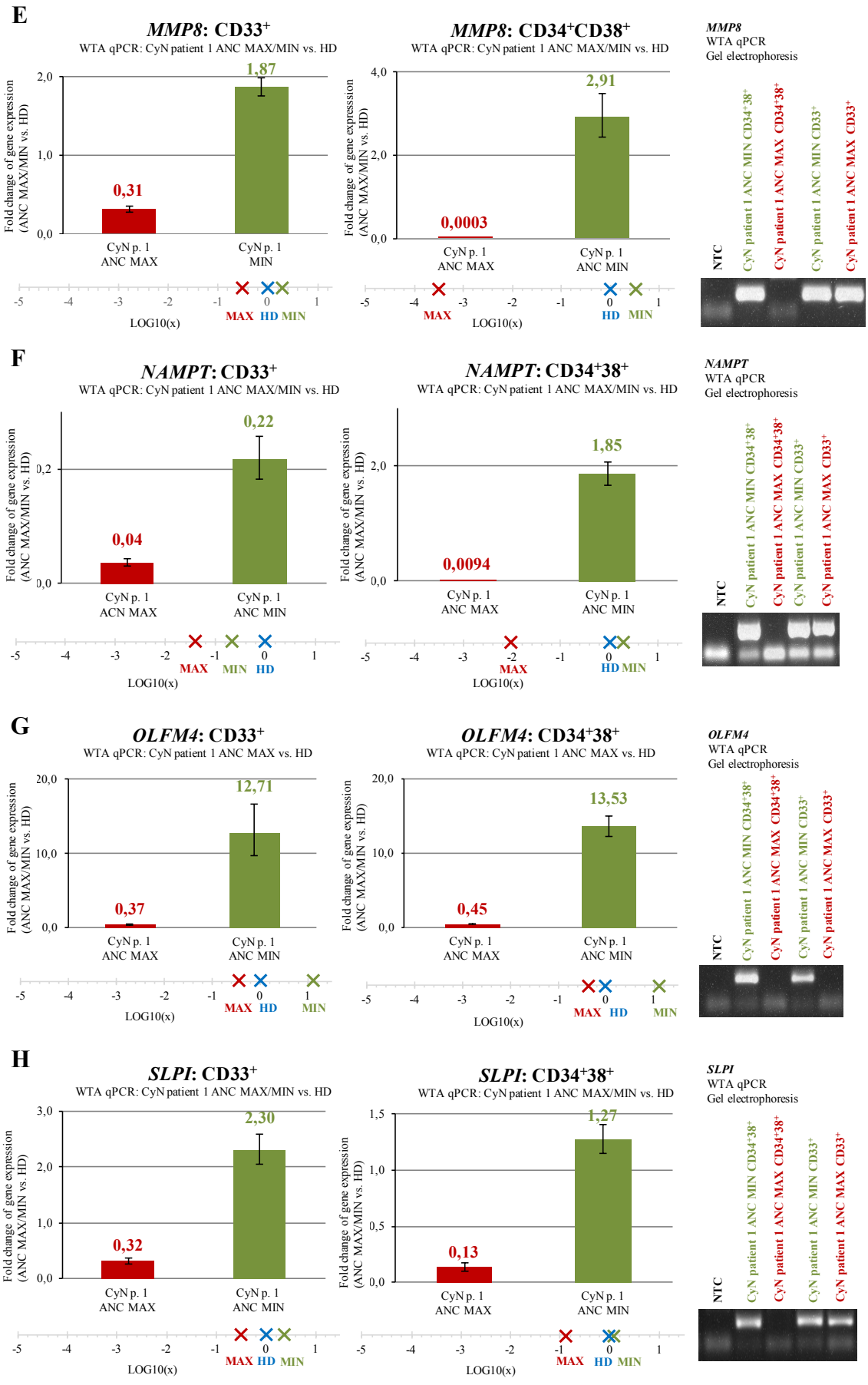
E
MMP8: CD33+
WTA qPCR: CyN patient 1 ANC MAX/MIN vs. HD
Fold change of gene expression (ANC MAX/MIN vs. HD)
1,87
0,31
CyN p. 1 ANC MAX
CyN p. 1 MIN
LOG10(x)
MAX HD MIN
MMP8: CD34+CD38+
WTA qPCR: CyN patient 1 ANC MAX/MIN vs. HD
2,91
0,0003
CyN p. 1 ANC MIN
MMP8
WTA qPCR
Gel electrophoresis
NTC
CyN patient 1 ANC MIN CD34+38+
CyN patient 1 ANC MAX CD34+38+
CyN patient 1 ANC MIN CD33+
CyN patient 1 ANC MAX CD33+
F
NAMPT: CD33+
WTA qPCR: CyN patient 1 ANC MAX/MIN vs. HD
0,22
0,04
CyN p. 1 ACN MAX
MAX MIN HD
NAMPT: CD34+38+
1,85
0,0094
MAX
HD MIN
NAMPT
G
OLFM4: CD33+
12,71
0,37
MAX HD MIN
OLFM4: CD34+38+
13,53
0,45
OLFM4
H
SLPI: CD33+
2,30
0,32
SLPI: CD34+38+
1,27
0,13
SLPI

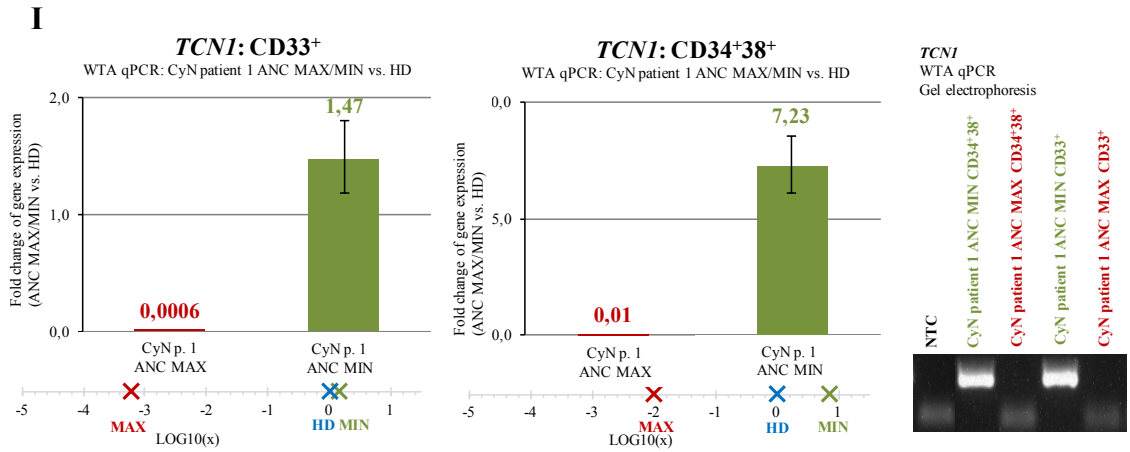

Figure 13: Relative gene expression of CyN patient 1 vs. HDs.
The bar graphs illustrate the WTA qPCR data of CyN patient 1's relative granule protein and *NAMPT* gene expression in $CD33^+$ and $CD34^+38^+$ cells in comparison to healthy donors. These data are presented in the form of fold changes of gene expression in CyN patient 1 at the ANC maximum versus healthy donors as well as the fold changes of CyN patient 1 at the ANC minimum versus healthy donors. The same data were simplified by being transformed into the logarithmic number lines below the bar graphs, that represents relations between the gene expression in CyN patient 1 and healthy donors. On the right side, gel electrophoresis data corresponding to each granule gene are illustrated. HD, healthy donor; MAX, maximum; MIN, minimum; NTC, negative template control; qPCR, real-time quantitative polymerase chain reaction; vs., versus; WTA, whole transcriptome amplification.

By analyzing the expressions of the nine granule protein genes (Figure 13), it was apparent that for all analyzed genes, the expression fold change of CyN patient 1 at the ANC minimum to healthy donors was higher than the fold change of CyN patient 1 at the ANC maximum to healthy donors. It was concluded that upregulation is manifested at the cycle nadir compared to the peak. The healthy donors' gene expression of *CRISP3, DEFA4, LCN2, MMP8, NAMPT, SLPI* and *TCN1* was approximately as high as the expression at the ANC minimum of CyN patient 1. In contrast, the gene expression at the cycle peak of ANC of CyN patient 1 was different from healthy donors. In the cases of *ELANE* and *OLFM4,* however, the expression of healthy donors resembled the expression rate at the ANC maximum of CyN patient 1. In summary, oscillating RNA granule protein and *NAMPT* gene expression could be seen in early progenitor cells of CyN patient 1. This oscillation became apparent with the up- and downregulation of gene expression in CyN patient 1's $CD33^+$ and $CD34^+38^+$ cells compared to healthy donors. This expression change oscillated between the two different samples obtained at the ANC minimum and maximum of CyN patient 1.

At this point, *TFRC* was tested (Figure 14). For this purpose, the same experimental setup was used as described for the other nine genes. In contrast to the nine cycling gene patterns already introduced, *TFRC* cannot be included in this group because CyN patient 1 has a *TFRC* expression corresponding to healthy donors at both times of the cycle. This is true for $CD33^+$ and $CD34^+38^+$ cells. Thus, *TFRC* underlined that the phenomenon observed in the other nine genes tested is specific to a special group and does not appear in every gene checked. Consequently, genes expressed in myeloid cells were identified that were not up- and downregulated between the ANC cycle compared to healthy donors.

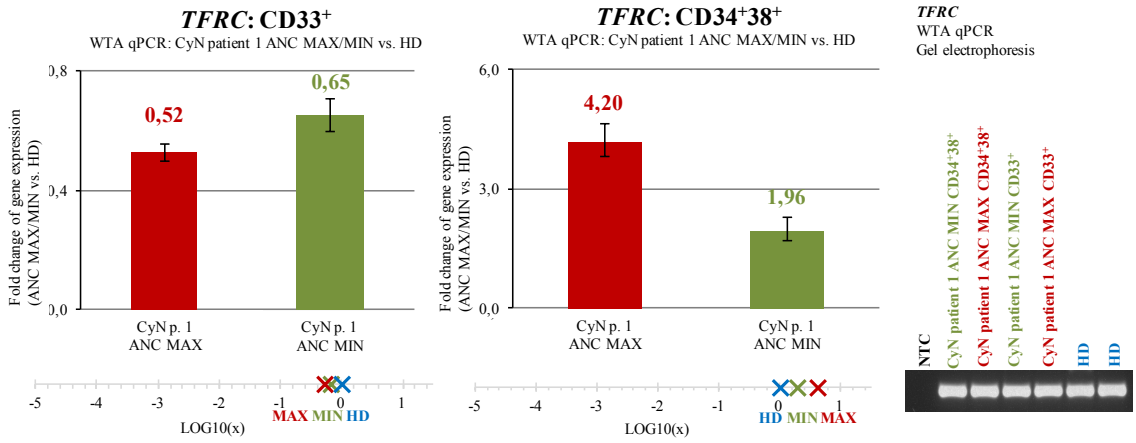

Figure 14: Relative *TFRC* expression of CyN patient 1 vs. HDs.
The bar graphs illustrate the fold changes of *TFRC* gene expression at the ANC maximum in CyN patient 1 versus healthy donors as well as the fold change at the ANC minimum of CyN patient 1 versus healthy donors. The WTA qPCR results of $CD33^+$ and $CD34^+38^+$ cells are shown. The same data were simplified by being transformed into the logarithmic number lines below the bar graphs, where relations between the gene expression in CyN patient 1 and healthy donors are symbolized. On the right side, the corresponding gel electrophoresis data are illustrated. HD, healthy donor; MAX, maximum; MIN, minimum; NTC, negative template control; qPCR, real-time quantitative polymerase chain reaction; vs., versus; WTA, whole transcriptome amplification.

4.1.2.3 Expression of granule protein genes in four other CyN patients

As a next step, the cycle pattern of granule protein genes and *NAMPT* confirmed in CyN patient 1 should be similarly verified in four other CyN patients (Table 1). These four patients were again selected according to the ANC at the date when the samples were obtained. Here, only $CD34^+38^+$ cells were included due to a lack of $CD33^+$ samples. Thereby two CyN patients, patient 2 and patient 3, represented the fraction of low ANC, whereas patient 4 and patient 5 represented the fraction of high ANC.

The first step was to perform qPCR for these four CyN patients and calculate the expression level of granule protein gene and *NAMPT* expression relative to a reference gene expression that was b-actin (Figure 15).

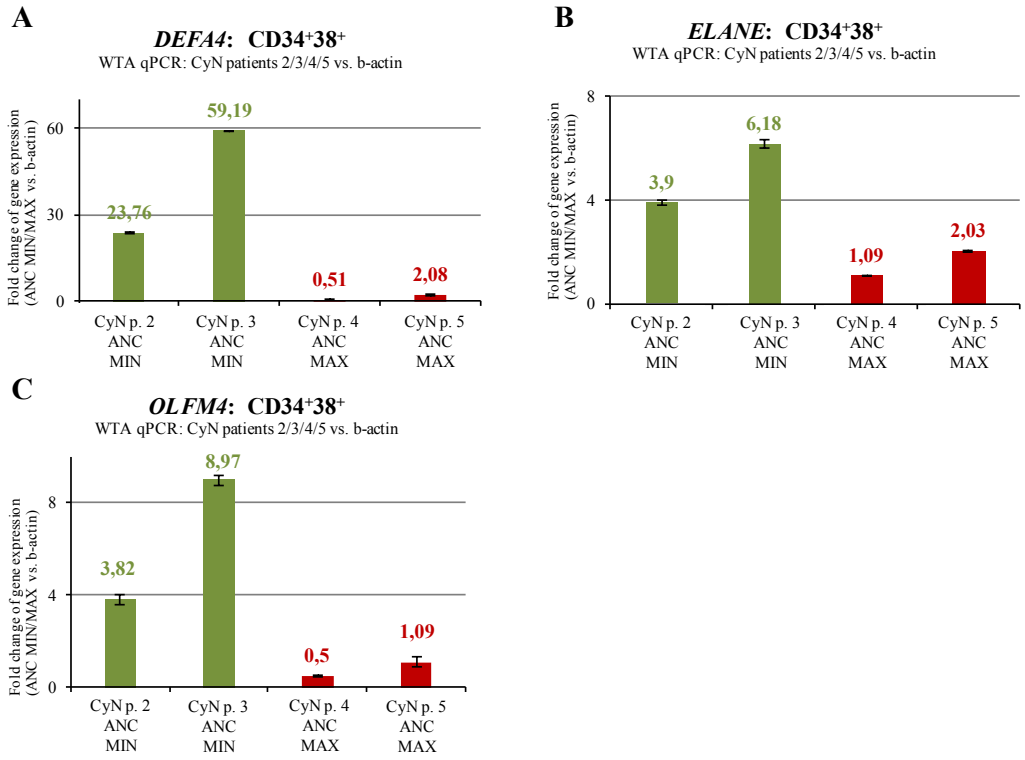

Figure 15: Relative gene expression of CyN patients 2, 3, 4 and 5 vs. b-actin.
The bar graphs illustrate the relative expression level of granule protein genes in those patients compared to the expression of the reference gene b-actin. Two CyN patients (patient 4 and 5) are referred to the ANC maximum whereas two (patient 2 and 3) are referred to the ANC minimum. MAX, maximum; MIN, minimum; qPCR, real-time quantitative polymerase chain reaction; WTA, whole transcriptome amplification.

Only the three granule protein genes of interest, *DEFA4, ELANE* and *OLFM4* showed the expected trend of an increased expression at the ANC minimum compared to the maximum. However, only in *DEFA4* the difference between ANC minimum and maximum was strikingly apparent. The expression at the ANC minimum appeared slightly increased in *ELANE* and *OLFM4*. To obtain direct information as to whether this trend is equivalent to what was seen in CyN patient 1, the fold changes between the four CyN patients and CyN patient 1 had to be calculated (Figure 16).

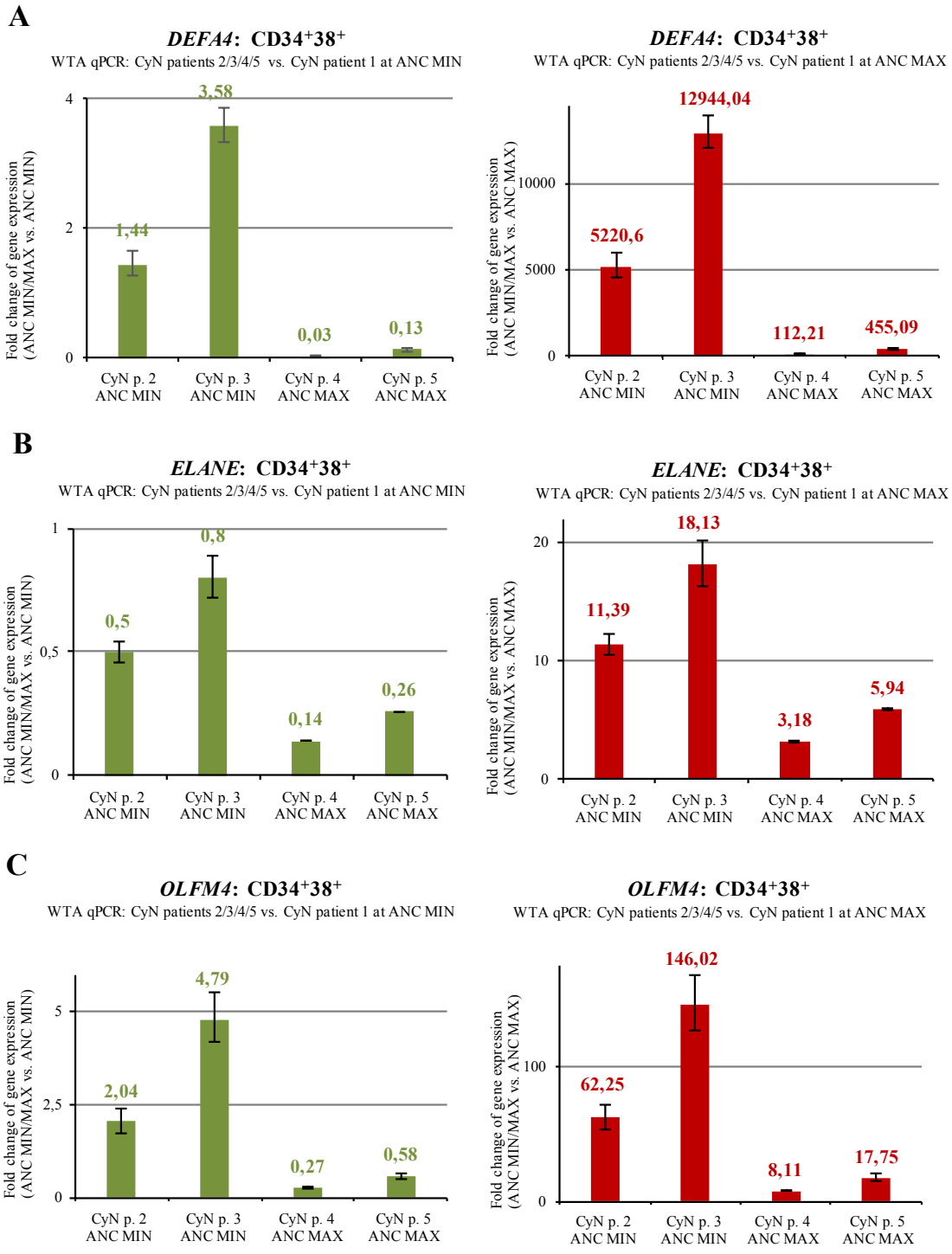

Figure 16: Relative gene expression of four further CyN patients vs. CyN patient 1.
While the green bars illustrate the fold changes of granule protein gene expression in the four CyN patients compared to the expression at the ANC minimum of CyN patient 1, the red bars visualize the four patients' gene expressions at the ANC maximum against CyN patient 1. ANC, absolute neutrophil count; MAX, maximum; MIN, minimum; qPCR, real-time quantitative polymerase chain reaction; vs., versus; WTA, whole transcriptome amplification.

In this setup, the expression of the granule protein genes in the four additional CyN patients was compared to either the expression at the ANC minimum or maximum of CyN patient 1 (Figure 16). As already mentioned before, not all granule protein genes showed the expected expression pattern in the four additional CyN patients. Only *DEFA4, ELANE* and *OLFM4* could reinforce the suspicion that there might also be an oscillating expression in other CyN patients. Samples of CyN patients 2 and 3, both belonging to the ANC minimum fraction, showed a substantially increased expression in comparison to CyN patient 1 at maximum ANC. On the other side, the expression of CyN patient 1 at the cycle minimum was approximately in the same range as in CyN patients 2 and 3. Samples of CyN patients 4 and 5, both of which were part of the ANC maximum fraction, showed an increased expression in comparison to CyN patient 1 ANC maximum. However, they had a decreased expression in comparison to CyN patient 1 at the ANC minimum.

As a result, the index CyN patient 1 at the ANC maximum is likely to be different from healthy donors as well as further CyN patients.

4.1.2.4 Expression of granule protein genes in four CyN patients vs. HDs

Before focusing on a possible reason for the unique phenomenon in CyN patient 1, the four additional CyN patients should be compared to healthy donors by qPCR.

Again, the three granule protein genes of interest, *DEFA4, ELANE* and *OLFM4* were highlighted, as they showed the expected trend in $CD34^{+}38^{+}$ cells (Figure 17).

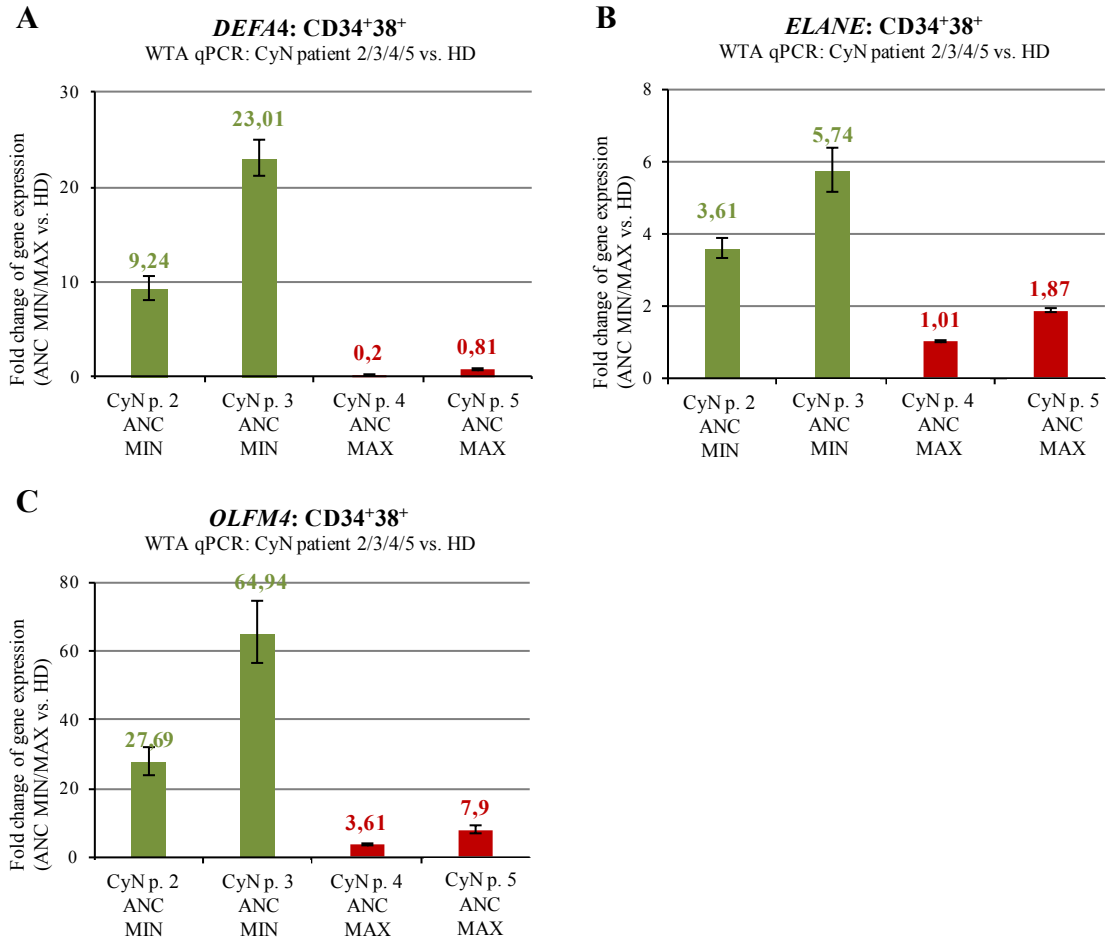

Figure 17: Relative gene expression of four CyN patients vs. HDs.
The WTA qPCR results of the granule protein gene expression in four CyN patients is illustrated as fold change to HDs. The green bars show the fold change at the ANC minimum of the two CyN patients to healthy donors, while the red bars show the fold change at the ANC maximum of the two patients to healthy donors. ANC, absolute neutrophil count; HD, healthy donor; CyN, cyclic neutropenia; MAX, maximum; MIN, minimum; qPCR, real-time quantitative polymerase chain reaction; vs., versus; WTA, whole transcriptome amplification.

In each gene, a remarkable difference was visible between the expression in patients at the cycle nadir and the expression in patients at the cycle peak (Figure 17). The highest difference could be seen in *OLFM4*, which has a 28- to 65-fold increased expression in patients at the ANC minimum compared to healthy donors. However, the expression amplitude between maximum and minimum in these four CyN patients was not to the same extent as seen in CyN patient 1.

Consequently, an oscillating trend was detectable in three out of ten gene expressions of the additional CyN patients with an upregulation in every patient at the ANC minimum. However, the other six genes of interest, *CRISP3, LCN2, MMP8, NAMPT, SLPI* and

TCN1, which were noticeably cycling in the case of CyN patient 1, showed a pattern that is rather comparable to healthy donors and thus totally differed from the oscillating phenomenon. Thus, these experiments confirmed a cycling granule protein gene and *NAMPT* expression in CyN patient 1 but could not be confirmed in the same manifestation in the additionally examined CyN patients. CyN patient 1 seemed to occupy a unique position. As a consequence, the question arose as to which variables might cause the oscillations in all tested granule protein genes and *NAMPT* in CyN patient 1.

4.1.3 *C/EBPe* and *TNFRSF1A* mutations of CyN patient 1

To explain the unique phenomenon of cycling *NAMPT* and granule protein genes in CyN patient 1, a whole genome sequencing (WGS) was performed of CyN patient 1 and the family of CyN patient 1. Two interesting mutations were found in CyN patient 1's sample: a *TNFRSF1A* mutation inherited from the mother and a *C/EBPe* mutation inherited from the father (Figure 5). C/EBPe is a transcription factor in the final differentiation steps towards eosinophils and neutrophils (Figure 2) and plays an indispensable role in granulopoiesis. In humans, four different isoforms are known (isoforms 32, 30, 27 and 14). While isoforms 32 and 30 are predicted to have an activating role on myeloid promoters, isoforms 27 and 14 are considered to be transcriptional repressors. Isoform 14, which is said to function as a dominant-negative *C/EBPe* repressor, might stimulate erythropoiesis at the expense of the maturation towards the granulocyte-macrophage lineage. Mutations in the *C/EBPe* gene are known to induce a lack of neutrophil secondary granule proteins (Bedi et al., 2009; Lekstrom-Himes et al., 1999; Yamanaka et al., 1997).

In the sample of CyN patient 1, we found the heterozygous *C/EBPe* p.Leu155Met single nucleotide variant (SNP). The *Sorting Intolerant from Tolerant* (SIFT) and *Polymorphism Phenotyping v2* (PolyPhen-2) tools predict the functional consequences of human single nucleotide polymorphisms (SNPs) (Adzhubei et al., 2010; Ng & Henikoff, 2001). Thereby, *C/EBPe* p.Leu155Met is predicted to be damaging by PolyPhen-2 and deleterious by SIFT.

C/EBPe p.Leu155Met is a known low-frequency SNP with an allele frequency of $p = 0.007$ and a homozygous amount of $p^2 = 4/60{,}706$ according to the ExAC browser.

The ExAC browser does not include samples of individuals with severe pediatric diseases (Karczewski et al., 2017). Therefore, it had to be proven whether the mentioned homozygous amount of the four people already corresponds to the total number of homozygotes, or rather, only the proportion that does not suffer from severe diseases. According to the allele frequency of $p = 0.007$, a homozygote frequency of $p^2 = 5/100{,}000$ could be calculated using the Hardy-Weinberg equation:

$$p^2 + 2pq + q^2 = 1$$

p = frequency of mutant *C/EBPe* p.Leu155Met allele
q = frequency of wildtype allele
p^2 / q^2 = frequency of according homozygous genotype
$2pq$ = frequency of heterozygous genotype

Thus, the homozygous amount of four listed in ExAC is what is expected according to the Hardy-Weinberg distribution. Consequently, there is no report of homozygous carriers of the *C/EBPe* p.Leu155Met mutation with severe disease. Since the number of homozygous carriers corresponds to the theoretical estimate, it is unlikely that this SNP has a pathogenic effect in the heterozygous state. Moreover, there is a significant number of heterozygous carriers of *C/EBPe* p.Leu155Met mutation. In total, the population frequency of the *C/EBPe* p.Leu155Met mutation is much higher than that of neutropenia in the general population.

The effect of the *C/EBPe* p.Leu155Met mutation is not fully understood. However, one cannot rule out that the mutation creates a new start codon so that a shorter isoform is induced besides the 32, 30, 27 and 14 isoforms (Figure 18). The mutated isoform has its start codon two base pairs downstream from the start codon of isoform 14. Thus, in theory this mutated isoform might have the same effect as the short isoform 14, which would lead to an inhibited expression of secondary granule proteins. In the case of CyN patient 1, this *C/EBPe* mutation could enhance neutropenia in addition to the *ELANE* mutation effect.

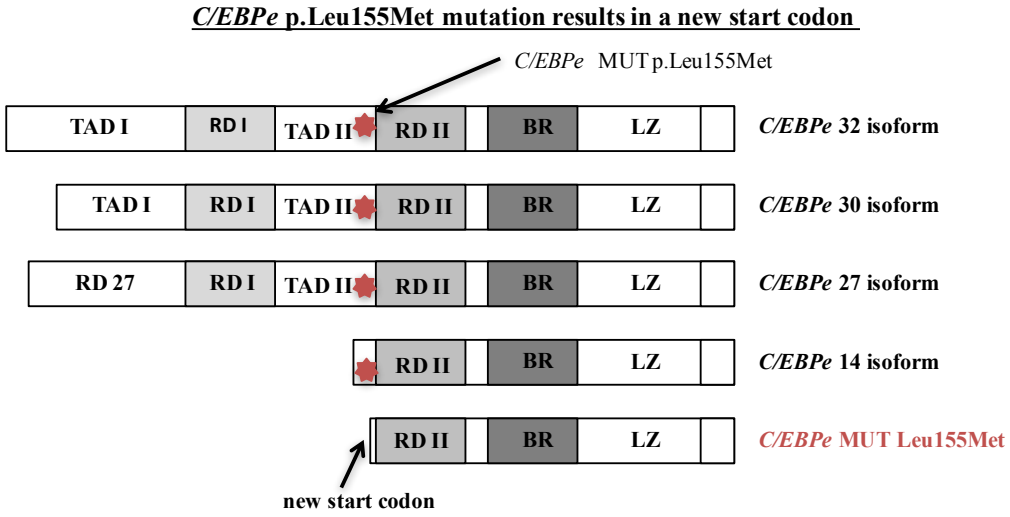

Figure 18: Overview of different *C/EBPe* isoforms.
In humans, four different *C/EBPe* isoforms are known (32, 30, 27 and 14). The *C/EBPe* mutation p.Leu155Met, indicated in red, leads to a short C/EBPe isoform due to a newly created start codon at the mutation site. The start codon of the mutated isoform is located two base pairs apart to the start codon of isoform 14. All indicated isoforms share the identical carboxyl terminus (Modified from Bedi et al., 2009; additional data have been kindly made available by Prof. Dr. J. Skokowa, Universitätsklinikum Tübingen).

To get an idea whether, due to the mutation, the *C/EBPe* expression in CyN patient 1 differs from other CyN patients and healthy donors, an isoform-specific qPCR run was performed. Also, to find out which *C/EBPe* isoform predominates in CyN patient 1, qPCR was done by using a *C/EBPe* C-terminal primer pair that binds to each isoform and a *C/EBPe* N-terminal primer pair that attaches only to the long isoforms (Figures 18 and 19).

Homo sapiens CCAAT/enhancer binding protein epsilon gene (*C/EBPe*), mRNA
Primer binding sites

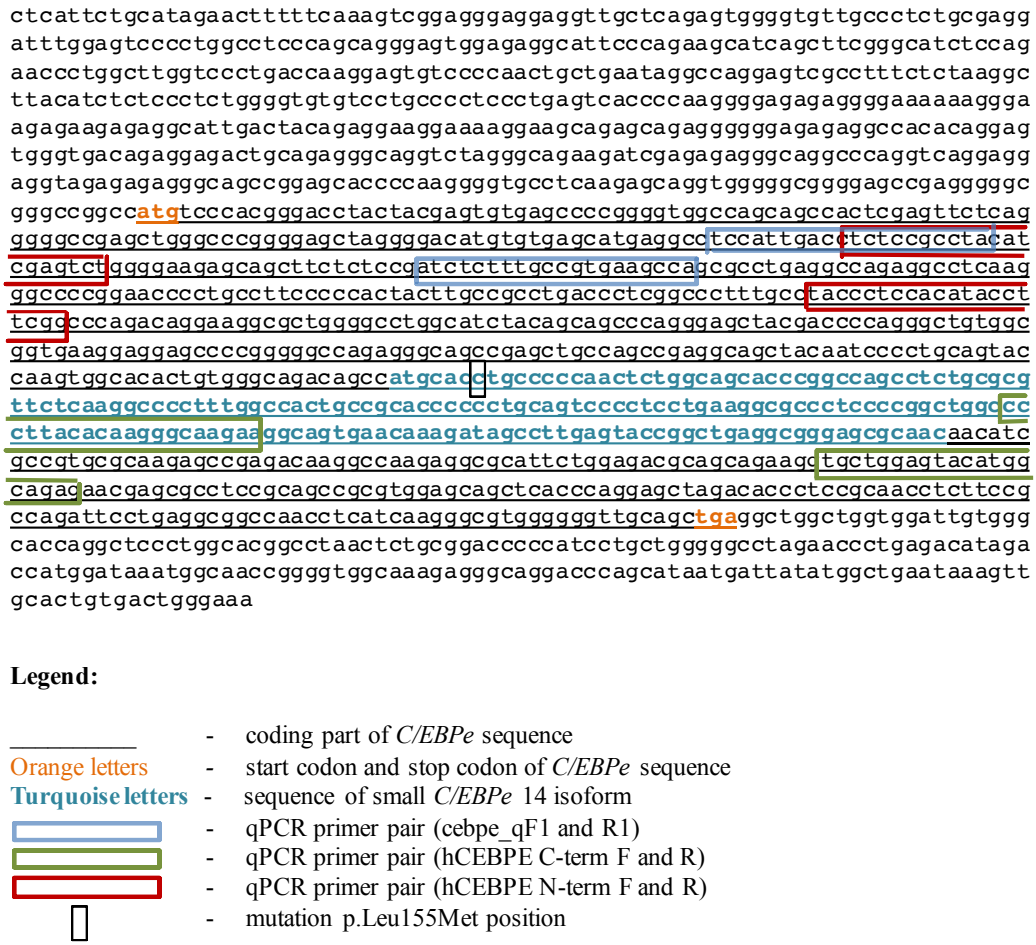

Legend:

_____	-	coding part of *C/EBPe* sequence
Orange letters	-	start codon and stop codon of *C/EBPe* sequence
Turquoise letters	-	sequence of small *C/EBPe* 14 isoform
	-	qPCR primer pair (cebpe_qF1 and R1)
	-	qPCR primer pair (hCEBPE C-term F and R)
	-	qPCR primer pair (hCEBPE N-term F and R)
	-	mutation p.Leu155Met position

Figure 19: Overview of *C/EBPe* mRNA sequence with primer binding sites.
The figure shows the entire *C/EBPe* mRNA sequence. The primer binding sites of the primer pairs used for the experiments are indicated. The coding part of the *C/EBPe* mRNA sequence is underlined, while the sequence of the small isoform 14 is indicated in light gray. The p.Leu155Met mutation position is framed in black. The *C/EBPe* primers utilized for our experiments are framed in different colors, which are listed below in the legend. mRNA, messenger ribonucleic acid; qPCR, real-time quantitative polymerase chain reaction.

4.1.3.1 Expression of *C/EBPe* in CyN patients vs. HDs

The *C/EBPe* expression in CyN patient 1 and further CyN patients were compared to healthy donors (Figures 20 and 21). The cebpε_qF1 and cebpε_R1 primer pair (Table 4 and Figure 19) was used.

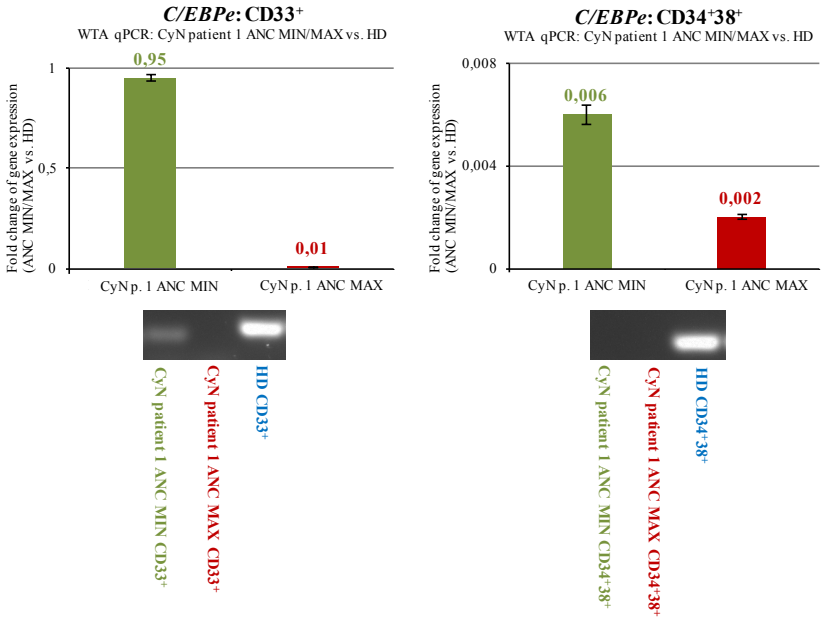

Figure 20: Relative *C/EBPe* expression of CyN patient 1 vs. HDs.
The bar graphs illustrate the fold changes of *C/EBPe* gene expression at the ANC maximum and minimum in $CD33^+$ and $CD34^+38^+$ cells of CyN patient 1versus healthy donors. Below each bar graph, gel electrophoresis data in relation to the WTA qPCR data are shown. HD, healthy donor; MAX, maximum; MIN, minimum; qPCR, real-time quantitative polymerase chain reaction; vs., versus; WTA, whole transcriptome amplification.

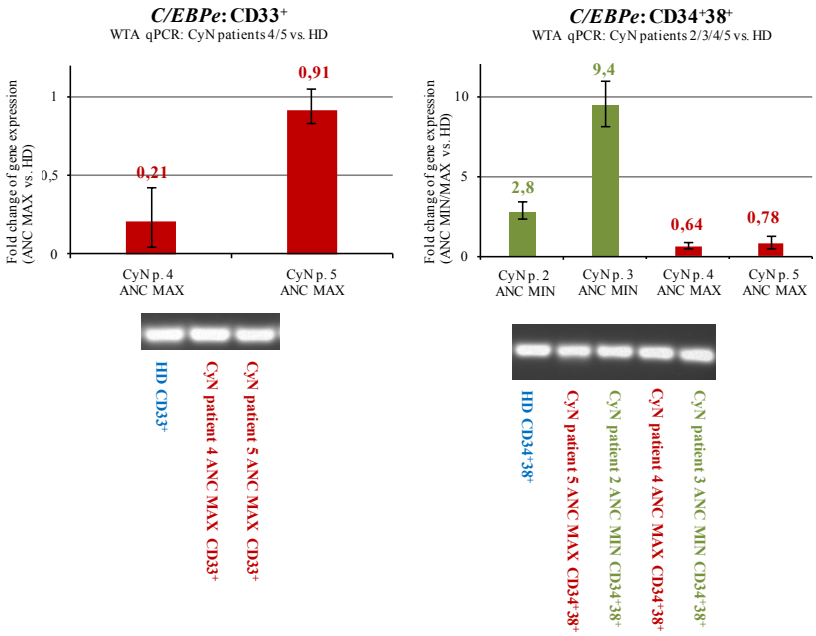

Figure 21: Relative *C/EBPe* expression of four CyN patients vs. HDs.
The bar graphs illustrate the fold changes of *C/EBPe* gene expression in $CD33^+$ and $CD34^+38^+$ cells of CyN patients that are either at the minimum or maximum of their ANC cycle, versus healthy donors. Below each bar graph, gel electrophoresis data in relation to the WTA qPCR data are illustrated. HD, healthy donor; MAX, maximum; MIN, minimum; qPCR, real-time quantitative polymerase chain reaction; vs., versus; WTA, whole transcriptome amplification.

As a result, no gene expression was measurable in qPCR and gel electrophoresis in the $CD34^{+}38^{+}$ cell fraction of CyN patient 1 (Figure 20). In comparison, a *C/EBPe* expression was seen in $CD33^{+}$ cells at the cycle minimum of CyN patient 1.

CyN patients 2, 3, 4 and 5, independently of their cycle stage and the cell fraction, showed a *C/EBPe* expression similar to healthy donors (Figure 21). Moreover, the trend of a cycling *C/EBPe* expression in other CyN patients can be considered, as the expression of the patients at the ANC minimum is increased compared to b-actin, while it is decreased at the ANC maximum (Figure 22).

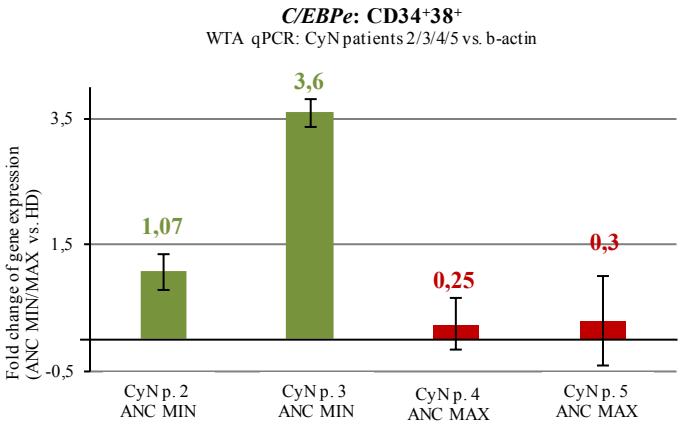

Figure 22: Relative *C/EBPe* expression of four CyN patients vs. HDs.
The bar graph illustrates the relative expression level of *C/EBPe* in the four CyN patients compared to the expression of the reference gene b-actin. Two CyN patients (patients 4 and 5) are referred to the ANC maximum, whereas two (patients 2 and 3) are referred to the ANC minimum. MAX, maximum; MIN, minimum; qPCR, real-time quantitative polymerase chain reaction WTA, whole transcriptome amplification.

It should be noted that the utilized primers did not cover the short isoform that was expressed due to the mutation. For this purpose, two new primer pairs were designed to distinguish between the long and short isoforms of *C/EBPe*. The first primer pair of *C/EBPe* are the *C/EBPe* C-terminal primers that cover every isotype because of their identical carboxyl terminus. The second primer pair, the *C/EBPe* N-terminal primers, however, only amplify the long isoforms so that isoform 14 and the novel isoform with the *C/EBPe* p.Leu155Met mutation will not be amplified (Figure 19). First, the *C/EBPe* C-terminal primers were utilized (Figures 23 and 24).

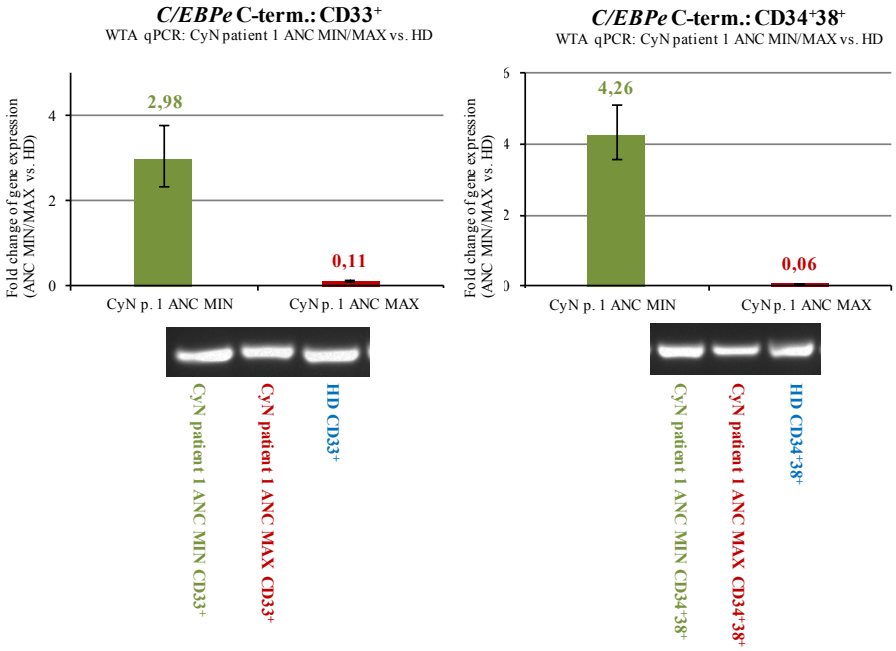

Figure 23: Relative *C/EBPe* C-terminal expression of CyN patient 1 vs. HDs.
The bar graphs illustrate the fold changes of *C/EBPe* gene expression at the ANC maximum and minimum in CyN patient 1 versus healthy donors. Below each bar graph, gel electrophoresis data according to the WTA qPCR data are illustrated. HD, healthy donor; MAX, maximum; MIN, minimum; qPCR, real-time quantitative polymerase chain reaction; vs, versus; WTA, whole transcriptome amplification.

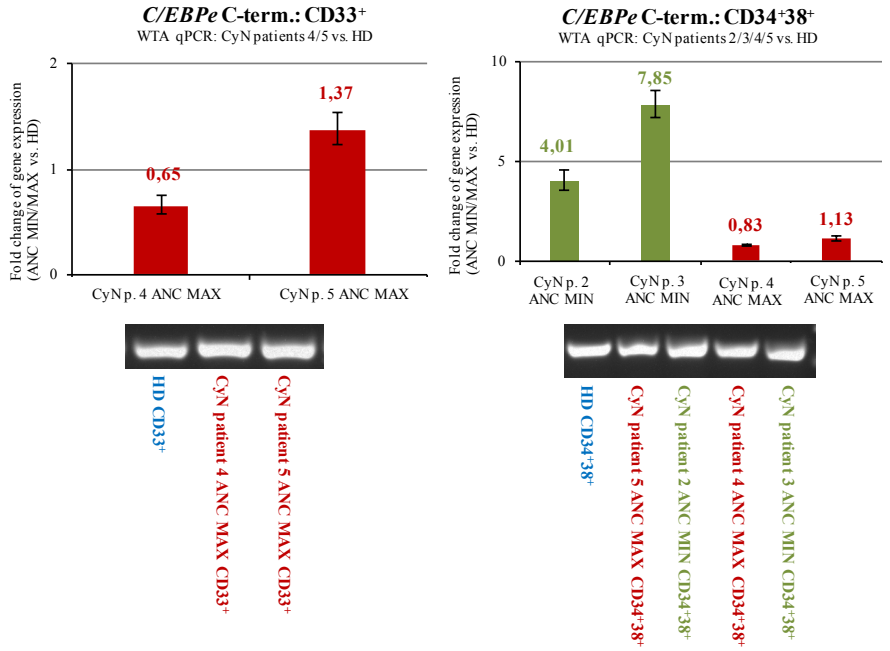

Figure 24: Relative *C/EBPe* C-terminal expression of four CyN patients vs. HDs.
The graph shows the fold changes of *C/EBPe* gene expression in CyN patients that are either at the minimum or maximum of ANC cycle versus healthy donors. Below each bar graph, the gel electrophoresis data in relation to the WTA qPCR data are shown. HD, healthy donor; MAX, maximum; MIN, minimum; qPCR, real-time quantitative polymerase chain reaction; vs, versus; WTA, whole transcriptome amplification.

Using the *C/EBPe* C-terminal primers, CyN patient 1 was analyzed and compared to healthy donors (Figure 23). According to the gel electrophoresis results, *C/EBPe* was expressed at the ANC minimum and maximum and in the two different cell lineages. This indicates that there was a *C/EBPe* expression in CyN patient 1, but it is not possible to say which isoform was expressed at this point. Next, in $CD33^+$ and $CD34^+38^+$ cells, the *C/EBPe* expression in CyN patient 1 is higher at the ANC minimum compared to the maximum.

In the next step, the CyN patients 2, 3, 4 and 5 were again compared to healthy donors (Figure 24). Again, their *C/EBPe* expression resembled that of healthy donors, and again, the expression at the ANC minimum was increased at the minimum compared to the maximum.

The same experimental setup was performed by using the *C/EBPe* N-terminal primers (Figures 25 and 26).

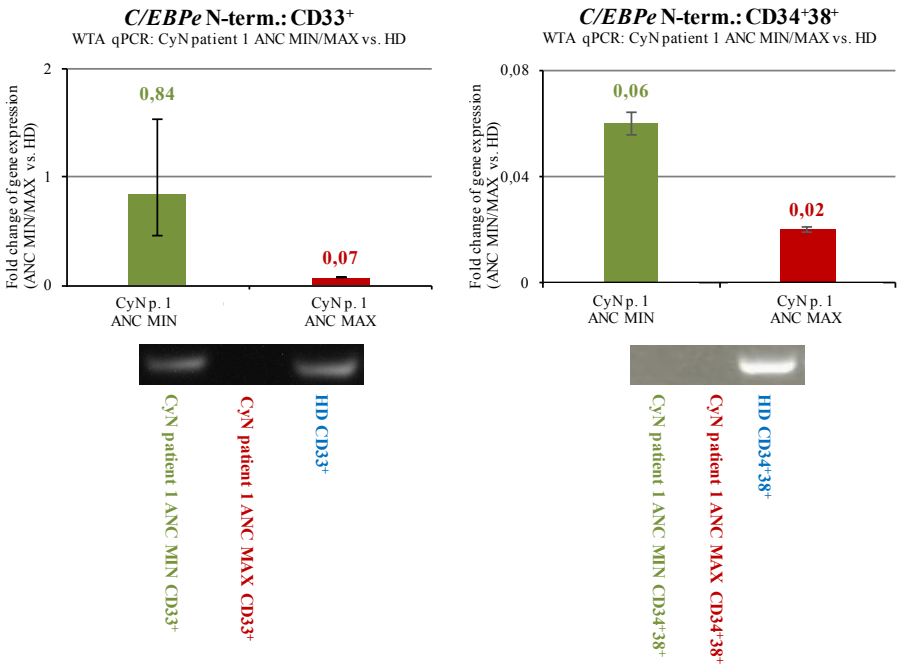

Figure 25: Relative *C/EBPe* N-terminal expression of CyN patient 1 vs. HDs.
The bar graphs show the fold changes of *C/EBPe* gene expression at the ANC maximum and minimum in CyN patient 1 versus healthy donors. Gel electrophoresis data in relation to the WTA qPCR data are illustrated below each bar graph. HD, healthy donor; MAX, maximum; MIN, minimum; qPCR, real-time quantitative polymerase chain reaction; vs, versus; WTA, whole transcriptome amplification.

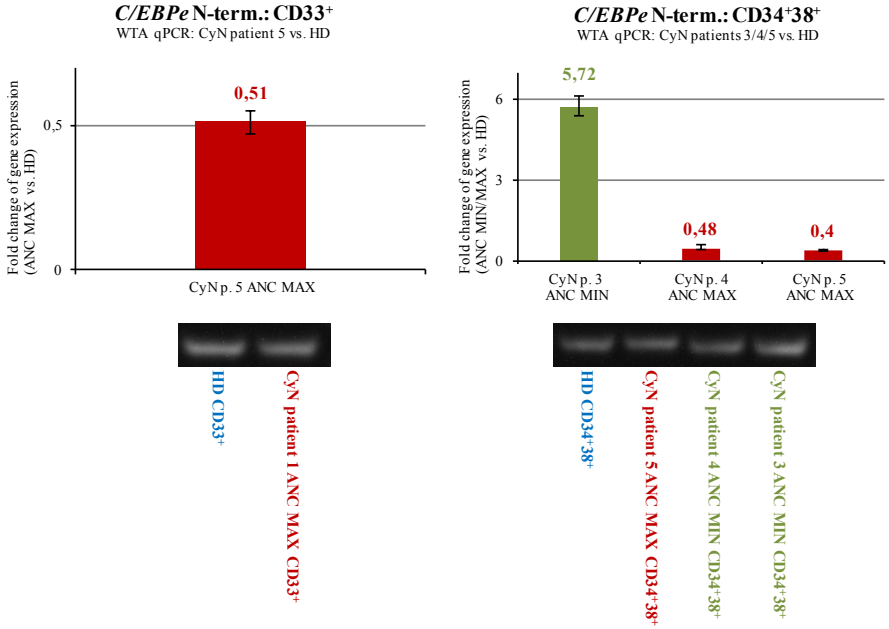

Figure 26: Relative *C/EBPe* N-terminal expression of four CyN patients vs. HDs.
The bar graphs illustrate the fold changes of *C/EBPe* N-terminal gene expression in CyN patients that are either at the minimum or maximum of their ANC cycle, versus healthy donors. Below each bar graph, gel electrophoresis data in relation to the WTA qPCR data are illustrated. HD, healthy donor; MAX, maximum; MIN, minimum; qPCR, real-time quantitative polymerase chain reaction; vs, versus; WTA, whole transcriptome amplification.

This last run again produced the expected results. In early matured $CD34^+38^+$ cells of CyN patient 1, almost no long *C/EBPe* isoforms are expressed (Figure 25). However, looking at the expression in further matured $CD33^+$ cells, long *C/EBPe* isoforms were expressed at the ANC minimum.

In summary, the expression of *C/EBPe* isoforms in the four CyN patients is comparable to what was measured in healthy donors. In CyN patient 1, the expression of the *C/EBPe* short isoform was measurable in both cell lineages, $CD34^+38^+$ and $CD33^+$ cells. However, it was increased in the ANC minimum samples compared to those obtained at the ANC maximum. In contrast, CyN patient 1 showed no expression of the *C/EBPe* long isoform in $CD34^+38^+$ cells at both time points. In further differentiated $CD33^+$ cells, the *C/EBPe* long isoform was expressed in the ANC minimum sample (Table 24).

Table 24: Overview of *C/EBPe* expression in CyN patients.

	C/EBPe N-term.		*C/EBPe* C-term.	
	Primer 1: cebpε	Primer 2: hCEBPE N-term.	Primer 3: hCEBPE C-term.	
CyN patient 1 MAX	−	−	+	Only short isoform
Other CyN patients	+	+	+	Long and short isoform
Healthy donors	+	+	+	Long and short isoform

The table simplifies the results discussed in Chapter 4.1.3.1. According to the different primers used, the results of qPCR and gel electrophoresis were summarized. The green plus sign symbolizes a detected expression of the *C/EBPe* gene, while the red minus sign means that no expression was measurable. MAX, maximum; MIN, minimum.

4.2 *CSF3R* and *RUNX1* mutations in CyN patients

SCN is well known to be associated with MDS and AML, while CyN has long been considered benign and *CSF3R* or *RUNX1* mutations have not been reported in CyN patients (Chapter 1.2.6) (Germeshausen et al., 2007). In 2016, however, Klimiankou et al. detected the first CyN patient with the AML associated *CSF3R* and *RUNX1* mutations, followed by a second with an acquired *CSF3R* mutation. These results, presented in the following part of this thesis, were published in *Blood*: "Two cases of cyclic neutropenia with acquired *CSF3R* mutations, with 1 developing AML" (Klimiankou et al., 2016). The acquired *CSF3R* mutations of CyN patient 4 are Gln743, Gln749 and Tyr752. CyN patient 6 has the acquired mutation Gln741 (Figure 27).

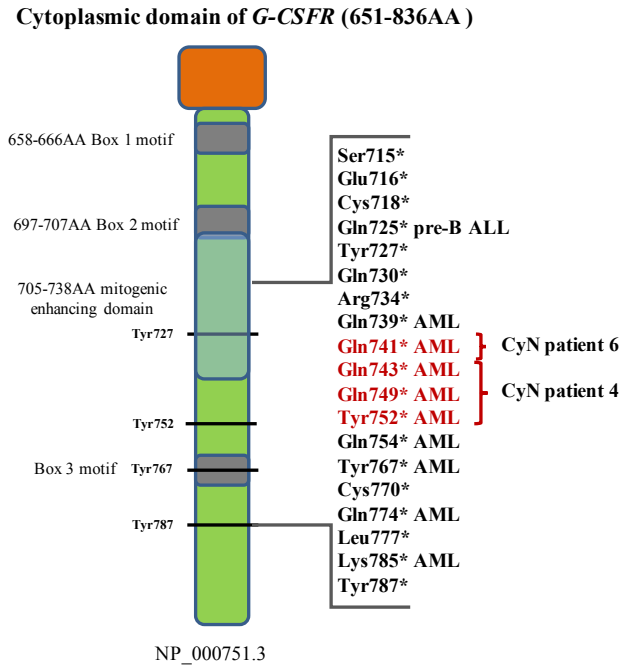

Figure 27: Acquired mutations in cytoplasmic domain of *G-CSFR*.
The cytoplasmic domain of *G-CSFR* is presented. The bracket beside the gene domain includes those locations, where known *G-CSFR* mutations are sited. Moreover, the association with AML development is added to the corresponding mutations. The four mutations that could be detected in CyN patients 4 and 6 are indicated in red. AML, acute myeloid leukemia (data have kindly been provided by M. Klimiankou).

4.2.1 *CSF3R* and *RUNX1* mutation in CyN patient 6

To get a follow-up examination, various CyN patients were screened with deep sequencing by the research group of Prof. Dr. J. Skokowa/Prof. Dr. K. Welte. CyN patient 6, who had previously been negative for leukemic mutations, attracted particular attention, as the sample, taken three years before the AML diagnosis, showed that 3% of the peripheral blood mononuclear cells (PB MNCs) had the *CSF3R* p.Gln741* mutation. The bone marrow mononuclear cell (BM MNC) sample, which was taken two years later (one year before AML diagnosis), showed a mutant allele frequency (MAF) of 8%. Then, in the latest sample of 2016, when the patient was 17 years old, the *CSF3R* mutation had increased to an amount of 50% according to the following deep sequencing run. Moreover, 10% of the BM MNCs carried the *RUNX1* mutation p.Asp171Asn. This was accompanied by an acquired trisomy 21 and monosomy 7 and a blast frequency of 33% in bone marrow (Figure 28). At this point, AML (French-American-British-classification M2) was diagnosed so that the first CyN patient developing AML was detected (Figures 28 and 29) (Klimiankou et al., 2016).

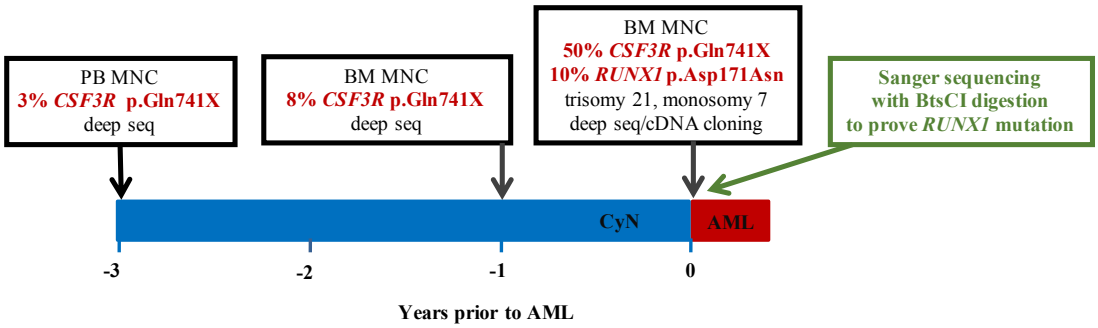

Figure 28: Time line of *CSF3R* and *RUNX1* mutation acquisition in CyN patient 6.
The black frames contain the examinations and results that were gained prior to this work, while the green frame contains the step that is part of this thesis. AML, acute myeloid leukemia; BM MNC, bone marrow mononuclear cells; CyN, cyclic neutropenia; deep seq, deep sequencing; PB MNC, peripheral blood mononuclear cells (data were kindly provided by M. Klimiankou).

The result of a 10% amount of *RUNX1* mutation in the BM MNCs of CyN patient 6, which was obtained by using deep sequencing, should be validated by a second, alternative method. Therefore, Sanger sequencing should be performed. In the first step, eight different colony-forming units (CFUs) of CyN patient 6 were amplified using the RUNX1ex3D17N_F/RUNX1D171N309.R primer pair (Table 5) and sent for Sanger sequencing. However, the sequencing results were negative for the *RUNX1* mutation in every CFU sample. One reason might have been that the cells with the *RUNX1* mutation

had not been growing in the in-vitro mediums. In the next step, cDNA of CyN patient 6 should be used. Two different samples were included. The first sample originated from $CD34^+$ cells that had been cultured in stem cell $CD34^+$ expansion cocktail + G-CSF + FCS for 1.5 months before RNA was isolated and transcribed into cDNA. The second sample originated from PM MNCs. As a tiny percentage of *RUNX1* mutation was expected, the use of a restriction enzyme should help to increase the amount of mutant allele. Thus, the detection limit of Sanger sequencing should be reached. In this process, the *RUNX1* cDNA allele was amplified by PCR, and then the product was incubated with the restriction enzyme. Having cut the wild-type *RUNX1* alleles, the entire mutant alleles were selectively amplified by PCR and could then be sent for Sanger sequencing (Chapter 3.3.5).

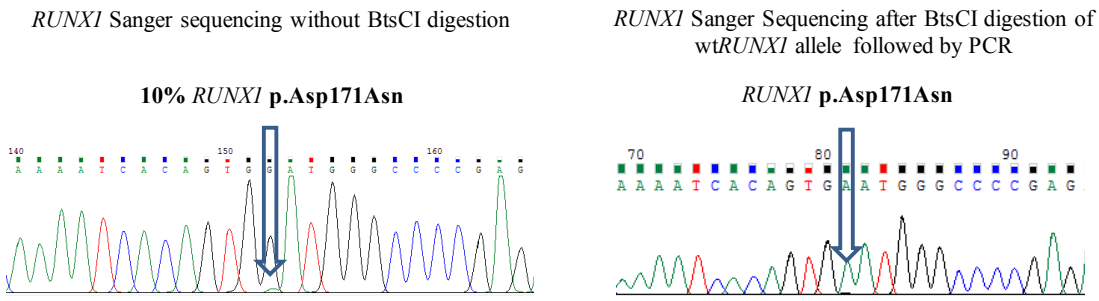

Figure 29: Sanger sequencing results of *RUNX1* mutation in CyN patient 6.
The figures show the detection of the *RUNX1* mutation in PM MNCs of CyN patient 6. The left figure contains the results obtained without BtsCI digestion. As indicated on the right, an elevated signal could be detected after the digestion step with BtsCI was included in the sample preparation. PCR, polymerase chain reaction; wt, wild type.

The results of Sanger sequencing showed that with the use of the BtsCI restriction enzyme an enrichment of the mutant *RUNX1* allele was observed in the sample of CyN patient 6 (Figure 29). In contrast, the sample that was not digested did not show mutant allele enrichment in Sanger sequencing. In this way, the presence of the *RUNX1* mutant clone was confirmed in both samples, in the cultured ones as well as in the PM MNCs.

4.2.2 *CSF3R* mutation in CyN patient 4

Having proven that there is a risk for myeloid transformation in CyN, 18 further patients were screened for *CSF3R* and *RUNX1* mutations by deep sequencing. In this process, this research group pointed out CyN patient 4, aged 15.4 years at that time, who had also

acquired the *CSF3R* mutation. This result was measured by deep sequencing in a BM MNC sample that has been obtained two years before the time of measurement. This sample showed a mutant allele frequency of 2.6%. To get further information, the same sample was sent for ultra-deep sequencing. Here, 2.2% of the cells showed the p.Gln734* mutation, 0.81% the p.Tyr752*, and the p.Gln749* mutation was represented in an amount of 1% with this method. These are all mutations of the *G-CSFR* gene and, furthermore, associated with AML (Figure 27). The latest PB MNC sample, obtained two years later, was examined with exome sequencing and showed an increased amount of 9% p.Gln749* mutated cells. In contrast to CyN patient 6, CyN patient 4 had not developed MDS or AML to date (Klimiankou et al., 2016). To get a confirming result of this data by an alternative method, Sanger sequencing was again performed (Figures 30 and 31).

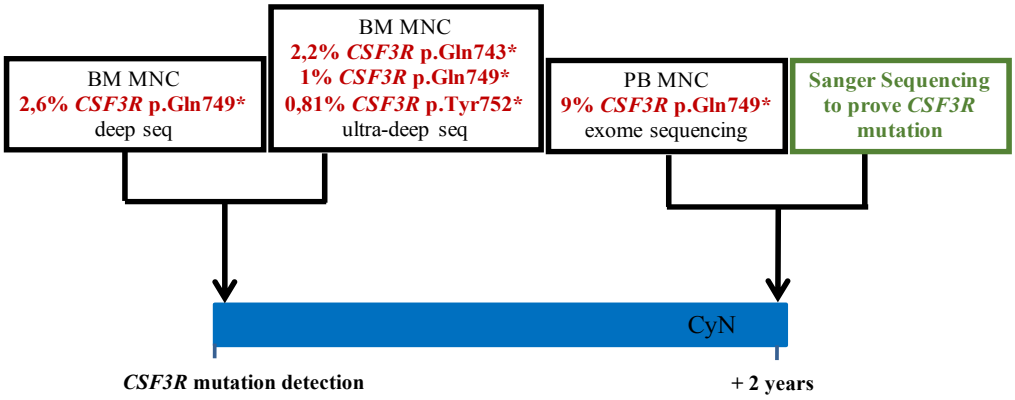

Figure 30: Time line of *CSF3R* mutation acquisition in CyN patient 4.
The black boxes contain the experiments and results obtained prior to this work, while the green box contains the step that is part of this thesis. BM MNC, bone marrow mononuclear cells; CyN, cyclic neutropenia; deep seq, deep sequencing; PB MNC, peripheral blood mononuclear cells (data were kindly provided by M. Klimiankou).

The mutated cell fraction in CyN patient 4 was below 10% in exome sequencing, and thus below the detection limit of Sanger sequencing. Different methods were tested to increase the level of mutant alleles. The use of a restriction enzyme could not show a signal elevation despite optimization of the protocol. Furthermore, COLD-PCR was established. This model is based on the optimization of the denaturation temperature in PCR, which barely divides mutant double-strands but not the wild-type double strands. In this way, only the mutant strands will be amplified. However, the use of this technique did not lead to success. Finally, molecular cloning was result-producing. For this purpose, 25 clones

of the latest PB MNC sample that was used for exome sequencing earlier were prepared (according to the protocol in Chapter 3.3.6) and sent for Sanger sequencing.

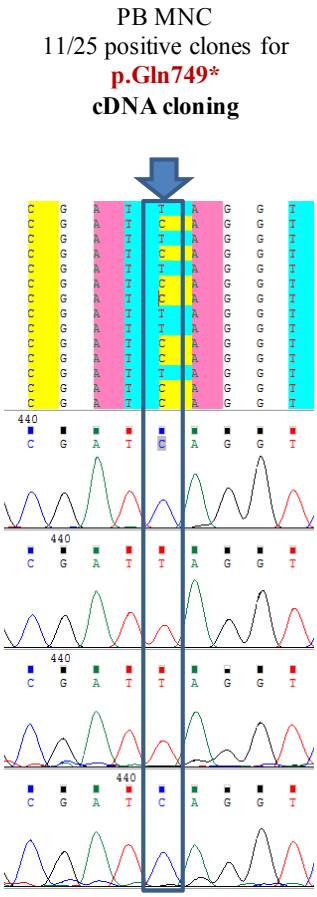

Figure 31: Sanger sequencing results of *CSF3R* mutation in CyN patient 4.
This Sanger sequencing result shows the presence of the *CSF3R* p.Gln749* mutation in 11 of 25 PB MNC clones. PB MNC, peripheral blood mononuclear cell.

Eleven of the 25 sequenced clones were positive for the p.Gln749* mutation after very clear signals in Sanger sequencing (Figure 31). Consequently, the mutant allele frequency has increased to 44%. As a result, the second CyN patient with an acquired *CSF3R* mutation was detected.

5 Discussion

5.1 Oscillating granule protein gene expression in CyN patient 1

5.1.1 Discussion of data collection and experimental setup

In the first project, the gene expression of an index CyN patient was compared to six healthy donors and four further CyN patients. It was imperative that the samples included in this study undergo a selection to guarantee high comparability. Thus, the selection criteria for the CyN patients were very specific: the diagnosis of CyN had to be documented. A BM sample obtained at either the ANC minimum or the maximum had to be available, which indicates that the ANC course of these patients had to be documented over a period of time. For reasons of comparability, only $CD33^+$ or $CD34^+38^+$ cells could be used. However, this selection had the disadvantage that the examined cohort was far to small for being able to draw a significant conclusion. Due to this lack of samples, except for CyN patient 1, only two patients could be included per granulocyte cycle time point (ANC maximum and minimum, respectively). Under the concept of this study, at least three patients should have been worked with per comparison group. In addition, only in the case of CyN patient 1 the corresponding samples of ANC maximum and minimum could be used. It would have been favorable to have both samples (ANC maximum and minimum) for each CyN patient.

Consequently, bias due to individual expression variabilities between those two time points could not be excluded. However, it was assumed that the same mechanisms of granulocyte number regulation (ANC maximum vs. minimum) exist in the HSCs of each CyN patient and are active permanently, independently of the patient's conditions at the time points of the study. Therefore, based on this assumption, the comparison of cells from different patient cycles was considered possible.

A positive aspect of the study is that every result obtained by qPCR was measured in triplicate. As shown in the various bar graphs, the standard deviation in most of the measurements is tolerably small so that measurement errors could be minimized. Moreover, the comparison of two different methods, namely microarray and qPCR, confirmed the results independently. An additional positive aspect worth mentioning is

that each group of comparison, CyN patient 1, the four other CyN patients (CyN patients 2, 3, 4 and 5) and the healthy donors, was set in relation to the others. This experimental setup allowed statements about the direct ratio between those groups.

5.1.2 Basic findings about cycling genes in CyN patient 1

The analysis of the granule protein genes and *NAMPT* expression of CyN patient 1 in comparison to healthy donors (Chapter 4.1.2.2) showed that CyN patient 1 differs clearly from the healthy ones. The detailed view of each divergent gene will be the subject of the subsequent chapter. In this context, basic perceptions about the tested gene expression in CyN patient 1 as well as the correlation of the patient's gene oscillation with the ANC cycle time will be discussed.

First, in this index patient, granule protein genes and *NAMPT* appeared to be coordinately expressed, as nine out of ten tested genes showed the same pattern. This confirms the hypothesis of Graubert et al. (1993) and Berliner et al. (1995) who described a tightly controlled and synchronized expression of secondary granule proteins and *defensin*. In addition to the known dependency on maturation level of granulopoiesis, granule protein gene expression also seems to depend on the timing of the ANC cycle (Graubert et al., 1993; Berliner et al., 1995). Accordingly, not only the gene expression in CyN patient 1 but also in the four other CyN patients oscillated in the opposite direction to the ANC (Figures 13 and 17). At the myelopoiesis level, this means that myelopoiesis is inhibited at the ANC peak and, conversely, an induction of myelopoiesis occurs at the ANC nadir. In other words, the elevation of ANC in CyN could lead to its subsequent drop. These observations made a negative feedback loop of neutrophil stimulation conceivable. In 1966, healthy individuals with oscillating neutrophil counts were already described. In this context, a negative feedback regulation of neutrophil production was first mentioned (Morley, 1966). Moreover, in 1998, Haurie et al. have set up the thesis of a negative feedback loop regulation of neutrophils in view of the same principle confirmed in erythropoiesis and thrombopoiesis. They especially focused on G-CSF, which is produced inversely to neutrophil counts and is thus highly expressed at the ANC minimum and vice versa (Haurie et al., 1998). G-CSF is known to induce granule protein

genes so that a connection could be expected between the expression of those genes and the cycling ANC (Nakajima & Ihle, 2001).

Additionally, gel electrophoresis results of CyN patient 1 (Figure 13) showed that three genes (*MMP8, SLPI* and *NAMPT*) were expressed in $CD33^+$ cells but not in $CD34^+38^+$ cells. This could support the hypothesis that granule protein genes and *NAMPT* expression increase in the course of neutrophil maturation.

5.1.3 *C/EBPe* mutation correlated with cycling genes in CyN patient 1

This chapter discusses the phenomenon of the unique presence of oscillating granule and NAMPT proteins in CyN patient 1. Therefore, the focus must once again be placed on the gene expression of CyN patient 1 compared to healthy donors (Chapter 4.1.2.2). The integrated view of WTA qPCR and gel electrophoresis data pointed out three groups of genes that needed to be separated from each other (Table 25). First, there was the group of four genes (*CRISP3, LCN2, OLFM4* and *TCN1*) that all showed a strongly decreased expression at the ANC maximum of CyN patient 1 compared to healthy donors in both cell lineages and, accordingly, had no PCR product in gel electrophoresis. This indicates that these genes are downregulated at the ANC maximum of CyN patient 1 at the different maturation levels of granulopoiesis. In contrast, there was another group of genes (*MMP8, SLPI* and *NAMPT*) that also had a decreased expression at the ANC maximum compared to healthy donors but showed an elevated expression in more matured $CD33^+$ cells compared to $CD34^+38^+$ cells. Thus, a product was visible at the ANC peak in $CD33^+$ cells but not in $CD34^+38^+$ cells. Finally, the third group contained two genes (*DEFA4* and *ELANE*) that indeed showed a downregulated expression at the ANC maximum of CyN patient 1 compared to healthy donors but still had a product in gel electrophoresis in both cell lineages. Interestingly, the genes of group one and two belong to the secondary granule protein genes and are known to modify the myeloid differentiation in case of *NAMPT*, while *DEFA4* and *ELANE,* belonging to group three, are primary granule protein genes (Yang-Feng et al., 1991; Faurschou & Borregaard, 2003; Skokowa et al., 2009; Kobayashi, 2015).

On the other hand, it was apparent, that the other four CyN patients did not show these obvious oscillating amplitudes in the granule protein gene and *NAMPT* expression (Chapter 4.1.2.3). Here we could only see a minimally downregulated expression at the ANC maximum compared to the minimum in three genes, *ELANE, DEFA4* and *OLFM4*.

Table 25: Simplified WTA qPCR and gel electrophoresis results of Figure 13.

Genes	WTA qPCR gene expression at the ANC MAX vs. HD		Gel electrophoresis product in the ANC MAX samples		Comment
	$CD33^+$ cells	$CD34^+38^+$ cells	$CD33^+$ cells	$CD34^+38^+$ cells	
CRISP3	↓↓↓	↓↓↓	–	–	Secondary granule protein gene
LCN2	↓↓↓	↓↓↓	–	–	
OLFM4	↓	↓	–	–	
TCN1	↓↓↓	↓↓	–	–	
MMP8	↓	↓↓↓	+	–	Myeloid diff. modifying protein
SLPI	↓	↓	+	–	
NAMPT	↓↓	↓↓↓	+	–	
DEFA4	↓	↓↓↓	+	+	Primary granule protein gene
ELANE	↓	↓	+	+	

WTA qPCR and gel electrophoresis results of nine genes (listed in Figure 13) in CyN patient 1. The gene expression, as well as the results in agarose gel, are indicated for both cell lineages, $CD33^+$ and $CD34^+38^+$ cells. The data were being simplified so that three different patterns of gene expression and the corresponding protein product were remarkable. The first group of genes is indicated in red, the second group in orange and the third group in blue. The arrows symbolize the intensity of downregulated expression at the ANC maximum of CyN patient 1 compared to HD. One arrow corresponds to low downregulation, while two arrows correspond to a middle and three arrows to a high downregulation. In case of the gel electrophoresis results, the plus sign indicates an existing product, while the minus sign indicates that there was no product in the gel. ANC, absolute neutrophil count; diff., differentiation; HD, healthy donor; qPCR, real-time quantitative polymerase chain reaction; vs., versus; WTA, whole transcriptome amplification.

The integration of the gene expression of CyN patient 1 into the classification of primary and secondary granule proteins leads back to the *C/EBPe* mutation of CyN patient 1, which was considered as a possible explanation for the unique phenomenon of cycling granule protein genes and *NAMPT* in this patient.

To summarize the findings concerning *C/EBPe,* it was confirmed that *C/EBPe* is expressed in CyN patient 1, but in a great surplus of the short and probable mutated isoform. It was also concluded that in CyN patient 1, *C/EBPe* expression is elevated at the cycle nadir compared to the peak. Considering other CyN patients, a similar *C/EBPe*

expression to healthy donors could be detected independently of the isoform. However, a slightly oscillating *C/EBPe* expression could also be seen in those patients between the ANC maximum and minimum.

Interestingly, *C/EBPe* expression is induced by G-CSF (Nakajima & Ihle, 2001). As already discussed, G-CSF levels in CyN patients depend on the ANC cycle in the form of a negative feedback loop. At the neutrophilic stage, the G-CSF level is decreased, while it is increased in the neutropenic phase (Kiyoshi Watari et al., 1989; Foley et al., 2006). Consequently, at the maximum of ANC, G-CSF levels are decreased in CyN patients, which induces a downregulation of *C/EBPe* (Figure 32). Against this background, an oscillation of the expression of *C/EBPe* or secondary granule protein genes could be explained in CyN patients.

However, CyN patients 1, 2, 3, 4 and 5 were all treated with G-CSF at the time the samples were obtained. So, due to unphysiologically high G-CSF levels, an increased *C/EBPe* expression over the time cycle was expected. Looking at the four CyN patients (CyN patients 2, 3, 4 and 5), a slightly oscillating pattern of *C/EBPe* expression was detected, which, however, was comparable to healthy donors (Figures 21, 24 and 26). The moderate level of up- and downregulation of *C/EBPe* expression that could nevertheless be measured in those four CyN patients, could be attributed to the additional specific G-CSF oscillation of the CyN patients, fluctuating between <30 pg/ml at the ANC maximum and up to 165 pg/ml at the ANC minimum in untreated patients (Kiyoshi Watari et al., 1989). In consequence of the almost steady *C/EBPe* expression, the secondary granule protein gene expression in the four CyN patients was possibly comparable to healthy donors or showed a discreetly cycling pattern in some genes.

CyN patient 1 has the heterozygous *C/EBPe* p.Leu155Met mutation (Chapter 4.1.3). Homozygous mutations in *C/EBPe*, in general, are known to provoke a lack of neutrophil secondary granule proteins (Lekstrom-Himes et al., 1999). However, the effect of the rare heterozygous SNP *C/EBPe* p.Leu155Met in CyN patient 1 can only be speculated. Referring to the research on this SNP in the ExAC database, a damaging effect of the heterozygous *C/EBPe* p.Leu155Met mutation seems unlikely. However, according to PolyPhen-2 and SIFT, this SNP is said to be damaging and deleterious (Chapter 4.1.3). This work has demonstrated changes in the *C/EBPe* isoforms in CyN patient 1. Thereby

one can imagine a potentially damaging effect of the heterozygous mutation in creating a new start codon leading to an isoform that is likely to have the same dominant-negative effect as the *C/EBPe* isoform 14 (Chapter 4.1.3). In other words, since CyN patient 1 has the heterozygous mutation in *C/EBPe*, the mutant protein must act in a dominant-negative manner to inhibit the wild-type protein.

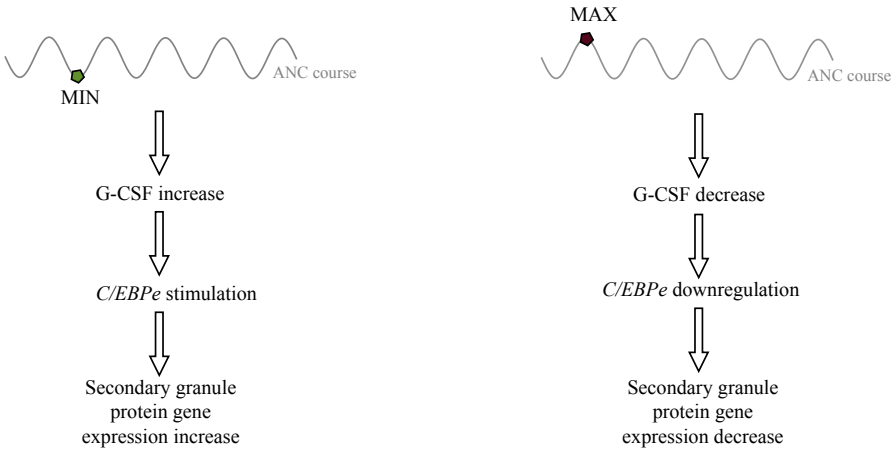

Figure 32: Influence of ANC on G-CSF level and *C/EBPe* expression.
The consequences of a neutropenic phase in CyN patients are indicated on the left side, while the neutrophilic state with its influences in CyN patients is indicated on the right side. ANC, absolute neutrophil count; G-CSF, granulocyte-colony stimulating factor; MAX, maximum; MIN, minimum.

5.2 Discussion of pathomechanism in general CyN

5.2.1 Role of ELANE as a cycling gene in CyN patients

As already discussed, the granule protein gene expression in the four CyN patients (CyN patients 2, 3, 4 and 5) did not show the same obvious oscillating trend that was detected in CyN patient 1. Only the three genes *DEFA4, ELANE* and *OLFM4* had a cycling pattern (Figures 15 and 17). *OLFM4* is known to be expressed heterogeneously in healthy individuals depending for example, on the maturation level of neutrophils. This complicates speculations about its influence on the cycling ANC (Clemmensen et al., 2012). However, since *ELANE* is the causative gene for CyN, it has been of particular interest (Horwitz et al., 1999). The hypothesis of a negative feedback loop inducing the cycling ANC was already mentioned (Chapter 5.1.2). Knowing that the majority of

granule protein genes oscillate only in CyN patient 1, this phenomenon can probably be attributed to influences of the *C/EBPe* mutation or, rather, other individual variables (Chapter 5.1.3). However, the fact that *ELANE* was also cycling in the four additional CyN patients brings the assumption that the *ELANE* mutation might be predominantly involved in the ANC oscillations. This observation had already been reported by Klimenkova et al. (2015), who identified cycling granule protein genes as possible regulators of oscillating myeloid cells. To confirm this observation, it would have been desirable to examine sample pairs (ANC maximum and minimum) of each CyN patient, instead of comparing the two cycle time points of different patients. Furthermore, it would have been interesting to see these oscillations also in $CD33^+$ myeloid cell populations. Next, measurements of *ELANE* expression in additional CyN patients may further prove whether a cycling pattern is detectable in every CyN patient and thus is an integral part of the disease's pathomechanism.

5.2.2 Regeneration of neutrophil production at the ANC nadir

Next, a closer look shall be taken at those three cycling genes (*DEFA4*, *ELANE* and *OLFM4*) in the additional four examined CyN patients. For each of these genes, it was seen that the expression at the ANC maximum resembled that of healthy donors, while an elevated expression at the ANC minimum was detectable compared to healthy donors. In other words, CyN patients appear to have stable, physiological expression of the primary granule protein genes *DEFA4* and *ELANE*, as well as *OLFM4* at the ANC peak, while their expression is boosted at the ANC nadir. Consequently, despite low ANC counts, the ANC minimum does not appear to be a time point of cycle at which granulopoiesis is deficient, but rather the point at which neutrophil production is stimulated. *DEFA4* and *ELANE,* being primary granule protein genes, are thus expressed in early neutrophil progenitors. Knowing that they are highly expressed at the ANC minimum in CyN patients compared to healthy donors underlines that the starting point of boosted granulopoiesis takes place at the nadir of ANC. Interestingly, comparable results for *DEFA4*, *ELANE* and *OLFM4* could be seen in CyN patient 1, with the expression at the ANC maximum more or less at the level of healthy donors and the expression at the ANC minimum higher than in healthy donors. As a result, the

phenomenon of enhanced early expressed neutrophil granule protein genes at the nadir of ANC could be reinforced in each examined CyN patient.

5.2.3 Biological difference of SCN and CyN in neutrophil production

At this point, a view of the biological difference between CyN and SCN becomes obvious. While the ANC is consistently low in SCN patients, one can conclude that those patients cannot produce enough neutrophils with the G-CSF level they naturally have without additional substitution. In contrast, CyN patients indeed have deficient mechanisms to produce a constant sufficient neutrophil count. However, in the case of low ANC, emergency pathways are active and lead to a strong recovery of neutrophil production.

5.3. Cooperativity of CSF3R and RUNX1 mutations in CyN

5.3.1 *CSF3R* and *RUNX1* mutations in SCN

As presented by Skokowa et al. in 2014, *CSF3R* mutations play an important role in the leukemogenesis of SCN. Interestingly, 80% of all AML/SCN patients harbor *CSF3R* mutations, making them an essential driver of MDS and AML development. However, it only leads to malignant transformation if other genetic defects contribute, with the *RUNX1* mutation being the most frequent example. Thus, the *CSF3R* mutation was suggested as the initial driver of MDS/AML, favoring cell growth and the acquisition of the crucial leukemic driver, the *RUNX1* mutation. This cooperativity appears to be pathognomic for MDS/AML development in SCN (Skokowa et al., 2014).

5.3.2 *CSF3R* and *RUNX1* mutations in CyN

Until 2016, it was a common knowledge that CyN patients do not acquire *CSF3R* mutations (Zeidler et al., 2009). Then, Klimiankou et al. (2016) identified the first two patients (CyN patients 4 and 6) harboring this preleukemic mutation in *CSF3R* (Chapter 4.2). CyN patient 4, same as her sister, has the *ELANE* mutation, p.Val190_Phe199del, that was found in both phenotypes, SCN and CyN. This mutation was inherited from her

father. CyN patient 6 has the sporadic p.Ala233Pro and the p.Val235TrpfsX5 mutations that were previously documented only in SCN cases. Clinically, both patients were specific for CyN so that bias due to masked SCN could be excluded (Klimiankou et al., 2016). This led to the assumption that the acquisition of *CSF3R* mutations might be correlated with *ELANE* mutations associated with SCN. This would imply, that any patient harboring an *ELANE* mutation related to SCN should be screened for *CSF3R* mutations as a precaution, regardless of whether the appropriate patient has the SCN or CyN phenotype. To date, a third CyN patient with an acquired *CSF3R* mutation was found. Consequently, the importance of regular screening procedures for CyN patients, in general, becomes even more apparent.

5.3.3 G-CSF dose dependence of *CSF3R* mutation

Daily treatment with G-CSF could raise the suspicion that the constant high level of influence and stimulation of HSCs of SCN and CyN patients with G-CSF might induce the acquisition of *CSF3R* mutations. Interestingly, G-CSF does not likely facilitate the occurrence of *CSF3R* mutations in SCN. The time of the first AML/SCN case was well before the introduction of G-CSF treatment (Skokowa et al., 2014; Gilman et al., 1970).

While the median G-CSF dose for CyN patients registered in the European section of SCNIR averages at 2.6 µg/kg per day, CyN patient 4 is treated with very low doses, namely 1.5 µg/kg per day. Whereas, CyN patient 6 receives comparatively high doses of 7.5 µg/kg per day. Despite the controversial data, the possibility of a G-CSF-induced risk of malignancy as a function of the treatment dose should be considered (Klimiankou et al., 2016).

5.4 Perspectives in CyN treatment

In addition to the known *ELANE* mutations, there are still many open questions about the cycling phenomenon of neutrophils in CyN patients (Grenda et al., 2007). The ultimate understanding of all modifiers and variables that induce these oscillations is indispensable

for an adequate adjustment of therapy. The actual treatment, based on the daily application of G-CSF, might be fraught with risk of malignant mutations, such as the acquisition of *CSF3R* and *RUNX1* mutations (Klimiankou et al., 2016). Thus, alternative ways to increase the ANC at the neutropenic stage are brought into focus.

In this context, vitamin B3 has gained importance. Vitamin B3, also called nicotinamide, is known to be converted by NAMPT into nicotinamide adenine dinucleotide (NAD+). NAD+, on the other hand, leads to the induction of G-CSF-triggered granulocyte differentiation and thus induces steady-state and stress-induced granulopoiesis. In vitro and in vivo studies proved elevated neutrophil granulocyte counts under vitamin B3 treatment (Skokowa et al., 2009). To get further information about the influence of G-CSF treatment on the acquisition of leukemic mutations, further studies are required; comparing G-CSF treated SCN and CyN patients to vitamin B3 treated patients would be interesting. This therapeutic approach is still in its trial phase. However, if this treatment is successful, G-CSF therapy could be replaced, or at least reduced, potentially resulting in the reduction of pre-leukemic cell clones.

6 Summary

6.1 Summary (English version)

CyN is a rare hematopoietic disorder characterized by an oscillating count of neutrophils ranging from less than 200 neutrophils per µl at the cycle nadir to a maximum of 2000 neutrophils per µl at the cycle peak in an average 21-day rhythm. At the nadir of the ANC cycle, the patients consequently suffer from multiple bacterial and fungal infections. As a subtype of SCN, which shows a constant low ANC, both phenotypes are known to be associated with mutations in *ELANE*. However, the pathomechanism leading to the typical ANC cycling in CyN is unclear.

This work focuses on the probable influences and regulatory mechanisms that could contribute to this cycling phenomenon. A microarray run performed with an index CyN patient represented the starting point of experiments. This microarray showed cycling patterns of granule protein genes and *NAMPT* expressions inverse to the ANC course. To confirm these findings, the index patient's data were verified by using qPCR. Additionally, four further CyN patients and six healthy donors served as comparison groups. While the cycling character in nine out of ten examined genes was confirmed in the index CyN patient, only three genes were cycling only slightly in the other CyN patients, among them *ELANE.* This inversely cycling *ELANE* expression, as compared to the ANC oscillations in all examined CyN patients, contributed to the hypothesis of a negative feedback regulation of neutrophil maturation. Moreover, as a reason for the difference in expression of the index patient to the others, the index patient's additionally inherited *C/EBPe* mutation was discussed. This mutation could lead to the inhibition of secondary granule proteins, thus contributing, besides other variables, to the unique protein expression and the neutropenic situation in this patient.

As another differentiating criterion to SCN, CyN was always described as benign and not to be associated with MDS/AML. However, in 2016, the author's research group identified the first two CyN patients harboring the preleukemic *CSF3R* mutation by deep, ultradeep, and exome sequencing. One of these patients additionally acquired the *RUNX1*

mutation and was diagnosed with AML. With this knowledge, a prophylactic screening of CyN patients becomes particularly important.

6.2 Summary (German version)

Die zyklische Neutropenie ist eine seltene Erkrankung aus der Gruppe der angeborenen Neutropenien und charakterisiert durch den oszillierenden Verlauf von neutrophilen Granulozyten. Dabei schwankt deren Zahl in einem durchschnittlich 21-tägigen Rhythmus zwischen <200 pro μl und maximalen Werten von etwa 2000 pro μl. In der neutropenischen Phase dieses Zyklus leiden die Patienten an diversen bakteriellen Infekten und Pilzerkrankungen. Dem gegenüber steht die schwere kongenitale Neutropenie mit einer durchgängig niedrigen Anzahl an Neutrophilen. Interessanterweise sind beide Phänotypen auf Mutationen im gleichen Gen *ELANE* zurückzuführen. Es ist bisher jedoch noch völlig unklar, welche Variablen letztlich zu dem typisch oszillierenden Neutrophilenmuster im Rahmen der zyklischen Neutropenie beitragen und damit den entscheidenden Unterschied zur schweren kongenitalen Neutropenie definieren.

Um dieser Frage auf den Grund zu gehen, wurden im ersten Teil der Arbeit Microarray-Daten einer Indexpatientin mit zyklischer Neutropenie untersucht. Diese zeigten einige neutrophile Granulaproteingene, deren Expression sich zyklisch verhielt, jedoch dem absoluten Neutrophilenwert im Blut entgegengesetzt war. Basierend auf dieser Erkenntnis wurde die Hypothese aufgestellt, dass ein negativer Rückkopplungsmechanismus die Granulopoese reguliert. Dementsprechend erwarteten wir, dass die Neutrophilenproduktion und damit die Proteingenexpression am Tiefpunkt des Neutrophilenzyklus hochreguliert und am Neutrophilenpeak entsprechend herabgesenkt sei. Nachdem die Microarray-Daten der Indexpatientin mittels qPCR in neun von zehn untersuchten Genen bestätigt werden konnten, dienten im weiteren Versuchsaufbau vier zusätzliche Patienten, sowie sechs gesunde Probanden als Vergleichsgruppen. Entgegen unserer Erwartungen zeigten die anderen Patienten hingegen lediglich eine leicht zyklische Tendenz in der Expression von drei der zehn untersuchten Genen, eines darunter *ELANE*. Dessen Expression verlief in allen Patienten

antizyklisch zum Neutrophilenwert und stützte damit die Hypothese eines negativen Rückkopplungsmechanismus der Granulopoese. Eine Bestätigung der antizyklischen Expression des *ELANE* Genes in weiteren Patienten mit zyklischer Neutropenie könnte zukünftig zu einem besseren Verständnis der Neutrophilenoszillation und damit des Pathomechanismus der Erkrankung beitragen.

Als mögliche Ursache für das abweichende Expressionsverhalten in der Indexpatientin im Vergleich zu den anderen Patienten, wurde deren vererbte *C/EBPe* Mutation als Ursache diskutiert. Die Mutation könnte zu einer Hemmung der sekundären Granulaproteine führen, hierdurch zu deren einzigartigen Expressionsmuster beitragen und letztendlich die Ausprägung der Neutropenie der Patientin verstärken.

Neben den Neutrophilenzahlen diente bisher der gutartige Verlauf der zyklischen Neutropenie als klares Abgrenzungsmerkmal zur schweren kongenitalen Neutropenie, die mit einem erhöhten Risiko für MDS/AML assoziiert ist. Im Jahr 2016 hingegen identifizierte die Arbeitsgruppe der Autorin die ersten beiden Patientinnen mit zyklischer Neutropenie, bei welchen die präleukämische *CSF3R* Mutation auftrat. Eine dieser Patientinnen wies zusätzlich die *RUNX1* Mutation auf und entwickelte im Verlauf eine AML. Im Zuge dieser Arbeit konnte mittels Sanger-Sequenzierung der betroffenen Allele, die Existenz der durch Deep-, Ultradeep- und Exome-Sequenzierung ermittelten Mutationen bestätigt werden. Durch diese neue Erkenntnis kommt dem prophylaktischen Screening von an zyklischer Neutropenie erkrankter Patienten ein besonderer Stellenwert zu.

7 References

Adzhubei, I.A., Schmidt, S., Peshkin, L., Ramensky, V.E., Gerasimova, A., Bork, P., Kondrashov, A.S. & Sunyaev, S.R. 2010. A method and server for predicting damaging missense mutations. *Nature Methods*, 7(4): 248–249.

Amulic, B., Cazalet, C., Hayes, G.L., Metzler, K.D. & Zychlinsky, A. 2012. Neutrophil function: From mechanisms to disease. *Annual Review of Immunology*, 30(1): 459–489.

Antonson, P., Stellan, B., Yamanaka, R. & Xanthopoulos, K.G. 1996. A novel human CCAAT/enhancer binding protein gene, C/EBPepsilon, is expressed in cells of lymphoid and myeloid lineages and is localized on chromosome 14q11.2 close to the T-cell receptor alpha/delta locus. *Genomics*, 35(1): 30–38.

Basu, S., Hodgson, G., Katz, M. & Dunn, A.R. 2002. Evaluation of role of G-CSF in the production, survival, and release of neutrophils from bone marrow into circulation. *Blood*, 100(3): 854–861.

Bedi, R., Du, J., Sharma, A.K., Gomes, I. & Ackerman, S.J. 2009. Human C/EBP-ε activator and repressor isoforms differentially reprogram myeloid lineage commitment and differentiation. *Blood*, 113(2): 317–327.

Berliner, N., Hsing, a, Graubert, T., Sigurdsson, F., Zain, M., Bruno, E. & Hoffman, R. 1995. Granulocyte colony-stimulating factor induction of normal human bone marrow progenitors results in neutrophil-specific gene expression. *Blood*, 85(3): 799–803.

Beutler, B. 2004. Innate immunity: An overview. *Molecular Immunology*, 40(12): 845–859.

Bonilla, M.A., Gillio, A.P., Ruggeiro, M., Kernan, N.A., Brochstein, J.A., Abboud, M., Fumagalli, L., Vincent, M., Gabrilove, J.L., Welte, K., Souza, L.M. & O'Reilly, R.J. 1989. Effects of recombinant human granulocyte colony-stimulating factor on neutropenia in patients with congenital agranulocytosis. *New England Journal of Medicine*, 320(24): 1574–1580.

Borregaard, N. 2010. Neutrophils, from marrow to microbes. *Immunity*, 33(5): 657–670.

Borregaard, N. & Cowland, J.B. 1997. Granules of the human neutrophilic polymorphonuclear leukocyte. *Blood*, 89(10): 3503–3521.

Borregaard, N., Sehested, M., Nielsen, B.S., Sengeløv, H. & Kjeldsen, L. 1995. Biosynthesis of granule proteins in normal human bone marrow cells. Gelatinase is a marker of terminal neutrophil differentiation. *Blood*, 85(3): 812–817.

Borregaard, N., Sørensen, O.E. & Theilgaard-Mönch, K. 2007. Neutrophil granules : A library of innate

immunity proteins. *Trends in Immunology*, 28(8): 340–345.

Boxer, L.A. & Newburger, P.E. 2007. A molecular classification of congenital neutropenia syndromes. *Pediatric Blood and Cancer*, 49(5): 609–614.

Boztug, K., Appaswamy, G., Ashikov, A., Schäffer, A. a, Salzer, U., Diestelhorst, J., Germeshausen, M., Brandes, G., Lee-Gossler, J., Noyan, F., Gatzke, A.-K., Minkov, M., Greil, J., Kratz, C., Petropoulou, T., Pellier, I., Bellanné-Chantelot, C., Rezaei, N., Mönkemöller, K., Irani-Hakimeh, N., Bakker, H., Gerardy-Schahn, R., Zeidler, C., Grimbacher, B., Welte, K. & Klein, C. 2009. A novel syndrome with congenital neutropenia caused my mutations in G6PC3. *The New England journal of medicine*, 360(1): 32–43.

Bustin, S.A., Benes, V., Garson, J.A., Hellemans, J., Huggett, J., Kubista, M., Mueller, R., Nolan, T., Pfaffl, M.W., Shipley, G.L., Vandesompele, J. & Wittwer, C.T. 2009. The MIQE guidelines: Minimum information for publication of quantitative real-time PCR experiments. *Clinical Chemistry*, 55(4): 611–622.

Cho, H.K. & Jeon, I.S. 2014. Different clinical phenotypes in familial severe congenital neutropenia cases with same mutation of the ELANE gene. *Journal of Korean Medical Science*, 29(3): 452–455.

Clemmensen, S.N., Bohr, C.T., Rorvig, S., Glenthoj, A., Mora-Jensen, H., Cramer, E.P., Jacobsen, L.C., Larsen, M.T., Cowland, J.B., Tanassi, J.T., Heegaard, N.H.H., Wren, J.D., Silahtaroglu, A.N. & Borregaard, N. 2012. Olfactomedin 4 defines a subset of human neutrophils. *Journal of Leukocyte Biology*, 91(3): 495–500.

Cottle, T.E., Fier, C.J., Donadieu, J. & Kinsey, S.E. 2002. Risk and benefit of treatment of severe chronic neutropenia with granulocyte colony-stimulating factor. *Seminars in hematology*, 39(2): 134–140.

Dale, D.C. 2002. ELANE-related neutropenia. *Gene Reviews [Internet] Seattle (WA): University of Washington, Seattle*: [Updated July 14, 2011].

Dale, D.C., Bonilla, M.A., Davis, M.W., Nakanishi, A.M., Hammond, W.P., Kurtzberg, J., Wang, W., Jakubowski, A., Winton, E., Lalezari, P., Glaspy, J.A., Emerson, S., Gabrilove, J., Vincent, M. & Boxer, L.A. 1993. A randomized controlled phase II trial of recombinant human granulocyte colony-stimulating factor (Filgrastim) for treatment of severe chronic neutropenia. *Blood*, 8(10): 2496–2502.

Dale, D.C., Cottle, T.E., Fier, C.J., Bolyard, A.A., Bonilla, M.A., Boxer, L.A., Cham, B., Freedman, M.H., Kannourakis, G., Kinsey, S.E., Davis, R., Scarlata, D., Schwinzer, B., Zeidler, C. & Welte, K. 2003. Severe chronic neutropenia: Treatment and follow-up of patients in the Severe Chronic Neutropenia International Registry. *American Journal of Hematology*, 72(2): 82–93.

Dale, D.C. & Hammond, W.P. 1988. Cyclic neutropenia: A clinical review. *Blood Reviews*, 2(3): 178–

185.

Dale, D.C., Person, R.E., Bolyard, A.A., Aprikyan, A.G., Bos, C., Bonilla, M.A., Boxer, L.A., Kannourakis, G., Zeidler, C., Welte, K., Benson, K.F. & Horwitz, M. 2000. Mutations in the gene encoding neutrophil elastase in congenital and cyclic neutropenia. *Blood*, 96(7): 2317–2322.

Donadieu, J., Fenneteau, O., Beaupain, B., Mahlaoui, N. & Chantelot, C.B. 2011. Congenital neutropenia: diagnosis, molecular bases and patient management. *Orphanet journal of rare diseases*, 6(26): 1–28.

Doulatov, S., Notta, F., Laurenti, E. & Dick, J.E. 2012. Hematopoiesis: A human perspective. *Cell Stem Cell*, 10(2): 120–136.

Faurschou, M. & Borregaard, N. 2003. Neutrophil granules and secretory vesicles in inflammation. *Microbes and Infection*, 5: 1317–1327.

Fernández, K.S. & de Alarcón, P.A. 2013. Development of the hematopoietic system and disorders of hematopoiesis that present during infancy and early childhood. In *Pediatric Clinics of North America*. Elsevier Inc: 1273–1289.

Foley, C., Bernard, S. & Mackey, M.C. 2006. Cost-effective G-CSF therapy strategies for cyclical neutropenia: Mathematical modelling based hypotheses. *Journal of Theoretical Biology*, 238(4): 754–763.

Fraga, D., Meulia, T. & Fenster, S. 2008. Real-Time PCR. In *Current Protocols Essential Laboratory Techniques*. 10.3.1-10.3.34.

Friedman, A.D. 2007. Transcriptional control of granulocyte and monocyte development. *Oncogene*, 26(47): 6816–6828.

Germeshausen, M., Ballmaier, M. & Welte, K. 2007. Incidence of CSF3R mutations in severe congenital neutropenia and relevance for leukemogenesis: Results of a long-term survey. *Blood*, 109(1): 93–99.

Germeshausen, M., Deerberg, S., Peter, Y., Reimer, C., Kratz, C.P. & Ballmaier, M. 2013. The spectrum of ELANE mutations and their implications in severe congenital and cyclic neutropenia. *Human Mutation*, 34(6): 905–914.

Gilman, P.A., Jackson, D.P. & Guild, H.G. 1970. Congenital agranulocytosis: Prolonged survival and terminal acute leukemia. *Blood*, 36(5): 576–585.

Graubert, T., Johnston, J. & Berliner, N. 1993. Cloning and expression of the cDNA encoding mouse neutrophil gelatinase: demonstration of coordinate secondary granule protein gene expression during terminal neutrophil maturation. *Blood*, 82(10): 3192–3197.

References

Grenda, D.S., Murakami, M., Ghatak, J., Xia, J., Boxer, L.A., Dale, D., Mary, C., Link, D.C. & Dinauer, M.C. 2007. Mutations of the ELA2 gene found in patients with severe congenital neutropenia induce the unfolded protein response and cellular apoptosis. *Blood*, 110(13): 4179–4187.

Guerry, D., Dale, D.C., Omine, M., Perry, S. & Wolff, S.M. 1973. Periodic hematopoiesis in human cyclic neutropenia. *Journal of Clinical Investigation*, 52(12): 3220–3230.

Hammond, W.P., Price, T.H., Souza, L.M. & Dale, D.C. 1989. Treatment of cyclic neutropenia with granulocyte colony-stimulating factor. *New England Journal of Medicine*, 320(20): 1306–1311.

Haurie, C., Dale, D.C. & Mackey, M.C. 1998. Cyclical neutropenia and other periodic hematological disorders: A review of mechanisms and mathematical models. *Blood*, 92: 2629–2640.

Heid, C.A., Stevens, J., Livak, K.J. & Williams, P.M. 1996. Real time quantitative PCR. *Genome Research*, 6(10): 986–994.

Hirai, H., Zhang, P., Dayaram, T., Hetherington, C.J., Mizuno, S., Imanishi, J., Akashi, K. & Tenen, D.G. 2006. C/EBPβ is required for 'emergency' granulopoiesis. *Nature Immunology*, 7(7): 732–739.

Horwitz, M., Benson, K.F., Person, R.E., Aprikyan, A.G. & Dale, D.C. 1999. Muations in ELA2, encoding neutrophil elastase, define a 21-day biological clock in cyclic haematopoiesis. *Nature Genetics*, 23(4): 433–436.

Iwasaki, A. & Medzhitov, R. 2010. Regulation of adaptive immunity by the innate immune system. *Science*, 327(5963): 291–295.

Iwasaki, H., Somoza, C., Shigematsu, H., Duprez, E.A., Iwasaki-Arai, J., Mizuno, S.I., Arinobu, Y., Geary, K., Zhang, P., Dayaram, T., Fenyus, M.L., Elf, S., Chan, S., Kastner, P., Huettner, C.S., Murray, R., Tenen, D.G. & Akashi, K. 2005. Distinctive and indispensable roles of PU.1 in maintenance of hematopoietic stem cells and their differentiation. *Blood*, 106(5): 1590–1600.

Karczewski, K.J., Weisburd, B., Thomas, B., Solomonson, M., Ruderfer, D.M., Kavanagh, D., Hamamsy, T., Lek, M., Samocha, K.E., Cummings, B.B., Birnbaum, D., Daly, M.J. & MacArthur, D.G. 2017. The ExAC browser: Displaying reference data information from over 60 000 exomes. *Nucleic Acids Research*, 45(D1): D840–D845.

Klein, C. 2011. Genetic defects in severe congenital neutropenia: emerging insights into life and death of human neutrophil granulocytes. *Annu Rev Immunol*, 29: 399–413.

Klein, C., Grudzien, M., Appaswamy, G., Germeshausen, M., Sandrock, I., Schäffer, A. a, Rathinam, C., Boztug, K., Schwinzer, B., Rezaei, N., Bohn, G., Melin, M., Carlsson, G., Fadeel, B., Dahl, N., Palmblad, J., Henter, J.-I., Zeidler, C., Grimbacher, B. & Welte, K. 2007. HAX1 deficiency causes autosomal recessive severe congenital neutropenia (Kostmann disease). *Nature Genetics*, 39(1): 86–

92.

Klimenkova, O., Klimiankou, M., Kanz, L., Zeidler, C., Welte, K. & Skokowa, J. 2015. Differential expression of neutrophil granule protein genes in bone marrow myeloid cells at the peak and nadir of neutrophil counts in cyclic neutropenia. *Blood*, 126(23): 2194.

Klimiankou, M., Mellor-Heineke, S., Klimenkova, O., Reinel, E., Uenalan, M., Kandabarau, S., Skokowa, J., Welte, K. & Zeidler, C. 2016. Two cases of cyclic neutropenia with acquired CSF3R mutations, with 1 developing AML. *Blood*, 127(21): 2638–2641.

Kobayashi, Y. 2015. Neutrophil biology: An update. *Excli Journal*, 14: 220–227.

Köllner, I., Sodeik, B., Schreek, S., Heyn, H., Von Neuhoff, N., Germeshausen, M., Zeidler, C., Krüger, M., Schlegelberger, B., Welte, K. & Beger, C. 2006. Mutations in neutrophil elastase causing congenital neutropenia lead to cytoplasmic protein accumulation and induction of the unfolded protein response. *Blood*, 108(2): 493–500.

Koschmieder, S., Rosenbauer, F., Steidl, U., Owens, B.M. & Tenen, D.G. 2005. Role of transcription factors C/EBPα and PU.1 in normal hematopoiesis and leukemia. *International Journal of Hematology*, 81(5): 368–377.

Kostmann, R. 1956. Infantile genetic agranulocytosis (Agranulocytosis infantilis hereditaria) a new recessive lethal disease in man. *Acta Paediatrica*, 45(3): 309–310.

Kurn, N., Chen, P., Don Heath, J., Kopf-Sill, A., Stephens, K.M. & Wang, S. 2005. Novel isothermal, linear nucleic acid amplification systems for highly multiplexed applications. *Clinical Chemistry*, 51(10): 1973–1981.

Leale, M. 1910. Recurrent furunculosis in an infant showing an unusual blood picture. *Journal of the American Medical Association*, 54(23): 1854–1855.

Lekstrom-Himes, J. a, Dorman, S.E., Kopar, P., Holland, S.M. & Gallin, J.I. 1999. Neutrophil-specific granule deficiency results from a novel mutation with loss of function of the transcription factor CCAAT/enhancer binding protein epsilon. *The Journal of experimental medicine*, 189(11): 1847–1852.

Makaryan, V., Zeidler, C., Bolyard, A.A., Skokowa, J., Rodger, E., Kelley, M.L., Boxer, L. a, Bonilla, M.A., Newburger, P.E., Shimamura, A., Zhu, B., Rosenberg, P.S., Link, D.C., Welte, K. & Dale, D.C. 2015. The diversity of mutations and clinical outcomes for ELANE-associated neutropenia. *Current opinion in hematology*, 22(1): 3–11.

Maximow, A. 1909. Der Lymphozyt als gemeinsame Stammzelle der verschiedenen Blutelemente in der embryonalen Entwicklung und im postfetalen Leben der Säugetiere. *Folia Haematologica*, 8: 125–

134.

Metcalf, D. 1989. The molecular control of cell division, differentiation commitment and maturation in haemopoietic cells. *Nature*, 339: 27–30.

Morley, A.A. 1966. A neutrophil cycle in healthy individuals. *The Lancet*: 1220–1222.

Morley, A.A., Carew, J.P. & Baikie, A.G. 1967. Familial cyclical neutropenia. *British Journal of Haematology*, 13(5): 719–738.

Nakajima, H. & Ihle, J.N. 2001. Granulocyte colony-stimulating factor regulates myeloid differentiation through CCAAT / enhancer-binding protein e. *Blood*, 98(4): 897–905.

Newburger, P.E., Pindyck, T.N., Zhu, Z., Bolyard, A.A., Aprikyan, A.A.G., Dale, D.C., Smith, G.D. & Boxer, L.A. 2010. Cyclic neutropenia and severe congenital neutropenia in patients with a shared ELANE mutation and paternal haplotype: Evidence for phenotype determination by modifying genes. *Pediatric Blood and Cancer*, 55(2): 314–317.

Ng, P.C. & Henikoff, S. 2001. Predicting deleterious amino acid substitutions. *Genome Research*, 11: 863–874.

Nielsen, J.S. & McNagny, K.M. 2008. Novel functions of the CD34 family. *Journal of Cell Science*, 121(22): 3683–3692.

Notta, F., Zandi, S., Takayama, N., Dobson, S., Gan, O.I., Wilson, G., Kaufmann, K.B., McLeod, J., Laurenti, E., Dunant, C.F., McPherson, J.D., Stein, L.D., Dror, Y. & Dick, J.E. 2016. Distinct routes of lineage development reshape the human blood hierarchy across ontogeny. *Science*, 351(6269).

Nüsse, O. & Lindau, M. 1988. The dynamics of exocytosis in human neutrophils. *Journal of Cell Biology*, 107(6): 2117–2123.

Ohlsson, K. & Odsson, I. 1974. The neutral proteases of human granulocytes. Isolation and partial charaterization of granulocyte elastases. *European Journal of Biochemistry*, 42(2): 519–527.

Orkin, S.H., Fisher, D.E., Ginsburg, D., Look, A.T., Lux, S.E. & Nathan, D.G. 2014. Phagocyte system and disorders of granulopoiesis and granulocyte function. In S. H. Orkin, ed. *Nathan and Oski's hematology and oncology of infancy and childhood*. Elsevier: 773–847.

Osgood, E.E., Brownlee, I.E., Osgood, M.W., Ellis, D.M. & Cohen, W. 1939. Total differential and absolute leukocyte counts and sedimentation rates determined for healthy persons nineteen years of age and over. *Archives of Internal Medicine*, 64(1): 105–120.

Rappeport, J.M., Parkman, R., Newburger, P., Camitta, B.M. & Chusid, M.J. 1980. Correction of

infantile agranulocytosis (Kostmann's syndrome) by allogeneic bone marrow transplantation. *The American Journal of Medicine*, 68(4): 605–609.

Rosenberg, P.S., Alter, B.P., Bolyard, A.A., Bonilla, M.A., Boxer, L.A., Cham, B., Fier, C., Freedman, M., Kannourakis, G., Kinsey, S., Schwinzer, B., Zeidler, C., Welte, K., Dale, D.C., Chronic, S. & International, N. 2006. The incidence of leukemia and mortality from sepsis in patients with severe congenital neutropenia receiving long-term G-CSF therapy. *Blood*, 107(12): 4628–4635.

Rosenberg, P.S., Zeidler, C., Bolyard, A.A., Alter, B.P., Bonilla, M.A., Boxer, L.A., Dror, Y., Kinsey, S., Link, D.C., Newburger, P.E., Shimamura, A., Welte, K. & Dale, D.C. 2010. Stable long-term risk of leukaemia in patients with severe congenital neutropenia maintained on G-CSF therapy. *British journal of haematology*, 150(2): 196–199.

Sieff, C.A. 1987. Hematopoietic growth factors. *The Journal of clinical investigation*, 79(6): 1549–1557.

Skokowa, J., Dale, D.C., Touw, I.P., Zeidler, C. & Welte, K. 2017. Severe congenital neutropenias. *Nature Reviews*, 3.

Skokowa, J., Lan, D., Thakur, B.K., Wang, F., Gupta, K., Cario, G., Schambach, A., Hinrichsen, L., Meyer, G., Gaestel, M., Stanulla, M., Tong, Q. & Welte, K. 2009. NAMPT is essential for the G-CSF – induced myeloid differentiation via a NAD + – sirtuin-1 – dependent pathway. *Nature Medicine*, 15(2): 151–158.

Skokowa, J., Steinemann, D., Jenny, K.-K., Zeidler, C., Klimenkova, O., Klimiankou, M., Ünalan, M., Kandabarau, S., Makaryan, V., Beekman, R., Behrens, K., Stocking, C., Obenauer, J., Schnittger, S., Kohlmann, A., Valkhof, M., Hoogenboezem, R., Göhring, G., Reinhardt, D., Schlegelberger, B., Stanulla, M., Vandenberghe, P., Donadieu, J., Zwaan, C.M., Touw, I.P., Van den Heuvel-Eibrink, M.M., Dale, D.C. & Welte, K. 2014. Cooperativity of RUNX1 and CSF3R mutations in severe congenital neutropenia: A unique pathway in myeloid leukemogenesis. *Blood*, 123(14): 2229–2238.

Spicer, S.S. & Hardin, J.H. 1969. Ultrastructure, cytochemistry, and function of neutrophil leukocyte granules. *Laboratory Investigation*, 20(5): 488–497.

Touw, I.P. 2015. Game of clones: the genomic evolution of severe congenital neutropenia. *Hematology American Society of Hematology Education Program 2015*, 2015(1): 1–7.

Vorachek, W.R., Bobe, G. & Hall, J.A. 2013. Reference gene selection for quantitative PCR studies in bovine neutrophils. *Advances in Bioscience and Biotechnology*, 4: 6–14.

Wang, X., Spandidos, A., Wang, H. & Seed, B. 2012. PrimerBank: A PCR primer database for quantitative gene expression analysis, 2012 update. *Nucleic Acids Research*, 40(D1).

Watari, K., Asano, S., Shirafuji, N., Kodo, H., Ozawa, K., Takaku, F. & Kamachi, S. 1989. Serum

granulocyte colony-stimulating factor levels in healthy volunteers and patients with various disorders as estimated by enzyme immunoassay. *Blood*, 73(1): 117–122.

Watari, K., Asano, S., Shirafuji, N., Kodo, H., Ozawa, K., Takaku, F. & Kamachi, S. 1989. Serum granulocyte colony-stimulating factor levels in healthy volunteers and patients with various disorders as estimated by enzyme immunoassay. *Blood*, 73(1): 117–122.

Welte, K. & Boxer, L. 1997. Severe chronic neutropenia: Pathophysiology and therapy. *Seminars in hematology.*, 34(4): 267–278.

Welte, K., Platzer, E., Lu, L., Gabrilove, J.L., Levi, E., Mertelsmann, R. & Moore, M.A. 1985. Purification and biochemical characterization of human pluripotent hematopoietic colony-stimulating factor. *Proceedings of the National Academy of Sciences of the United States of America*, 82(5): 1526–1530.

Welte, K., Zeidler, C. & Dale, D.C. 2006. Severe congenital neutropenia. *Seminars in hematology*, 43(3): 3–5.

Williams, G.T., Smith, C.A., Spooncer, E., Dexter, T. & Taylor, D. 1990. Haemopoietic colony stimulating factors promote cell survival by suppressing apoptosis. *Nature*, 343(6253): 76.

Winkler, I.G., Barbier, V., Wadley, R., Zannettino, A.C.W., Williams, S. & Lévesque, J.P. 2010. Positioning of bone marrow hematopoietic and stromal cells relative to blood flow in vivo: Serially reconstituting hematopoietic stem cells reside in distinct nonperfused niches. *Blood*, 116(3): 375–385.

Wong, G.G., Witek, J.S., Temple, P.A., Wilkens, M.M., Leary, A.C. & Luxenberg, D. 1985. Human GM-CSF: Molecular cloning of the complementary DNA and purification of the natural recombinant proteins. *Science*, 228: 810–816.

Wriedt, K., Kauder, E. & Mauer, A.M. 1970. Defective myelopoiesis in congenital neutropenia. *The New England journal of medicine*, 283(20): 1072–1077.

Wright, D.G., Dale, D.C., Fauci, A.S. & Wolff, S.M. 1981. Human cyclic neutropenia: Clinical review and long-term follow-up of patients. *Medicine*, 60(1): 1–13.

Yamanaka, R., Kim, G.-D., Radomska, H.S., Lekstrom-Himes, J., Smith, L.T., Antonson, P., Tenen, D.G. & Xanthopoulos, K.G. 1997. CCAAT/enhancer binding protein epsilon is preferentially up-regulated during granulocytic differentiation and its functional versatility is determined by alternative use of promoters and differential splicing. *Proceedings of the National Academy of Sciences of the United States of America*, 94(12): 6462–6467.

Yang-Feng, T., Berliner, N., Deverajan, P. & Johnston, J. 1991. Assignment of two human neutrophil

secondary granule protein genes, transcobalamin I and neutrophil collagenase to chromosome 11. *Cytogenetics and Cell Genetics*, 58(3–4).

Ye, J., Coulouris, G., Zaretskaya, I., Cutcutache, I., Rozen, S. & Madden, T.L. 2012. Primer-BLAST: A tool to design target-specific primers for polymerase chain reaction. *BMC Bioinformatics*, 13(1): 134.

Zeidler, C., Germeshausen, M., Klein, C. & Welte, K. 2009. Clinical implications of ELA2-, HAX1-, and G-CSF-receptor (CSF3R) mutations in severe congenital neutropenia. *British Journal of Haematology*, 144(4): 459–467.

Zhang, P., Iwasaki-Arai, J., Iwasaki, H., Fenyus, M.L., Dayaram, T., Owens, B.M., Shigematsu, H., Levantini, E., Huettner, C.S., Lekstrom-Himes, J.A., Akashi, K. & Tenen, D.G. 2004. Enhancement of hematopoietic stem cell repopulating capacity and self-renewal in the absence of the transcription factor C/EBPα. *Immunity*, 21(6): 853–863.

8 Declaration of Authorship

This work was developed in the laboratory for translational oncology of the *Universitätsklinikum Tübingen* in the department *Innere Medizin II, Medizinische Universitätsklinik* under the supervision of Prof. Dr. Julia Skokowa. I hereby certify that the thesis I am submitting is my own original work except for the parts mentioned in the text below and where otherwise indicated. All direct or indirect sources used are acknowledged as references, including those sources of information that are integrated into graphs and figures.

The conception of this thesis was done by Prof. Dr. Julia Skokowa and Prof. Dr. Karl Welte in cooperation with Maksim Klimiankou, Ph.D. The supervision of the experimental procedure and the data analysis, as well as the correction of the thesis, was done by Maksim Klimiankou, Ph.D. The evaluation of results was done under the supervision and help of Maksim Klimiankou, Ph.D. and Prof. Dr. Julia Skokowa. The patient data have been made available by the SCNIR and Dr. Cornelia Zeidler. I was introduced to the experimental methods by Ingeborg Steiert, Karin Hähnel and Ursula Hermanutz-Klein. The isolation of MNCs from bone marrow samples, as well as the magnetic separation of $CD33^+$ and $CD34^+38^+$ cells, was carried out in collaboration with Ingeborg Steiert, Karin Hähnel and Ursula Hermanutz-Klein. The detection of isolated cell fractions and the molecular cloning was performed with the support of Karin Hähnel. Microarray as well as deep sequencing, ultradeep sequencing and exome sequencing, which formed the fundamentals of this work, have been performed by the members of the research group of Prof. Dr. Julia Skokowa/Prof. Dr. Karl Welte before I had started my work. RNA purification, the quantification of RNA by NanoDrop/ cDNA by Qubit, reverse transcription, the WTA Ovation method, qPCR, PCR, restriction digestion, Sanger sequencing and gel electrophoresis were done independently by me.

Concerning the paper “Two cases of cyclic neutropenia with acquired *CSF3R* mutations, with one developing AML” published in *Blood* in 2016 (Chapter 9), Maskim Klimiankou, Ph.D. performed the main part of experiments. Sabine Mellor-Heineke and Dr. Cornelia Zeidler provided the patient data and materials. Olga Klimenkova, Ph.D. performed the CFU assays. I performed the Sanger sequencing and cloning. Dr. Murat Uenalan, in

cooperation with Maksim Klimiankou, Ph.D. and Siarhei Kandabarau, analyzed the deep-sequencing data of *CSF3R*. Prof. Dr. Julia Skokowa, Prof. Dr. Karl Welte, Dr. Cornelia Zeidler, Sabine Mellor-Heineke and Maksim Klimiankou, Ph.D. analyzed the data and wrote the manuscript.

Tübingen, 15.10.2018

_____

9 Publication

Parts of this thesis have already been published in the following paper:

Klimiankou, M., Mellor-Heineke, S., Klimenkova, O., Reinel, E., Uenalan, M., Kandabarau, S., Skokowa, J., Welte, K. & Zeidler, C. 2016. Two cases of cyclic neutropenia with acquired CSF3R mutations, with 1 developing AML. *Blood*, 127(21): 2638–2641.

Acknowledgement

Firstly, my special thanks are extended to my advisor Prof. Dr. Julia Skokowa for her continuous support of my work. I am very grateful for the patience and permanent willingness to make the most out of a project, which created an encouraging and motivating work atmosphere. Knowing that she would always have an open ear for concerns and suggestions, I always felt insightfully supervised. In this context, I would also like to thank Prof. Dr. Karl Welte, who always enriched our lab meetings with his positive attitude and constructive feedback. As a relative of patients included in this research, I am particularly grateful to know their concerns in the hands of such competent leaders with a high degree of responsibility and human closeness.

I also want to take this opportunity to express my special gratitude to my supervisor Maksim Klimiankou, Ph.D., who helped me to learn laboratory work from scratch. I am extremely thankful for the tolerance and patience and for the great deal of time he has invested in giving me a better understanding of diverse issues. The way of scrutinizing and discussing my progress positively challenged me a great deal. His profound knowledge combined with the conscientious working methods was for me the best example and eye-opener for how science should be practiced.

I also want to give warm thanks to the entire team of the research group of Prof. Dr. Julia Skokowa/Prof. Dr. Karl Welte for the excellent cooperation and helpful atmosphere. The friendly way of welcoming and integrating new members in the team left a lasting impression on me. Without the precious help and support of especially Ingeborg Steiert, Karin Hähnel and Ursula Hermanutz-Klein, it would not have been possible to me to conduct this research.